A novel mycovirus Rosellinia necatrix megabirnavirus 1: Biological and molecular characterization, gene expression strategy and genome rearrangements

2014, March

LAKHA SALAIPETH

The Graduate School of Natural Science and Technology

(Doctor Course)

OKAYAMA UNIVERSITY

Table of Contents

List of Tables

List of Figures

Northern blotting of serial dilutions of RnMBV1 mRNA. SsRNA fractions were prepared from RnMBV1-infected *C. parasitica* strains Δ*dcl*-2 and EP155. The same amounts (10 μg) of RNA from the strains were applied to the left- and right-most lanes of 1% denatured agarose gel, while the middle lanes were loaded with serial dilutions derived from RnMBV1-infected Δ*dcl-2*, as shown on the top of the blot. Specific cDNA probe for dsRNA1 was used. EtBr-stained rRNAs were shown as loading control.

15 Virus particles purified from Δ*dcl-2* infected with RnMBV1. (A) Photographs of the 20-50% cesium sulfate gradient tubes, RnMBV1 (left tube) and D*dcl-2/*RnMBV1 (right tube). Crude lysate from a virus preparation was layered on tubes containing a cesium sulphate gradient. After 15 hr at 28,000 rpm in a SW41Ti swing out rotor, virus band was clearly visible in the cesium sulphate gradient. The particle bands and other minor containing nonfully mature or empty capsids appear white with a light shadow. (B) Top; agarose gel electrophoresis analysis shows the dsRNA patterns of the viral particles present in the bands detected in the gradients shown in (A). DsRNA from 10 μl of virus particle suspension were obtained after phenol/chloroform and chloroform extraction. DsRNA fractions were loaded into each well of 1% agarose gel and electrophoresed in 1X TAE buffer. Below; analysis of the virus particles preparation by 8% SDS-PAGE. Protein from virus particles was prepared as described in method. The migration of the viral structural proteins in the gel is indicated. 70

16 Infection of a RnMBV1 purified from *C. parasitica*. (A) Agarose gel electrophoretic analysis of dsRNA from transfectants. Spheroplasts of Δ*dcl-2* (Left) and W1015 (right) were transfected by purified RnMBV1 particles from *C. parasitica* and *R. necatrix* W1015. (B) Top; colony morphology of RnMBV1-infected *C. parasitica*. Δ*dcl*-2, uninfected and and parental strain were grown on PDA for 6 days on a bench top and then photographed. Below; colony morphology of RnMBV1-infected *R. necatrix* W1015, uninfected and parental strain were grown on PDA for 7 days in dark at 25 ^{o}C and then photographed. 72

Chapter 1. General Introduction

1.1 Background and history of white root rot disease

Rosellinia necatrix (Hart.) Berl. Prill. is a phytopathogenic ascomycete fungus, which causes white root rot disease on a broad range of commercial crops such as apple, grape vine, pear, plum, poplar and walnut (Whalley, 1996). Arakawa *et al*. (2002) reported more than 197 different hosts of this fungus. There is a little information about the origin of *R. necatrix* and it has been argued that there is a possibility that, in some countries, it could have been introduced on infected material from the tropical and subtropital areas (Thomas *et al.,* 1953; Mantell and Wheeler, 1973 cited in Pérez-Jiménez, 2006). It has been known to occur in Europe since the middle of 19th century (Viala, 1891 cited in Pérez-Jiménez, 2006). The pathogen is a limiting factor in apple and vineyard orchards in France, Portugal and many other European countries (Teixeira de Sousa *et al*., 1995). Teixeira de Sousa *et al*. (1995) reported that in Alcobaça region (Portugal) 42% of the orchards were infected by *R. necatrix* and 14% of the apple trees exhibited advanced disease symptoms. In Italy the fungus represents one of the most dangerous pathogens of root-rot in poplar (Anselmi & Giorcelli, 1990a) and is widely diffused on fruit trees like sweet cherry, almond, peach, olive and grapevine. In Asia, the disease is very common in Japan on a variety of hosts. It causes particular damage on tea bushes and is considered one of the most serious pathogens of fruit trees such as grapevine (Kanadani, Date & Nasu, 1998), orchards (Behdad, 1976), Japanese pear and apple (Arakawa *et al.*, 2002). In Taiwan, it is a problem on loquats (Lin and Duan, 1988; Duan *et al*., 1990). On the other side of the Asiatic continent, it is also very common in Iran (Behdad, 1976) mostly on apple trees, sour cherry trees and poplars.

Sztejnberg and Madar (1980) found that the fungus attacked and killed artificially inoculated deciduous trees (apple, pear, plum, almond), olive trees, citrus rootstocks, grape rootstocks, avocado, mango, macadamia, field crops (cotton, alfalfa, bean) and weeds. The same authors suggested that weeds like *Prosopis farcta* , *Aechmea gracilis* and *Conyza bonariensis* could promote the disease spreading.

1.2 Biology and symptoms of *R. necatrix*

1.2.1 Biology of *R. necatrix*

The fungal pathogen *R. necatrix* belongs to the family Xylariaceae, phylum Ascomycetes, which includes more than one hundred species (Petrini, 1993). *R. necatrix* produces both asexually and sexually. There are three different spore types (chlamidospores, conidiospores and ascospores). Chlamidospores, a thick-walled asexual fungal spore that is derived from a hyphal cell and can function as a resting spore, can be found under exceptional environmental conditions. They are formed from pyriform swelling in which protoplasm is condensed and a wall is formed that divides the spherical zone from the remaining hypha. They are spherical of approximately 15 μm in diameter. Conidiospores (asexual) originate at synnemata conidiogenous cells. The length of conidiospores are 3-5 μm long and 2.3-3 μm wide (Petrini, 1993). The conidiospore germination is very difficult to introduce *in vitro*. Ascospores (sexual) are formed inside the perithecium and when they reach maturity are expelled in a mucilaginous mass from the pore or papilla located on the top of the perithecium. They are ellipsoidal and cymbiform (boat-shaped) and their size vary between 36-46 μm in length and 5.5-6.3 μm in width (Petrini, 1993; Sivanesan, 1985).

Aimi *et. al.* (2002) reported genetic differences among single ascospore culture isolated from the same perithecium. Pérez-Jiménez et. al. (2002) revealed the existence of high genetic diversity in this fungus. Based on this results, the life cycle of *R. necatrix* appears to be heterothallic. Aimi *et al.* (2002) using molecular biological methods estimated the number of chromosome of field isolates and single ascospore isolate as about seven. It means normal heterokaryon formation does not occur in *R. necatrix*. The causal fungus rarely produces teleomorph, the sexual reproductive stage, on diseased plants in nature (Teixeira de Sousa, 1993).

1.2.2 Symptoms of *R. necatrix*

The fungus invades the root system of a tree by white mycelial fans. Infection by the

pathogen causes wilting, chlorosis and defoliation and under conducive environmental conditions it may result in rapid death of a tree. *R. necatrix* spreads from an infected tree by mycelia aggregates or strands which grow through soil and may contact root of so far healthy tree. On trees, *R. necatrix* causes a root and collar rot. Both the physical destruction of the root system and the transport of phytotoxins by the sap quickly provoke symptoms on the aerial parts which include slowing down of growth, small size, discoloration and wilting of the leaves, and general dieback of the tree with death of the extremities of the twigs. According to the nature and age of the tree, disease development can be slow, death occurs after several years of decline, or very rapid, sudden wilting occurs following a period of drought or the first onset of fruiting.

1.3 Control strategies of *R. necatrix*

Various strategies have been used to reduce the impact of *R. necarix*. However, control of the white root rot is complicated by its resistance to drought, tolerance to a wide range of soil pH, high number of hosts, penetration deep into the soil and resistance to various common fungicides (Khan, 1959 cited in Schena *et al*., 2003). Control strategies in the fields should be based on the avoidance of the pathogen through the utilization of certified healthy propagating materials; however, once introduced in the field control strategies should be directed to the management of the disease rather than to the pathogen eradication, which is very difficult and too expensive to be economically justifiable.

1.3.1 Physical Control

There are many strategies for physical control of *R. necatrix.* For example, the steam soil (Runia, 2000) which has been proposed as a valid control strategy to devitalize a number of soil borne pathogens. The use of a hot-water for treatment of *Cyperus esculentus* L. tubers was studied as a control strategy to prevent the spread of *R. necatrix* through infected tubers (García-Jiménez *et al*., 2004). Soil solarization has been largely exploited all over the world wherever the climatic conditions are favorable

and proved to be effective and reliable against a number of soil pests including *R. necatrix* (Sztejnberg *et al*., 1987). The physical control provided a good control of disease, which didn't effect the environment. However, the physical control consumes high costs, high initial investment and energy consumption.

1.3.2 Chemical control

Several chemicals have shown high in vitro efficacy against *R. necatrix* and among these carbendazim (Gupta, 1977), benomyl and thiabendazol (Behdad, 1976) stand out for their inhibitory effect. Field trials to control *R. necatrix* are more limited and provided more variable results. Benomyl and thiophanatemethyl were highly effective in controlling the disease in apple trees when they were used in winter rather than in spring, and also when they were used as a preventive treatment on healthy trees close to diseased loquat trees (Teixeira de Sousa, 1985). A detailed list of chemicals including antibiotics tested against *R. necatrix* is reported by Ten Hoopen and Krauss (2006). However, most of them have not been utilised in field trials or provided inconsistent levels of protection or, finally, are not practically relevant, since their use is not permitted by national specific legislations. Many fungicides/chemicals have been used to control *R. necatrix*. but the residual of the chemicals may cross contaminate in the environment and may cause mutation in the fungus. So the use of biological control was established.

1.3.3 Biological control

There are many organisms that were studied for use as a biological control agent in *R. necatrix*. Fungal genus *Trichoderma* received high attention. *Trichoderma harzianum* and *T. hamatum* were assayed at different dosages of inocula in soils of apple orchards, which were artificially or naturally infested by *R. necatrix* (Freeman *et al.,* 1986).
Mendoza *et al.*, (2003) showed that mixtures of *Clonostachys* and *Trichoderma* can be effective against *Rosellinia bunodes* in the greenhouse. Not only fungal genus but several bacterial species isolated from soil and rhizosphere have also been investigated as biocontrol agents against *R. necatrix* (Cazorla-López *et al*., 2001; González-Sánchez

et al., 2004). Species of *Agrobacterium* and *Pseudomonas* showed a strong antagonistic effect against *R. necatrix* and were able to colonize and survive on tree roots (Yasuda & Katoh, 1989). However, the effectiveness depended on soil pH, natural inoculum, levels of the pathogen, sensitivity to different temperatures and the amount of soil organic matter. The success of using mycovirus, Cryphonectria parasitica hypovirus 1 (CHV1) as a biocontrol agent against chestnut blight in Europe inspired many group of researchers to conduct work on *R. necatrix* that might contain mycoviruses.

1.4 *R. necatrix* and mycoviruses

Mycoviruses (fungal viruses) are reviewed with importance on plant pathogenic fungi. The 8th ICTV report on virus taxonomy (Fauquet *et al*., 2005) with lists of over 90 mycovirus species that have been recognized from ten virus families. Studies of mycoviruses in *R. necatrix* started at the prospect of virocontrol (biological control using viruses, Ghabrial and Suzuki (2009)). Arakawa *et. al*. (2001) reported the double-stranded (ds)RNA of various types were detected in 65 out of 298 isolates (21.8%) from hyphae of *R. necatrix*. Arakawa *et. al*. (2001) also reported that dsRNAs having the same profiles were restricted to isolates of the same mycelial compatibility groups (MCG) from the same trees, with an exception where different profiles were detected in different isolates of the same MCGs. There were 45 distinct dsRNA profiles in the 65 isolates: they varied in the number of electrophoretic bands from 1 to 12 and in size from less than 1000 bp to more than 10kbp. Molecular characterization of these viruses revealed that *R. necatrix* is a natural host of at least 5 mycovirus families including *Partitiviridae* (Chiba *et. al.*, 2012; Sasaki *et.al*., 2005), *Quadriviridae* (Lin *et. al*., 2012 and 2013), *Reoviridae* (Wei *et. al*., 2003), *Totiviridae* (Yaegashi *et. al*., 2012) and *Megabirnaviridae* (Chiba et. al., 2009). Mostly mycoviruses infecting *R. necatrix* seem to be cryptic (non-symptomatic) species except for *Reoviridae* and *Megabirnaviridae.*

Under natural condition mycoviruses rely on their fungal host for intracellular transmission (Buck, 1998) that occurs in two ways, horizontally via protoplasmic fusion and vertically by sporulation. Horizontal transmission of mycoviruses between different fungal strains via hyphal anastomosis is a well-established phenomenon and has been

used to transmit mycoviruses experimentally (Suzuki *et al*., 2005; Xie *et al*., 2006). Anastomosis occurs when hyphae from different fungal individuals fuse together and genetic and cytoplasmic exchange occurs. Mycoviruses exist within the cytoplasm, and are therefore included in this exchange. Successful anastomosis relies on the two fungi being vegetatively compatible, i.e. in the same vegetative compatibility group (VCG). In ascomycete fungi, this process is controlled by a series of gene loci, variously known as *vic* (vegetative incompatibility) or *het* (heterokaryon incompatibility) loci (Glass and Dementhon, 2006; Saupe, 2000). Vertical transmission from the fungal mycelium to spores is a primary means of mycovirus spread, although observed rates vary greatly for different fungus/virus combinations and for different spore types (sexual vs. asexual) of the same fungus. Asexual spores are produced from modified hyphae and mycoviruses are readily transmitted to these spores through the cytoplasm as the spores develop (Buck, 1998). Some authors have concluded that virus transmission through sexual spores is less common and that infection rates are usually lower for those fungi whose sexual stage occurs frequently in the life cycle (Varga *et al*., 2003).

Irregular distribution of viruses within isolates of the same MCGs seems to be unique to *R. necatrix*. In the former, all or a part of the dsRNA segments could have been eliminated on isolation or through transfer. DsRNA is considered to have coexisted in the fungal cytoplasm through the process of speciation of hosts (Ghabrial 1998), but host– dsRNA interaction in *R. necatrix* is considered to be incompatible in most cases. For example, vertical transmission of dsRNA into ascospores is unlikely to occur, and consequently sexual reproduction is effective to remove dsRNA in *R. necatrix*. In conclusion, host–dsRNA interaction is not stable in *R. necatrix*, and mechanisms of dsRNA infection and removal may operate in nature (Arakawa *et. al*., 2001)

1.5 Expansion of host range of *R. necatrix* infected virus

The natural host range of mycoviruses is thought to be limited to the same or closely related vegetative compatibility groups that allow lateral transmission. The finding that closely related mitoviruses (>90% sequence identity) were isolated from two taxonomically distinct fungal hosts, *Sclerotinia homoeocarpa* and *Ophiostoma novo-*

ulmi, raises interesting questions regarding potential occurrence of natural vectors and/or unknown modes for horizontal transmission (Deng *et al*., 2003). Experimental host ranges for fungal viruses are essentially nonexistent because of lack of suitable infectivity assays. Expanding the experimental host range of mycoviruses and hypovirulence factors increases the potential to study biocontrol of fungal diseases, virus–host interactions and may serve as virocontrol agents. The term "virocontrol" is defined as one form of biological control that uses viruses capable of infection and compromises organisms that are pathogens of useful organisms, such as crops and livestock (Ghabrial and Suzuki, 2009). If mycoviruses can be introduced into a wide range of phytopathogenic fungi to reduce virulence, mycoviruses should have great potential as virocontrol agents.

1.6 Virus genome rearrangement

Virus genomes are highly streamlined. Compared with more complex organisms, viruses tend to have small genomes with a high percentage of coding sequences, none or little intronic sequences, and only short stretches of intergenic sequences (Lynch, 2006; Belshaw *et al*., 2007). Moreover, viruses have evolved strategies to further compress their genomes, such as frameshifts and overlapping open reading frames (ORFs) (e.g., Belshaw *et al*., 2007; Chung *et al*., 2008). The studies on the evolution of RNA viruses have revealed that RNA recombination is a widespread phenomenon that has shaped modern viruses by rearranging viral genomes or disseminating functional modules among different viruses (Strauss and Strauss, 1988; Dolja and Carrington, 1992; Lai, 1992; Simon and Bujarski, 1994). In addition, an important short-term function of genetic recombination may be the rescue of functional sequences from mutated parental molecules, which is of particular significance given the high mutation rates associated with replication by RNA-dependent RNA polymerases (RdRp) (Domingo *et al*., 1996). There are still many questions to be addressed; that is, known about which host factors interact with viral factors, at which steps those events occur. Faruk *et al*., 2008 developed a genetic screen protocol and they reported that characterization of a mutant *C. parasitica* strain shows usually altered symptoms upon infection with hypovirus.

Kanematsu *et al*., (2004) discovered a mutant of *R. necatrix* MyRV3 lacking of segment 8 during sub cultured and remained stable after more than 10 subcultures. Small remnants of the S8 dsRNA were not detected.

1.7 Objectives of the study

The aim of this study is to characterize molecularly and biologically a novel mycovirus, Rosellinia megabirnavirus 1 (RnMBV1)-W779 detected in a *R. necatrix* field isolate from Japan. Specifically, this study involves the determination of full-length nucleotide sequence, phylogenetic analyses, phenotype analysis to investigate possible association of the virus with hypovirulence of its fungal host and the ability of this virus to be used as biological control agent. In addition, this study was designed to extend the host range of this novel virus in an experimental host, *Cryphonectria parasitica* whose merits lie in the availability of its genome sequence, RNA-silencing mutants, artificial inoculation, among others that makes it amenable to determine virus-host, virus-virus interaction of the novel virus. These advantages allowed to perform its phenotypic characterization, and explore expression strategy and occurrence of rearranged segment in the new experimental host.

	agarose gel in TAE buffer, and excised the band of dsRNAS1a and -S1b from the gel. Eluted dsRNA was used as template. Primers used for RT-PCR are denoted above line, and their positions are indicated in Fig. 3. Primer sequences are listed in Table 5.	
16	Genome organization of dsRNAS1a and -S1b compared with the genome of wild type RnMBV1. Open boxes indicate ORFs, and the numbers above refer to map positions of the initiation and terminal codons of the respective ORFs. Red and blue double lines indicate the rearranged segments of dsRNAS1a and -S1b, and dotted lines indicate deletions in the rearranged segments. The sequences around the junction sites are at the bottom. Arrow heads indicate the RT-PCR primer positions in Fig. 16 and the probe position for the northern analyses in Fig. 12 and Fig. 17.	106
17	Fungal strains used in the analyses were: lane1, W97/RnMBV1; lane2, W97/RnMBV1-RS1a+RS1b; lane3, W97/RnMBV1-RS1b; lane4, W97/RnMBV1-RS1a+RS1b, lane5, W370T1/RnMBV1; Lane6, W370T1/RnMBV1-RS1a; lane7, W370T1/RnMBV1-RS1b. (A) Northern blot analyses of the genome segments in RnMBV1-R. The same amount of genomic dsRNA segments as shown in Fig. 8. were separated in denatured agarose gel and capillary transferred to Hybond N+ membrane. The membrane was probed with the DIG-labeled probes specific to ORF2 (RDRP) in dsRNA1 (the upper picture) and ORF3 in dsRNA2 (the below picture). The position of the probes was denoted in the Fig. 17. (B) RT-PCR analysis of dsRNAs extracted from mycelia. Specific primers for ORF1 and ORF3 were used for RT-PCR. Primer sequences are listed in Table 5.	107
18	Detection of genome and protein products of wild-type RnMBV1 and RnMBV1-RS1 in mycelia of *R. necatrix*. The fungal strains used were W97/RnMBV1 (lane 1), W97/RnMBV1-RS1a+S1b, -RS1b, RS1a+S1b (lanes 2 to 4), W370T1/ RnMBV1 (lane5), W370T1/RnMBV1-RS1a, -RS1b, (lanes 6, 7), and virus-free strains W97 and W370T1. (A) Agarose gel electrophoresis of 1.5 mg total RNA in 8 days mycelial culture on PDA with cellophane. (C) Western blot	108

Chapter 1. General Introduction

1.1 Background and history of white root rot disease

Rosellinia necatrix (Hart.) Berl. Prill. is a phytopathogenic ascomycete fungus, which causes white root rot disease on a broad range of commercial crops such as apple, grape vine, pear, plum, poplar and walnut (Whalley, 1996). Arakawa *et al*. (2002) reported more than 197 different hosts of this fungus. There is a little information about the origin of *R. necatrix* and it has been argued that there is a possibility that, in some countries, it could have been introduced on infected material from the tropical and subtropital areas (Thomas *et al.,* 1953; Mantell and Wheeler, 1973 cited in Pérez-Jiménez, 2006). It has been known to occur in Europe since the middle of 19th century (Viala, 1891 cited in Pérez-Jiménez, 2006). The pathogen is a limiting factor in apple and vineyard orchards in France, Portugal and many other European countries (Teixeira de Sousa *et al*., 1995). Teixeira de Sousa *et al*. (1995) reported that in Alcobaça region (Portugal) 42% of the orchards were infected by *R. necatrix* and 14% of the apple trees exhibited advanced disease symptoms. In Italy the fungus represents one of the most dangerous pathogens of root-rot in poplar (Anselmi & Giorcelli, 1990a) and is widely diffused on fruit trees like sweet cherry, almond, peach, olive and grapevine. In Asia, the disease is very common in Japan on a variety of hosts. It causes particular damage on tea bushes and is considered one of the most serious pathogens of fruit trees such as grapevine (Kanadani, Date & Nasu, 1998), orchards (Behdad, 1976), Japanese pear and apple (Arakawa *et al.*, 2002). In Taiwan, it is a problem on loquats (Lin and Duan, 1988; Duan *et al*., 1990). On the other side of the Asiatic continent, it is also very common in Iran (Behdad, 1976) mostly on apple trees, sour cherry trees and poplars.

Sztejnberg and Madar (1980) found that the fungus attacked and killed artificially inoculated deciduous trees (apple, pear, plum, almond), olive trees, citrus rootstocks, grape rootstocks, avocado, mango, macadamia, field crops (cotton, alfalfa, bean) and weeds. The same authors suggested that weeds like *Prosopis farcta* , *Aechmea gracilis* and *Conyza bonariensis* could promote the disease spreading.

1.2 Biology and symptoms of *R. necatrix*

1.2.1 Biology of *R. necatrix*

The fungal pathogen *R. necatrix* belongs to the family Xylariaceae, phylum Ascomycetes, which includes more than one hundred species (Petrini, 1993). *R. necatrix* produces both asexually and sexually. There are three different spore types (chlamidospores, conidiospores and ascospores). Chlamidospores, a thick-walled asexual fungal spore that is derived from a hyphal cell and can function as a resting spore, can be found under exceptional environmental conditions. They are formed from pyriform swelling in which protoplasm is condensed and a wall is formed that divides the spherical zone from the remaining hypha. They are spherical of approximately 15 μm in diameter. Conidiospores (asexual) originate at synnemata conidiogenous cells. The length of conidiospores are 3-5 μm long and 2.3-3 μm wide (Petrini, 1993). The conidiospore germination is very difficult to introduce *in vitro*. Ascospores (sexual) are formed inside the perithecium and when they reach maturity are expelled in a mucilaginous mass from the pore or papilla located on the top of the perithecium. They are ellipsoidal and cymbiform (boat-shaped) and their size vary between 36-46 μm in length and 5.5-6.3 μm in width (Petrini, 1993; Sivanesan, 1985).

Aimi *et. al.* (2002) reported genetic differences among single ascospore culture isolated from the same perithecium. Pérez-Jiménez et. al. (2002) revealed the existence of high genetic diversity in this fungus. Based on this results, the life cycle of *R. necatrix* appears to be heterothallic. Aimi *et al.* (2002) using molecular biological methods estimated the number of chromosome of field isolates and single ascospore isolate as about seven. It means normal heterokaryon formation does not occur in *R. necatrix*. The causal fungus rarely produces teleomorph, the sexual reproductive stage, on diseased plants in nature (Teixeira de Sousa, 1993).

1.2.2 Symptoms of *R. necatrix*

The fungus invades the root system of a tree by white mycelial fans. Infection by the

pathogen causes wilting, chlorosis and defoliation and under conducive environmental conditions it may result in rapid death of a tree. *R. necatrix* spreads from an infected tree by mycelia aggregates or strands which grow through soil and may contact root of so far healthy tree. On trees, *R. necatrix* causes a root and collar rot. Both the physical destruction of the root system and the transport of phytotoxins by the sap quickly provoke symptoms on the aerial parts which include slowing down of growth, small size, discoloration and wilting of the leaves, and general dieback of the tree with death of the extremities of the twigs. According to the nature and age of the tree, disease development can be slow, death occurs after several years of decline, or very rapid, sudden wilting occurs following a period of drought or the first onset of fruiting.

1.3 Control strategies of *R. necatrix*

Various strategies have been used to reduce the impact of *R. necarix*. However, control of the white root rot is complicated by its resistance to drought, tolerance to a wide range of soil pH, high number of hosts, penetration deep into the soil and resistance to various common fungicides (Khan, 1959 cited in Schena *et al*., 2003). Control strategies in the fields should be based on the avoidance of the pathogen through the utilization of certified healthy propagating materials; however, once introduced in the field control strategies should be directed to the management of the disease rather than to the pathogen eradication, which is very difficult and too expensive to be economically justifiable.

1.3.1 Physical Control

There are many strategies for physical control of *R. necatrix.* For example, the steam soil (Runia, 2000) which has been proposed as a valid control strategy to devitalize a number of soil borne pathogens. The use of a hot-water for treatment of *Cyperus esculentus* L. tubers was studied as a control strategy to prevent the spread of *R. necatrix* through infected tubers (García-Jiménez *et al*., 2004). Soil solarization has been largely exploited all over the world wherever the climatic conditions are favorable

and proved to be effective and reliable against a number of soil pests including *R. necatrix* (Sztejnberg *et al*., 1987). The physical control provided a good control of disease, which didn't effect the environment. However, the physical control consumes high costs, high initial investment and energy consumption.

1.3.2 Chemical control

Several chemicals have shown high in vitro efficacy against *R. necatrix* and among these carbendazim (Gupta, 1977), benomyl and thiabendazol (Behdad, 1976) stand out for their inhibitory effect. Field trials to control *R. necatrix* are more limited and provided more variable results. Benomyl and thiophanatemethyl were highly effective in controlling the disease in apple trees when they were used in winter rather than in spring, and also when they were used as a preventive treatment on healthy trees close to diseased loquat trees (Teixeira de Sousa, 1985). A detailed list of chemicals including antibiotics tested against *R. necatrix* is reported by Ten Hoopen and Krauss (2006). However, most of them have not been utilised in field trials or provided inconsistent levels of protection or, finally, are not practically relevant, since their use is not permitted by national specific legislations. Many fungicides/chemicals have been used to control *R. necatrix*. but the residual of the chemicals may cross contaminate in the environment and may cause mutation in the fungus. So the use of biological control was established.

1.3.3 Biological control

There are many organisms that were studied for use as a biological control agent in *R. necatrix*. Fungal genus *Trichoderma* received high attention. *Trichoderma harzianum* and *T. hamatum* were assayed at different dosages of inocula in soils of apple orchards, which were artificially or naturally infested by *R. necatrix* (Freeman *et al.,* 1986).
Mendoza *et al.*, (2003) showed that mixtures of *Clonostachys* and *Trichoderma* can be effective against *Rosellinia bunodes* in the greenhouse. Not only fungal genus but several bacterial species isolated from soil and rhizosphere have also been investigated as biocontrol agents against *R. necatrix* (Cazorla-López *et al*., 2001; González-Sánchez

et al., 2004). Species of *Agrobacterium* and *Pseudomonas* showed a strong antagonistic effect against *R. necatrix* and were able to colonize and survive on tree roots (Yasuda & Katoh, 1989). However, the effectiveness depended on soil pH, natural inoculum, levels of the pathogen, sensitivity to different temperatures and the amount of soil organic matter. The success of using mycovirus, Cryphonectria parasitica hypovirus 1 (CHV1) as a biocontrol agent against chestnut blight in Europe inspired many group of researchers to conduct work on *R. necatrix* that might contain mycoviruses.

1.4 *R. necatrix* and mycoviruses

Mycoviruses (fungal viruses) are reviewed with importance on plant pathogenic fungi. The 8th ICTV report on virus taxonomy (Fauquet *et al*., 2005) with lists of over 90 mycovirus species that have been recognized from ten virus families. Studies of mycoviruses in *R. necatrix* started at the prospect of virocontrol (biological control using viruses, Ghabrial and Suzuki (2009)). Arakawa *et. al*. (2001) reported the double-stranded (ds)RNA of various types were detected in 65 out of 298 isolates (21.8%) from hyphae of *R. necatrix*. Arakawa *et. al*. (2001) also reported that dsRNAs having the same profiles were restricted to isolates of the same mycelial compatibility groups (MCG) from the same trees, with an exception where different profiles were detected in different isolates of the same MCGs. There were 45 distinct dsRNA profiles in the 65 isolates: they varied in the number of electrophoretic bands from 1 to 12 and in size from less than 1000 bp to more than 10kbp. Molecular characterization of these viruses revealed that *R. necatrix* is a natural host of at least 5 mycovirus families including *Partitiviridae* (Chiba *et. al.*, 2012; Sasaki *et.al*., 2005), *Quadriviridae* (Lin *et. al*., 2012 and 2013), *Reoviridae* (Wei *et. al*., 2003), *Totiviridae* (Yaegashi *et. al*., 2012) and *Megabirnaviridae* (Chiba et. al., 2009). Mostly mycoviruses infecting *R. necatrix* seem to be cryptic (non-symptomatic) species except for *Reoviridae* and *Megabirnaviridae.*

Under natural condition mycoviruses rely on their fungal host for intracellular transmission (Buck, 1998) that occurs in two ways, horizontally via protoplasmic fusion and vertically by sporulation. Horizontal transmission of mycoviruses between different fungal strains via hyphal anastomosis is a well-established phenomenon and has been

used to transmit mycoviruses experimentally (Suzuki *et al*., 2005; Xie *et al*., 2006). Anastomosis occurs when hyphae from different fungal individuals fuse together and genetic and cytoplasmic exchange occurs. Mycoviruses exist within the cytoplasm, and are therefore included in this exchange. Successful anastomosis relies on the two fungi being vegetatively compatible, i.e. in the same vegetative compatibility group (VCG). In ascomycete fungi, this process is controlled by a series of gene loci, variously known as *vic* (vegetative incompatibility) or *het* (heterokaryon incompatibility) loci (Glass and Dementhon, 2006; Saupe, 2000). Vertical transmission from the fungal mycelium to spores is a primary means of mycovirus spread, although observed rates vary greatly for different fungus/virus combinations and for different spore types (sexual vs. asexual) of the same fungus. Asexual spores are produced from modified hyphae and mycoviruses are readily transmitted to these spores through the cytoplasm as the spores develop (Buck, 1998). Some authors have concluded that virus transmission through sexual spores is less common and that infection rates are usually lower for those fungi whose sexual stage occurs frequently in the life cycle (Varga *et al*., 2003).

Irregular distribution of viruses within isolates of the same MCGs seems to be unique to *R. necatrix*. In the former, all or a part of the dsRNA segments could have been eliminated on isolation or through transfer. DsRNA is considered to have coexisted in the fungal cytoplasm through the process of speciation of hosts (Ghabrial 1998), but host– dsRNA interaction in *R. necatrix* is considered to be incompatible in most cases. For example, vertical transmission of dsRNA into ascospores is unlikely to occur, and consequently sexual reproduction is effective to remove dsRNA in *R. necatrix*. In conclusion, host–dsRNA interaction is not stable in *R. necatrix*, and mechanisms of dsRNA infection and removal may operate in nature (Arakawa *et. al*., 2001)

1.5 Expansion of host range of *R. necatrix* infected virus

The natural host range of mycoviruses is thought to be limited to the same or closely related vegetative compatibility groups that allow lateral transmission. The finding that closely related mitoviruses (>90% sequence identity) were isolated from two taxonomically distinct fungal hosts, *Sclerotinia homoeocarpa* and *Ophiostoma novo-*

ulmi, raises interesting questions regarding potential occurrence of natural vectors and/or unknown modes for horizontal transmission (Deng *et al*., 2003). Experimental host ranges for fungal viruses are essentially nonexistent because of lack of suitable infectivity assays. Expanding the experimental host range of mycoviruses and hypovirulence factors increases the potential to study biocontrol of fungal diseases, virus–host interactions and may serve as virocontrol agents. The term "virocontrol" is defined as one form of biological control that uses viruses capable of infection and compromises organisms that are pathogens of useful organisms, such as crops and livestock (Ghabrial and Suzuki, 2009). If mycoviruses can be introduced into a wide range of phytopathogenic fungi to reduce virulence, mycoviruses should have great potential as virocontrol agents.

1.6 Virus genome rearrangement

Virus genomes are highly streamlined. Compared with more complex organisms, viruses tend to have small genomes with a high percentage of coding sequences, none or little intronic sequences, and only short stretches of intergenic sequences (Lynch, 2006; Belshaw *et al*., 2007). Moreover, viruses have evolved strategies to further compress their genomes, such as frameshifts and overlapping open reading frames (ORFs) (e.g., Belshaw *et al*., 2007; Chung *et al*., 2008). The studies on the evolution of RNA viruses have revealed that RNA recombination is a widespread phenomenon that has shaped modern viruses by rearranging viral genomes or disseminating functional modules among different viruses (Strauss and Strauss, 1988; Dolja and Carrington, 1992; Lai, 1992; Simon and Bujarski, 1994). In addition, an important short-term function of genetic recombination may be the rescue of functional sequences from mutated parental molecules, which is of particular significance given the high mutation rates associated with replication by RNA-dependent RNA polymerases (RdRp) (Domingo *et al*., 1996). There are still many questions to be addressed; that is, known about which host factors interact with viral factors, at which steps those events occur. Faruk *et al*., 2008 developed a genetic screen protocol and they reported that characterization of a mutant *C. parasitica* strain shows usually altered symptoms upon infection with hypovirus.

Kanematsu *et al*., (2004) discovered a mutant of *R. necatrix* MyRV3 lacking of segment 8 during sub cultured and remained stable after more than 10 subcultures. Small remnants of the S8 dsRNA were not detected.

1.7 Objectives of the study

The aim of this study is to characterize molecularly and biologically a novel mycovirus, Rosellinia megabirnavirus 1 (RnMBV1)-W779 detected in a *R. necatrix* field isolate from Japan. Specifically, this study involves the determination of full-length nucleotide sequence, phylogenetic analyses, phenotype analysis to investigate possible association of the virus with hypovirulence of its fungal host and the ability of this virus to be used as biological control agent. In addition, this study was designed to extend the host range of this novel virus in an experimental host, *Cryphonectria parasitica* whose merits lie in the availability of its genome sequence, RNA-silencing mutants, artificial inoculation, among others that makes it amenable to determine virus-host, virus-virus interaction of the novel virus. These advantages allowed to perform its phenotypic characterization, and explore expression strategy and occurrence of rearranged segment in the new experimental host.

Chapter 2. A novel bipartite dsRNA mycovirus from the white root rot fungus *Rosellinia necatrix*: Molecular and biological characterization, taxonomic considerations, and potential for biological control

2.1 Introduction

Viruses are found ubiquitously in major groups of filamentous fungi (Nuss, 2005), and an increasing number of novel mycoviruses are being reported (Aoki *et al*., 2009 and Liu *et al*., 2009). Mycoviruses with RNA genomes are now classified into 9 families, of which 4 accommodate dsRNA viruses and the remaining 5 families comprise ssRNA viruses (Ghabrial & Suzuki, 2009). While many ssRNA mycoviruses like hypoviruses and endornaviruses do not produce particles, dsRNA virus genomes, whether undivided (the family *Totiviridae*) or divided (Chen *et al*., 1994; Choi & Nuss, 1992) segments for the family *Reoviridae*, 4 segments for the *Chrysoviridae* and 2 segments for the *Partitiviridae*, are encapsidated in rigid particles. Most mycoviruses are considered to cause cryptic infections, while some cause phenotypic alterations that include hypovirulence and debilitation. However, the lack of artificial introduction methods for most mycoviruses has greatly hampered progress in exploring mycovirus/host interactions (Ghabrial & Suzuki, 2009; Nuss, 2005). Thus, virus etiology of altered fungal phenotypes was established only for a limited number of examples including the hypovirus/*C. parasitica* and mycoreovirus/*C. parasitica*.

White root rot is one of the most devastating diseases of perennial crops worldwide, 68 particularly highly valued fruits in Japan like apple, Japanese pear, and grapevine. The causal fungus, *Rosellinia necatrix*, is an ascomycete with a wide range of host plants over 197 species spanning 50 families (Ito & Nakamura, 1984), and is difficult to control by conventional methods, as is often the case for soil-borne pathogens. Fungicide application, though may be effective, is labor-intensive and raises environmental concerns, while cultural practices may not be effective. Successful biocontrol in Europe of the chestnut blight disease using hypovirulent strains

(Heiniger & Rigling, 1994; Milgroom & Cortesi, 2004) inspired a group of Japanese researchers to conduct an extensive search of a large collection of over 1,000 field fungal isolates for mycoviruses that might serve as virocontrol agents. Virocontrol or virological control refers to one form of biological control utilizing viruses that infect organisms pathogenic to useful organisms (Ghabrial & Suzuki, 2009). Approximately 20% of the collected isolates of *R. necatrix* were found to be dsRNA-positive and presumed to be infected by mycoviruses (Arakawa *et al*., 2002; Ikeda *et al*., 2004). Agarose gel profiles of dsRNAs suggested infections by members in the families *Totiviridae*, *Partitiviridae*, *Reoviridae*, and *Chrysoviridae* as well as unassigned viruses (S. Kanematsu & A. Sasaki, unpublished results). Among those dsRNAs, the genomic segments of *Mycoreovirus 3* (MyRV3) (Wei *et al*., 2004), and *Rosellinia necatrix partitivirus 1* (RnPV1) (Sasaki *et al*., 2005) were well characterized. However, many of other dsRNAs remain uncharacterzied.

Artificial virion introduction protocols, which are often unavailable for mycoviruses, have been developed for specific viruses infecting the white root rot fungus. Using a PEG-mediated method as established for MyRV1 and MyRV2 infecting *C. parasitaca* (Hillman & Suzuki, 2004; Hillmam *et al*., 2004), RnPV1 and MyRV3 were shown to be infectious as particles (Sasaki *et al*., 2007; Sakaki *et al*., 2006). Subsequently, the cause-effect relationship was established: MyRV3 was demonstrated to confer hypovirulence (attenuated virulence) to an isogenic and a few vegetatively incompatible virulent strains of *R. necatrix* (Kanematsu *et al*., 2004; Sasaki *et al*., 2007), while RnPV1 was shown to be associated with symptomless infection. Protoplast fusion is also available for introduction of partitiviruses and uncharacterized viruses into recipient fungal strains that are vegetatively incompatible with virus-containing ones (A. Sasaki, unpublished results). Furthermore, DNA tranformation systems are available for foreign gene expression in *R. necatrix* (Kanematsu *et al*., 2004; Pliego *et al*., 2009). These technical advances have made the *R. necatrix*/mycovirus systems attractive for studies of virus/host interactions and virocontrol (Ghabrial & Suzuki, 2009; Matsumoto, 1998).

2.2 Materials and Methods

2.2.1 Fungal isolates and culturing

The *R. necatrix* W779 strain was isolated by the baiting method using mulberry twigs from the soil of Japanese pear orchard infested with white root rot in Ibaraki prefecture (Ikeda *et al*., 2004). Although asexual sporulation is often used to obtain virus-free isolates for filamentous fungi, asexual spores of *R. necatrix* are known to germinate but never develop into mycelia under laboratory conditions (Nakamura *et al*., 2002). Thus, an isogenic virus (dsRNA)-free strain W1015 was prepared from spheroplasts of W779 and used as a reference strain. Two virus-free fungal strains W97 and W370T1 were previously described (Kanematsu *et al*., 2004; Sasaki *et al*., 2007) and used in transfection with W779 virus particles. Strains W779, W97, and W370T1 are vegetatively incompatible with each other and belong to different mycelial compatibility groups (MCGs), MCG351, MCG80, and MCG139, respectively (Arakawa *et al*., 2002, Ikeda *et al*., 2005). All strains were cultured at 25ºC on DifcoTM potato dextrose agar (PDA) (Becton Dickinson, Sparks, MD, USA) or in DifcoTM potato dextrose broth (PDB) in the dark, and kept at 5ºC until used.

2.2.2 DsRNA isolation and cDNA library construction

Double-stranded RNA was extracted as described by Sun and Suzuki (Sun & Suzuki, 2008). W779 was cultured for 10 days in PDB at room temperature. Mycelia were homogenized in liquid nitrogen. Nucleic acid fractions were obtained by treatments with phenol, phenol/chloroform, and chloroform. This was followed by digestion with S1 nuclease and subsequently with DNase I, as described by Suzuki *et al*. (Suzuki *et al*., 2003). Double-stranded RNA was further purified by CC41 cellulose column chromatography. A cDNA library of total dsRNA and L1 dsRNA was constructed using a classic non-PCR based method to minimize misincorporations during cDNA synthesis (Hillman *et al*., 2004). After denaturation at 65ºC in 90% dimethyl sulfoxide (DMSO) (Asamizu *et al*., 1985), dsRNA was used as a template for cDNA synthesis with random hexamers using a TimeSaverTM cDNA synthesis kit (Amersham). The resulting cDNA was cloned into the vector pGEM-T Easy (Promega) following

addition of an A by Taq polymerase, and used for transformation of *Escherichia coli* strain DH5α.

2.2.3 Terminal sequence determination

Two methods were used to determine the terminal sequences of the genome segments. A classic 5'-RACE (rapid amplification of cDNA ends) protocol using terminal deoxynucleotidyl transferase, was performed as described by Suzuki *et al*. (Suzuki *et al*., 2003). Approximately 20 ng of purified dsRNA along with specific primers denatured by the DMSO method was reverse-transcribed in a reaction mixture, 50 mM Tris-HCl, pH 8.3, 50 mM KCl, 4 mM MgCl2, 10 mM DTT, 40 units of MMLV reverse transcriptase (Fermentas), and 20 units of RNase inhibitor (Toyobo, Osaka, Japan). Primers used for the respective dsRNA segments were SC1 and SC2 for L1 and SC3 and SC4 for L2 (Table 1 for primers' sequences). After d(C) tailing, cDNA products were used as template with the 5' abridged anchor primer and a nested specific primer. For RNA ligase mediated RACE (RLM-RACE) (Suzuki *et al*., 2004), 5'-phosphorylated oligodeoxynucleotide (5'-PO_4 CAATACCTTCTGACCATGCGT GACAGTCAGCATG-3') (3' RACE-adaptor) was ligated to each of the 3'-termini of the L1 and L2 segments (single stranded form) with T4 RNA ligase at 16ºC for 16 h. Ligated DNA-RNA strands were denatured in 90% DMSO together with an oligonucleotide 3' RACE-1st (Table 1) as described above, and used as templates for cDNA synthesis. 3' RACE-1st is complementary to the 3'-half of the 3' RACE-adaptor. The resulting cDNA was amplified by PCR with the primer set, 3' RACE-2nd (Table 1) complementary to the 5'-half of 3' RACE-adaptor and gene specific primers (GSP). Four PCR reactions were set for the plus- and minus sense strands of L1 and L2. Amplified DNA fragments were cloned into pGEM-T Easy for sequence analysis.

2.2.4 Sequencing and sequence analysis

Plasmid DNA was prepared by spin columns (LaboPass Mini, Hokkaido System Science, Sapporo) and sent to Macrogen Japan, Inc., (Tokyo) for sequencing. Sequences were analyzed using the Genetyx DNA-processing software (SDC, Tokyo). Database searches were performed with the BLAST program (Altschul *et al*., 1997) at http://www.ncbi.nlm.nih.gov/ provided by from National Center for

Biotechnology Information (NCBI), and with the FASTA 3 program (Pearson & Lipman, 1988) at http://www.ddbj.nig.ac.jp/Welcome-j.html from DNA Data Bank of Japan (DDBJ). Motif searches were carried against the Pfam database at http://pfam.sanger.ac.uk/ (Finn *et al*., 2008) and PROSITE database at http://www.expasy.ch/. Multiple sequence alignments and phylogenetic trees were constructed using the Clustal X program (Thompson *et al*., 1997). RNA structures and motifs were analyzed at http://www.bioinfo.rpi.edu/applications/mfold/ and http://wilab.inha.ac.kr/fsfinder2/ using the Mfold (version 3.2) (Zuker, 2003), and FSFinder programs (Byun *et al*., 2007), respectively.

2.2.5 RNA preparation and RNA blot analysis

Total nucleic acid preparations were obtained by the method of Suzuki and Nuss (Suzuki & Nuss, 2002). Northern blot analysis of total RNA isolated as above was as described by Suzuki et al. (Suzuki *et al*., 2003). RNA was separated by electrophoresis in 1.0% agarose gels under denaturing conditions and capillary-transferred onto Hybond-N+ nylon membrane (Amersham Biosciences, Buckingham, England). Probes were Dioxigenin (DIG)-11-dUTP-labeled DNA fragments amplified by PCR according to the method recommended by the manufacturer (Roche Diagnostics, Mannheim). Chemiluminescent signals of probe-RNA hybrids were detected using a DIG detection kit and a CDP star kit (Roche).

2.2.6 Purification of virus particles

The fungal strain W779 was grown in PDB or cellophane-PDA for 10 days. Mycelia (approximately 30 g, wet weight, for PDB cultures and 10 g for cellophane-PDA cultures) were harvested and ground to powder in the presence of liquid nitrogen. The homogenates were mixed with 150 ml of 0.1 M sodium-phosphate, pH 7.0 using a Warning blender, and clarified twice with CCl4 for PDB culture or 13% Vertrel XF (Du Pont-Mitsui Fluorochemicals Co., Tokyo) for PDA-cellophane cultures. NaCl and PEG 6000 were added to final concentration of 1% and 8%, respectively for PDB culture. After being stirred for 3 h at 4ºC, the suspension was centrifuged at 16, 000 x g for 20 min. Resultant pellets suspended in 10 ml of 0.05 M sodium-phosphate buffer, pH 7.0 were centrifuged at 7,000 x g for 20 min. Centrifugation at 119,000 x g for 2 hour was substituted for the precipitation by PEG-NaCl, when cellophane-PDA

cultures were used. The supernatant was re-centrifuged through a 20% sucrose cushion (3 ml) in a Beckman SW41Ti rotor at 80, 000 x g for 2 h. The pellet was suspended in 1 ml 0.05 M Na-phosphate. After centrifugation at 7, 000 rpm for 5 min, the supernatant was fractionated through a 10-40% sucrose gradient by centrifugation at 70, 000 x g for 2 h. Fractions at the middle portion subjected to measurement of UV absorbance and ultracentrifugation. Recovered virus particles were resuspended in 100 µl of 0.05 M sodium-phosphate buffer, pH 7.0.

2.2.7 Peptide mass fingerprinting (PMF)

Protein preparation was according to the protocol recommended by the manufacturer (Bruker Daltonics) based on the method of Charoenpanich et al. (Charoenpanich *et al*., 2006). Purified virus preparations were electrophoresed in a preparative SDS-polyacrylamide (10%) gel. The major coat protein band of 135 kDa, stained by Coomassie Brilliant Blue, was excised, decolorized, and treated with DTT to break disulfide bonds, followed by carboxymethylation of cysteine residues with iodoacetoamide. Modified protein was subjected to in-gel digestion with trypsin (sequencing grade for HPLC, Promega), elution in acetonitrile-trifluoroacetic acid solution (ACN-TFA), and desalting by Zip-Tips (Clean up C18 pipette tips, Millipore). After re-dissolved in ACN-TFA, cleaved peptides were analyzed by matrix-assisted laser desorption ionization-time of flight mass spectrometry (MALDI-TOF MS) and MALDI-TOF tandem mass spectrometry (MS/MS) on a UltraFLEX mass spectrometer (BRUKER Daltonics) in which α-cyano-4-hydroxycinnamic acid (HCCA) was spotted as matrix on an HCCA AnchorChipTM (Bruker Daltonics) target plate along with protein preparations. 204 MS/MS spectra were obtained from some selected tryptic peptides in a reflector mode. Peptide masses were compared to those deduced from sequences of L1 and L2 ORFs using the MASCOT program (Matrix Science).

2.2.8 Protoplast transfection

"Transfection" is defined as inoculation of protoplasts with virus virions (Hillman *et al*., 2004). Protoplasts derived from two virus-free strains of *R. necatrix*, W97 and W370T1 were prepared according to the method of Kanematsu *et al*. (Kanematsu *et al*., 2004). These two trains are vegetatively incompatible with strain W779. Purified

virus particles (from PDA-cellophane cultures) were passaged through Ultrafree-MC sterile centrifugal filter units (Millipore, Tokyo Japan) and introduced into protoplasts using PEG, as described by Sasaki et al. (Sasaki *et al*., 2007; Sasaki *et al*., 2006).

2.2.9 Virulence assay

Virulence was assessed using the method of Kanematsu et al. (Kanematsu *et al*., 2004) with minor modifications. *R. necatrix* strains were cultured on PDA at 25°C in the dark for 2 weeks. Autoclaved apple twig segments were added to each plate and the plates were incubated for additional 2 weeks. Five apple nursery plants (*Malus pruniforia* var. ringo), frequently used as rootstocks in apple cultivation, were grown in a single plastic container (20 x 65 x 18 cm) containing autoclaved orchard soil and pearlite for 43 days. Two segments of the incubated twigs covered with freshly grown mycelia were placed as inocula in the soil, approximately 7 cm below the soil surface, in contact with the taproots of apple plants. Inoculated containers were kept in a greenhouse at approximately 25°C.

2.2.10 Nucleotide sequence deposition

The complete nucleotide sequences of L1 and L2 were deposited in the GenBank/EMBL/DDBJ databases under accession numbers AB512282 and AB512283.

2.3 Results

2.3.1 *R. necatrix* strain W779 carries a dsRNA virus with a bipartite genome that is associated with phenotypic alterations

R. necatrix strain W779 carries a dsRNA virus with a bipartite genome that is associated with phenotypic alterations. A previously conducted screen of field isolates revealed the presence in strain W779 of two differently sized dsRNAs, termed dsRNA-1 and dsRNA-2, of approximately 9 and 7 kbp, respectively. The present study showed that virus particles and the two dsRNAs occurred concomitantly.

However, no such particles or dsRNAs were found in isogenic strain W1015, which was derived from spheroplasts of W779 and which was cured of the virus (dsRNA) (Fig. 1).

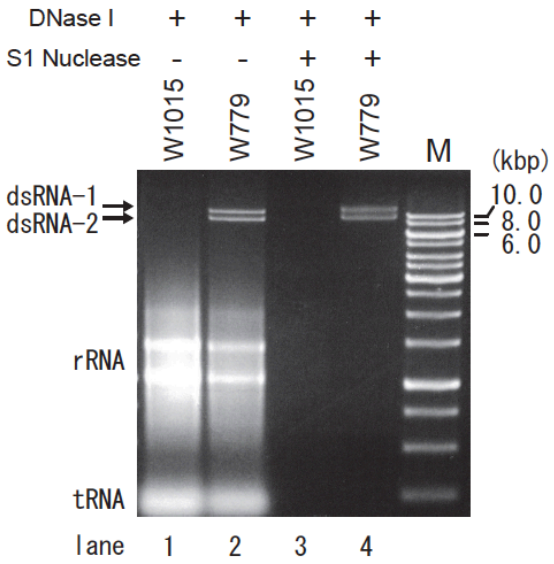

Fig. 1. Nuclease resistance and size estimation of W779 dsRNA. (A) Resistance of W779 dsRNA to nucleases. Total RNA factions were isolated from 50-ml PDB cultures of dsRNA-carrying W779 (lanes 2 and 4) and dsRNA-cured W1015 (lanes 1 and 3), and treated (+) or untreated (-) with RNase-free DNase I (5 units, Promega) alone or together with S1 nuclease (40 units, Takara). After extracted with phenol/chloroform, RNA was electrophoresed in 1.5% agarose gel in 1X TAE [40 mM Tris/acetate (pH 7.8), 1 mM EDTA]. DsRNA isolated from virus particles showed the identical gel profile to that of lane 4.

The two segments are thought to make up the bipartite genome of a novel virus. The two strains, W779 and W1015, are distinguishable in colony morphology and virulence. W779 showed a much smaller colony size on PDA than did W1015 (Fig. 2A). Comparison of vegetative mycelial growth on the surface (Fig. 2B) and inside of the bark of apple rootstocks clearly indicated a higher level of mycelial growth in virus-free W1015 than in W779. That is, the whitish mycelia (shown by arrows) of strain W1015 grew and expanded from the site of inoculation much faster than virus-containing W779 on apple rootstocks buried in the soil. No apparent mycelial growth of strain W779, however, was observed in the 2 weeks postinoculation (Fig. 2B).

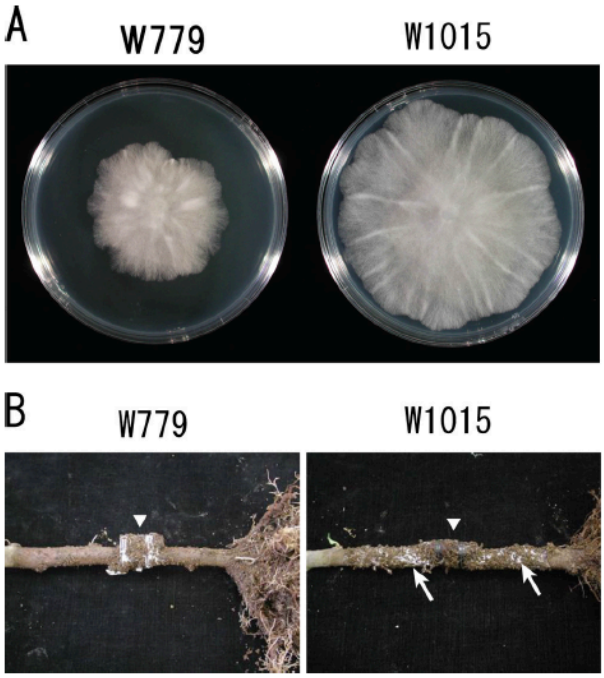

Fig. 2. Mycelial growth of virus-carrying field strain W779 and virus-cured isogenic strain W1015 of *R. necatrix*. (A) Colony morphology of *R. necatrix* strains W779 and W1015. The virus-carrying W779 and virus-cured W1015 fungal strains were grown on PDA for 5 days in the dark and photographed. (B) Mycelial growth on apple rootstocks. Twigs of Japanese pear (1.5 cm long) were placed for 3 weeks on 5-day-old PDA cultures of fungal strains W779 and W1015. Japanese pear twigs covered with mycelia of each fungal strain were fixed on stems of apple rootstocks (*M. prunifolia* var. ringo) that had been precultured in a soil medium for horticulture (Kenbyou, Yae Agricultural Co., Ltd., Nagasaki, Japan). Inoculated apple plants were cultured in the soil for an additional 2 weeks. Mycelial expansion is shown by white arrows, while inoculation sites are denoted by arrowheads. Levels of mycelial growth on apple rootstocks are equivalent to virulence level.

To further confirm the effects of the virus in the W779 host background, W1015 hyphae were fused as a recipient with W779 to transfer dsRNA-1 and -2 back to W1015. Interestingly, the phenotype of W1015, upon receipt of the virus, was converted to that of W779. This suggests that the virus comprising dsRNA-1 and -2 is likely responsible for the phenotypic differences between the two strains.

2.3.2 Composition of virus particles

Particles could be purified by a conventional method entailing differential centrifugation and subsequent sucrose density gradient centrifugation. Twenty fractions (fractions 1 to 20, from top to bottom) were obtained from a sucrose

gradient. A profile of absorbance at 260 nm showed a single peak at fraction 14. Electron micrographs of negatively stained virus particles purified from the peak fraction showed spherical particles ~50 nm in diameter with a rough surface (Fig. 3). The estimated size of the particles was slightly greater than that of those reported for members of the families *Partitiviridae* (30 to 40 nm), *Chrysoviridae* (30 to 40 nm), and *Totiviridae* (30 to 40 nm) and smaller than that of those of members of the genus Mycoreovirus (approximately 80 nm) that are known to infect fungi. When compared, on the same grid, to particles (approximately 40 nm) of the victorivirus HvV190S (provided by S. A. Ghabrial), the W779 particles were slightly larger (data not shown).

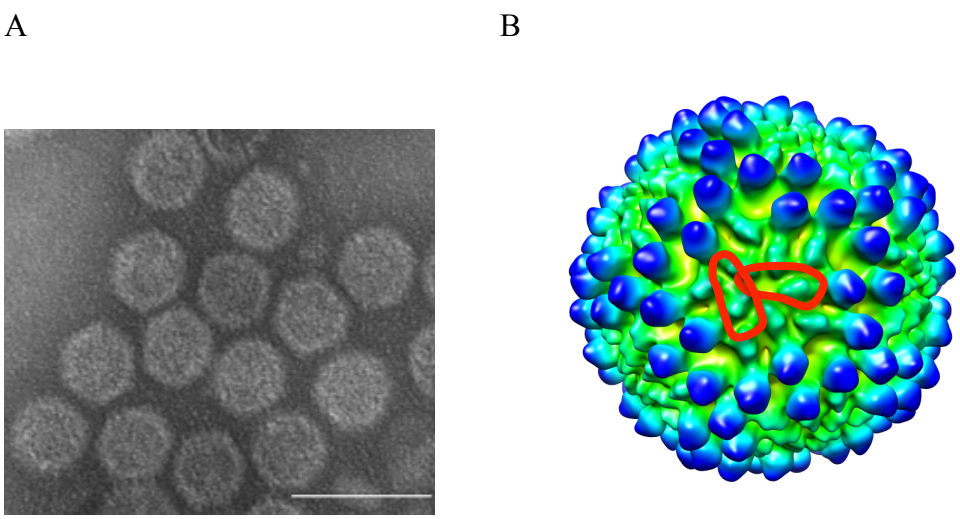

Fig. 3. (A) Electron micrograph of virus particles. Virus particles purified differential and sucrose gradient density centrifugation were negatively strained with 2% uranyl acetate and observed in a Hitachi model H-7000 transmission electron microscope. The scale bar indicates 100 nm. (B) The surface of RnMBV1 representations of cryo-EM.

Extraction of nucleic acids by the SDS-phenol method provided an RNA profile indistinguishable from that of nucleic acids prepared from mycelia of the same W779 culture as was used for particle preparations (Fig. 4). The larger dsRNA-1 segment migrated slightly faster than the dsRNA replicative forms of CHV3- GH2 (9.8 kbp; reference 48) or CHV1-EP713 mutant Δp69b, which lacks 96.1% of the p69 coding domain (10.9 kbp; Suzuki & Nuss, 2002) (Fig. 5).

Table 1. Deoxyoligonucleotides used in the experiment.

Primer name	Sequence	Map position	Used in
T7	5'-AATACGACTCACTATAG-3'	-	sequencing, cDNA probe synthesis
SP6	5'-ATTTAGGTGACACTATAG-3'	-	sequencing, cDNA probe synthesis
M13F	5'-GTAAAACGACGGCCAGT-3'	-	sequencing
M13R	5'-GCGGATAACAATTTCACACAGG-3'	-	sequencing
abridged anchor GI	5'-GGCCACGCGTCGACTAGTACGGGIIGGGIIGGGIIG-3'	-	5'RACE (1st PCR)
G (I)-2	5'-GTCGACTAGTACGGGGGG-3'	-	5'RACE (2nd PCR)
3RACE-adaptor	5'-CAATACCTTCTGACCATGCAGTGACAGTCAGCATG-3'	-	3'RLM-RACE (ligation)
3RACE-1st	5'-CATGCTGACTGTCACTGCAT-3'	-	3'RLM-RACE (1st strand)
3RACE-2nd	5'-TGCATGGTCAGAAGGTATTG-3'	-	3'RLM-RACE (PCR)
SC1	5'-AAGCCACATAAACGTGACCG-3'	dsRNA-1 682-700	5'RACE (1st strand)
SC2	5'-CACAGGTTGCTTGGATTAATG-3'	dsRNA-1 8303-8323	5'RACE (1st strand)
SC3	5'-TTGCATCAGCAAGCCTGTAG-3'	dsRNA-2 687-706	5'RACE (1st strand)
SC4	5'-GACGTTACTTGCCCACGAC-3'	dsRNA-2 6639-6657	5'RACE (1st strand)
SC5	5'-CAACTCGTAATCAGTTACAAGT-3'	dsRNA-1 508-529	RACE PCR (5'/3')
SC6	5'-TGTGCAGAAAAGGGGCTCG-3'	dsRNA-1 8413-8431	RACE PCR (5'/3')
SC7	5'-ATTCTGTTACAACAACAGGCG-3'	dsRNA-2 565-585	RACE PCR(5'/3')
SC8	5'-GATGGATATTAGCTGTGAGAC-3'	dsRNA-2 6763-6783	RACE PRC (5'/3')
SC9	5'-AGCCATTAGACTAAGAAG-3'	dsRNA-2 1936-1953	RT-PCR (1st strand, PCR)
SC10	5'-GTTTTTACCCTTGCGCG-3'	dsRNA-2 881-897	RT-PCR (1st strand)
SC11	5'-GAGAAATCCATTGCCAC-3'	dsRNA-2 1912-1928	RT-PCR (PCR)
SC12	5'-TGCAGGATTTCTTATGTTG-3'	dsRNA-2 120-138	RT-PCR (1st strand)
SC13	5'-CATATGTTTTTGAAGTTTTCC-3'	dsRNA-2 1032-1051	RT-PCR (1st strand)
SC14	5'-GAGACATCGAACACAAAC-3'	dsRNA-2 149-166	RT-PCR (PCR)
SC15	5'-ATAGATGATTGAATTGTCCC-3'	dsRNA-2 976-665	RT-PCR (PCR)
SC16	5'-TCCTTTCCTCTAACGGC-3'	dsRNA-2 1741-1757	RT-PCR (1st strand)
SC17	5'-TGAGTGGTAAAATTTTCATCCC-3'	dsRNA-2 60-81	cDNA probe synthesis
SC18	5'-GATAAGCAATAAAAAATCCCGAG-3'	dsRNA-2 231-253	cDNA probe synthesis
SC19	5'-TGTACGTAAGATATTGAATATAATA-3'	dsRNA-1 1402-1427	cDNA probe synthesis
SC20	5'-CATTTTAATCGTTTTTTGTTTTTAG-3'	dsRNA-1 1615-1639	cDNA probe synthesis

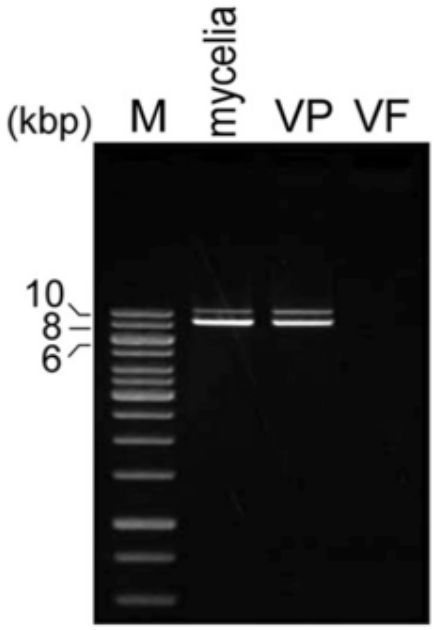

Fig. 4. RNA components of W779 particles. Nucleic acids were extracted from virus particles by the SDS-phenol method, electrophoresed in a 1% agarose gel, and stained with ethidium bromide (lane VP). dsRNAs were isolated from mycelia of the same W779 culture as used for virus purification (lane mycelia) and a virus-free W1015 culture (VF) and applied to an agarose gel in parallel. M refers to the 1-kb DNA ladder (GeneRuler; Fermentas).

Together with the resistance of the segments to S1 nuclease and DNase I, their ability to bind CC41 cellulose strongly suggested their dsRNA nature. When examined by band intensity on ethidium bromide-stained agarose gels, interestingly, the molar ratio of dsRNA-1 to dsRNA-2 varied, depending on the cultures (compare Fig. 1 with Fig. 4). Although dsRNA-1 is generally less abundant than dsRNA-2, the dsRNA profiles from purified particles and mycelia from single cultures are consistently similar (Fig. 4, compare lanes mycelia and VP).

SDS polyacrylamide gel electrophoresis analysis of purified virions showed a single major band corresponding to 135 kDa and a minor protein migrating slightly slower than the size standard of 250 kDa (shown by black and gray arrowheads, Fig. 6, lane VP). No major protein was detected in preparations obtained by the same procedure as for particle purification from virus-free mycelia of W1015 (Fig. 6, lane VF). Only a few

minor protein bands were occasionally detected. The 135- kDa protein possibly represents the major capsid protein. PMF analysis was performed to determine the sequence of peptides derived by digestion of the 135-kDa protein with trypsin. The analysis provided peptide sequences of a total of 24 peptide fragments, which perfectly matched those from the deduced amino acid sequence coded for by one of the dsRNA-1 ORFs, as discussed in Table 2.

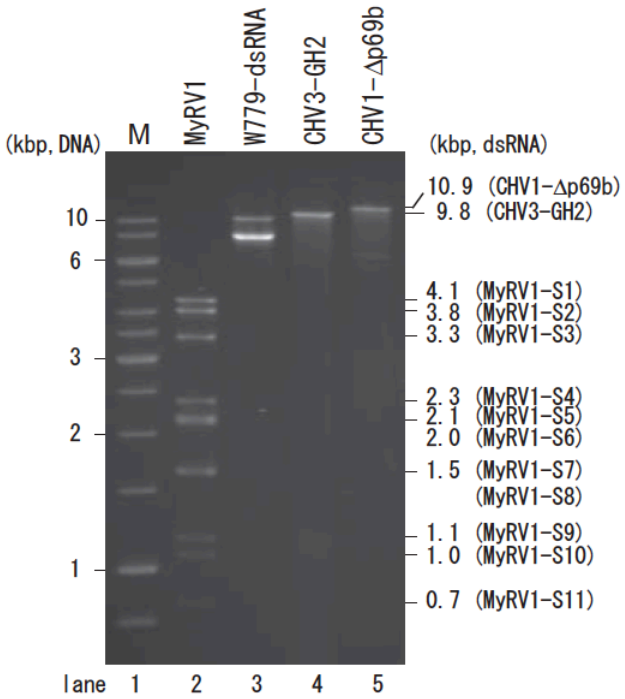

Fig. 5. Agarose gel electrophoresis of purified W779 dsRNA elements. Purified W779 dsRNA was analyzed by 1% agarose gel electrophoresis in 1X TAE (lane 2). The 1-kb DNA ladder (GeneRuler, Fermentas) (lane M), genomic dsRNAs of MyRV1 (0.7-4.1 kbp) (lane 1), and the replicative forms of genomic RNA of CHV1-GH2 (9.8 kbp) (lane 3), and CHV1-Δp69b (10.9 kbp) (lane 4) were used to estimate approximate sizes of W779 L1 and L2.

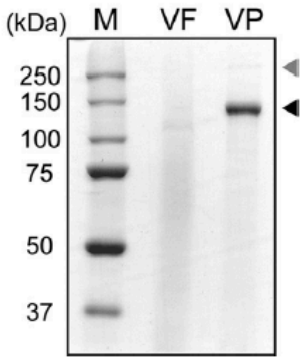

Fig. 6. Protein components of particles from strain W779. Purified particle preparations were denatured by boiling for 3 min in Laemmli's sample buffer containing 2% SDS and 0.05% -mercaptoethanol and electrophoresed in a 10% polyacrylamide gel (lane VP) (Sambrook & Russell, 2001). A fraction obtained from virus-free strain W1015 by the same method as for virus particles was also analyzed (lane VF). Proteins were stained by Coomassie brilliant blue. Prestained protein size standards are from Bio-Rad (Precision Plus Protein Standards) (lane M). The black and gray arrowheads denote the major and minor protein bands, respectively.

Table 2. Peptide mass fingerprinting analysis of the 135-kDa capsid protein.

amino acid positon	Observed	Mr(expt)	Mr(calc)	Delta	Sequence
42 - 71	3235.57	3234.56	3234.53	0.03	FADGADAIANVLQQMEHGVAQHQLGDMNVR
89 - 102	1742.81	1741.80	1741.81	-0.00	IANQYMMHFDLFGR
130 - 140	1349.65	1348.64	1348.65	-0.01	FHNQLSGVYER
151 - 173	2319.24	2318.23	2318.25	-0.02	ILATDTDLGGTSGLSVVFNGLLR
226 - 258	3435.82	3434.81	3434.73	0.08	WYGAPGQPIVPPAPNNPPAHVAPMETVMAGLQK
284 - 303	2083.15	2082.14	2082.16	-0.02	NLIAVLAAVSKPNLGFDANR
333 - 367	3754.04	3753.03	3752.89	0.14	VVANEAGVNDAGFIVPNAAPPQFLQNTNQQVIDFR
433 - 447	1785.84	1784.83	1784.83	-0.00	ADFGVYHNVVTNMYR
505 - 533	2987.50	2986.49	2986.49	0.01	QPLLDEAFGAGVVQPGNMDLVGAGIDFTR
557 - 581	2756.20	2755.19	2755.20	-0.01	DLGDFTAGTVDAAASGYEWDNYVYR
627 - 645	2096.00	2094.99	2094.99	-0.00	WGYDAAPLCSIPIPAGHDR
650 - 679	3281.69	3280.69	3280.64	0.05	NWSWVNVHNVHSVTGTSENVVLAGYVGLSR
711 - 723	1406.77	1405.77	1405.78	-0.01	MLSLTFGLAGQLR
852 - 862	1309.63	1308.62	1308.61	0.01	AYEQVEMGNIR
883 - 899	1774.91	1773.90	1773.92	-0.02	GASQQIAAVGGFHIQYK
922 - 928	955.47	954.47	954.49	-0.03	YLNNYLR
929 - 952	2612.20	2611.19	2611.22	-0.03	MSDCAPTSVLNAVSPLFWMAGTTR
953 - 977	2920.37	2919.37	2919.37	-0.00	VVLCEAANGYKPMAYDISQTSFWNR
978 - 991	1653.76	1652.76	1652.75	0.01	ENGLWAFTWGESEK
1051 - 1069	2065.00	2063.99	2064.01	-0.02	MFIIQDVAGGEHAAYSSLR
1078 - 1090	1542.75	1541.74	1541.74	0.00	AAHTWDTFVQNPR
1097 - 1113	1750.80	1749.80	1749.80	0.00	GYGNTGFTDTYSAAGIR
1123 - 1139	1963.94	1962.94	1962.95	-0.01	LSALTDDFEFTMHPLAR
1162 - 1181	2059.03	2058.02	2058.03	-0.01	DLSLPTGTVEDIIGAVDGMR

2.3.3 Genetic organization of dsRNA-1 and dsRNA-2

The complete sequence of each segment was obtained by sequencing recombinant plasmid clones derived from the cDNA library, reverse transcription (RT)-PCR, 5'-RACE, and RLM-RACE. For the sequencing strategy used, see Fig. 7. From the cDNA library prepared from a mixture of dsRNA-1 and -2, cDNA plasmid clones with relatively large inserts of ~700 bp were randomly chosen for sequence assembly. Assembly of sequences of the cDNA clones and gap-filling RT-PCR clones resulted in the generation of two contigs, 1 and 2. More than 75 cDNA clones were analyzed, and yet no clones were found to constitute an additional contig. This suggested that no dsRNAs other than dsRNA-1 and -2 were present in strain W779 that might co-migrate with them in gel. At least two cDNA clones were sequenced in both directions for a single site (Fig. 7). Contigs 1 and 2 were 8,894 and 7,135 nucleotides (nt) long, respectively, and were considered to be from dsRNA-1 and -2 and cover more than 95% of the dsRNA-1 and dsRNA-2 sequences based on the agarose gel electrophoresis profile of the dsRNAs of MyRV1 (Suzuki *et al*., 2004), CHV3-GH2 (Smart *et al*., 1999), and the -Δp69b mutant of CHV1 (Suzuki & Nuss, 2002) as size markers (Fig. 5).

Interestingly, the 5'-terminal regions of the coding strand from both contigs showed high levels of sequence similarity (approximately 70% identity), with gaps of 9 to 27 nt. Many identical sequence stretches of ~10 nt were found between the 5' UTRs of the two segments (Fig. 8). Sequence similarities could be attributed to template switches during cDNA synthesis and/or errors during sequence assembly. To eliminate this possibility and assign the contigs experimentally, Northern blotting using two cDNA clones representing contigs 1 (probe 1) and 2 (probe 3) and one cDNA clone of dsRNA-1 spanning a region similar in sequence to the corresponding portion of dsRNA-2 (probe 2) were carried out. As shown in Fig. 9A, probes 1 and 3 detected single bands of dsRNA-1 and -2 on a Northern blot, respectively. However, probe 2 hybridized to both segments (Fig. 9A), confirming the sequence similarities between them. The relative positions of these probes are shown in Fig. 9B. When cDNA fragments corresponding to regions of unique sequences of the 5' UTRs of dsRNA-1 (map positions 1402 to 1639) and dsRNA-2 (map positions 60 to 253) were used as probes,

the respective segments were detected specifically (data not shown), providing further evidence of the correctness of the sequences.

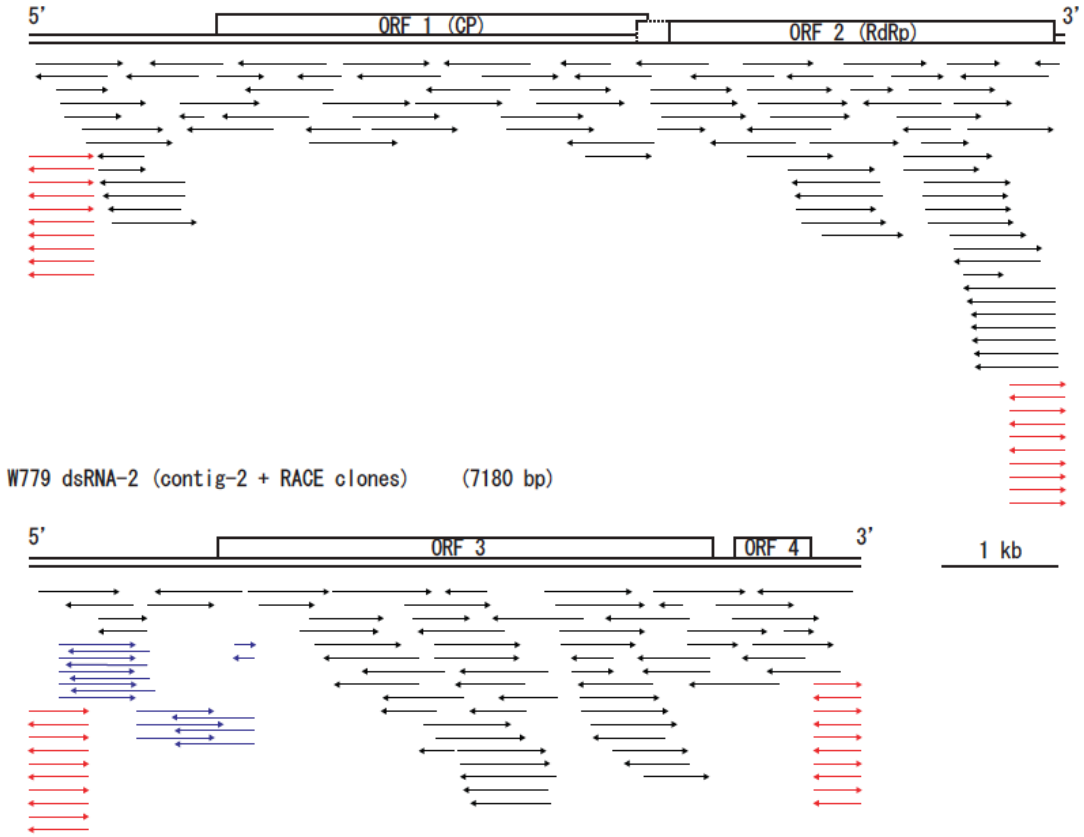

Fig. 7. Sequencing strategy of W779 L1 and L2. Black and blue arrows indicate sequence readings and directions obtained from cDNA and RT-PCR clones, respectively. For the determination of the terminal sequences, RACE clones shown by red arrows were used.


dsRNA-1 GCAUAAAAAGAGAAGGAAGGUUUAACUUCUGGAACUUUUAUGC---GAACUCGAUGAAAA
dsRNA-2 GCAUAAAAAGAGAAGGAAGGUUUAUCUUCUGGA-CUUUUAUGCAAAGAACUCGAUGAAAA
dsRNA-1 AUUCUCAAAAAGUUUUCAUUUCAGU---UCUAAUCCUUGGAUAUGAAAGUCAUACC-----
dsRNA-2 UGAGUGGUAAAAUUUUCAUCCCGGUGUUUCUGGCGCUUUUGCGCGUUCAUUCUUUCCUCU
dsRNA-1 ---ACGACUUCCAUUGUUCU---CUGAUGGUCCUGAUCUACUCAACCCUCUGC--CCAUA
dsRNA-2 UGCAGGAUUUCUUAUGUUGUGGACUGACGGAGACAUCGAACACAAACCGCUGCGGCCUUA
dsRNA-1 UGGGCGGAG-GGUGUCU----------ACUUUCUUG--------GGUAUU
dsRNA-2 GGGCCGCAGCGGUUUGUGGUUAGAGACCUCUGGAAGACAUUCUUUUGAAGGCUCGGGAUU
dsRNA-1 U----------GGAUUCGAGGUAGGGAAUCUUGUUCCUCCCCACACGUGGCUCUCAG
dsRNA-2 UUUUAUUGCUUAUCGAAUUCGAGUGUAGGACUCUUGUUCCUCCCCACGCGUGGUUCUCAA
dsRNA-1 UACAUGUGUAGUGCAUUUGGCUUAAGACGGCCGGAAAACUAAGGACAAGAAAGACUAA-A
dsRNA-2 CACAUGCGUAGUGUGGCUG-CUUAAGACGGCAGUGAAGCUA-GGACAAGGUGCUCUACUA
dsRNA-1 CCUUAUCCCAUCCUGAAUGAACAGGUUUGAGGACGGAAGCCUGCGCCAUUAUGCGGCAUG
dsRNA-2 CCUAACUCCAUCGUGAAUUGACACGUG-AAGGACGGAAGCCUCCGCCAUAA-AUGGCAUG
dsRNA-1 CCAGUUAACGACUGGCUGUAAGAACAGGCACGCUGCCCCCGGCAUUAUGGGGUCCGAAUG
dsRNA-2 CUGGUUAAUGGCCAGCUGUGAGAAGAGGCACGCUGCCCCCGGCAUAAUGGGGUCCGAAUG
dsRNA-1 GAUAAGGGCUGUGCGAUUGAUCCGGCGCGCAGCGAUAA--UGUUUAGUUUUUCUAUAUGC
dsRNA-2 GAUAAGGGCUGUUGGAUUGAUCCGGCCAACGGCAGUUAGGUAUGUAAAACACCACUCUUU
dsRNA-1 UUAGCAACCGCCUUCUUAGCCUCUGCACACACUUGUAACUGAUUACGAGUUGCGUGUGGG
dsRNA-2 CUUCUUCUCUCCUUCUUAGCCACCACACACGCCUGUUGUUGUAACAGAAUUGCGUGUGGG
dsRNA-1 GACUGAGAAGGAGCAAGAUUUUUUAUUGGUACUGGAUACCAUCAU-CCGCUGGCGGAUGU
dsRNA-2 GGUUGAGAAGGAACAAGAUUUUUUAUUGGUGCUGGACACCAAUGCACUGCUGGCGGUGCU
dsRNA-1 CC--CUACUGGGCACCGCUGAUGAU----------GGCCUCCC
dsRNA-2 CCUACUACUGGGCACCGCUGAUGACCUGAUGCUACAGGCUUGCUGAUGCAAGGGACUCCC
dsRNA-1 AGUAUAAACAUAAUGGCCGAAACCU-----GUUAGGUACGGUGUAGCUAGUGGUGCCGGCG
dsRNA-2 AGUCUAAAUAUAAUGUCCGAAACCUCGGUGUGAGGUACGGUGUAGCUGGGUGGUUCAGAU
dsRNA-1 GUCACGUUUAUGUGGCUUUGGCCCCACUGGCGCGUCACUCUCCUAUUAAAGGAAUUUAAU
dsRNA-2 GCUGUGUUUAAACAGCCUAGGGCCAUUCGGCGCGUCUUCACCCUAUUAAGAGGGUGUUUU

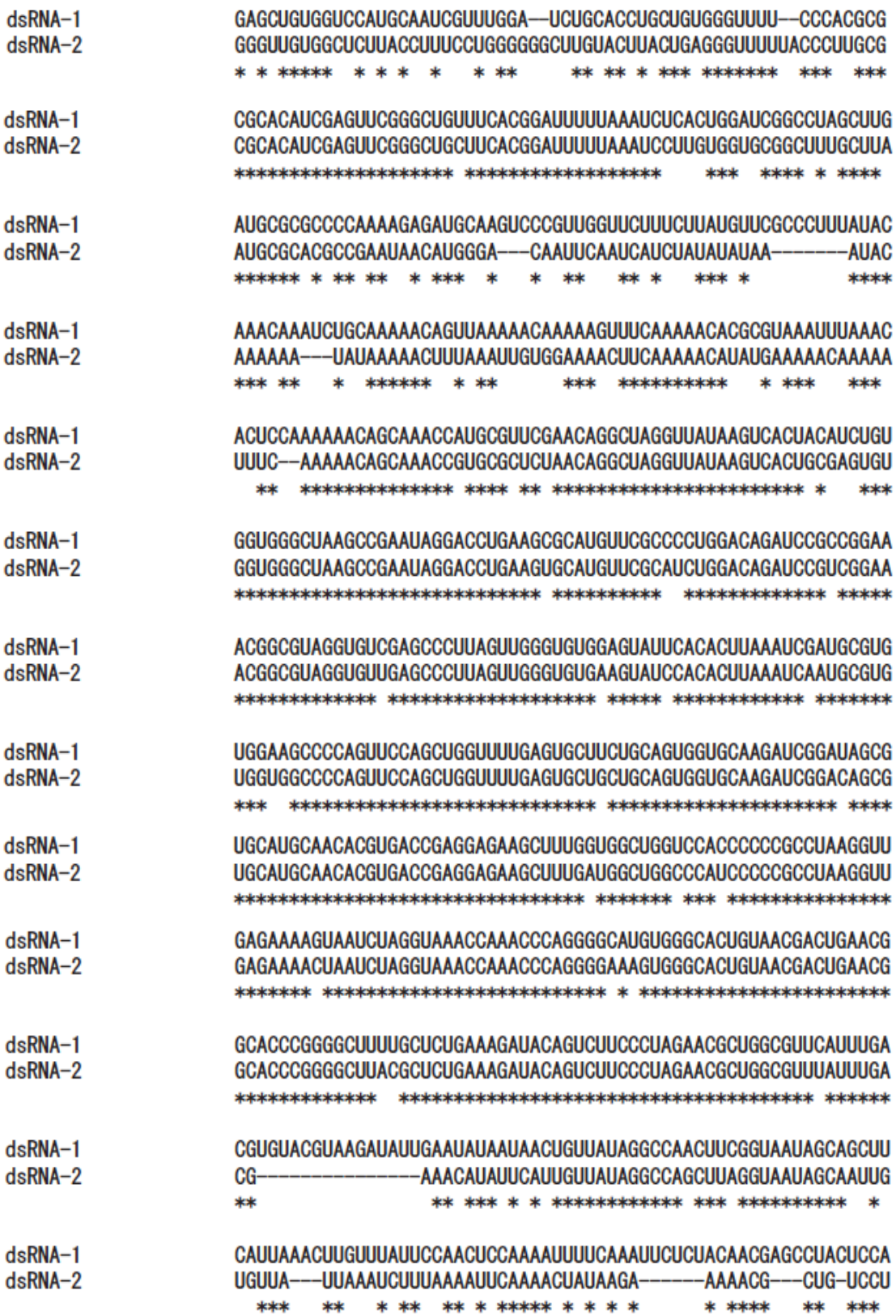
dsRNA-1 GAGCUGUGGUCCAUGCAAUCGUUUGGA—UCUGCACCUGCUGUGGGUUUU—CCCACGCG
dsRNA-2 GGGUUGUGGCUCUUACCUUUCCUGGGGGGCUUGUACUUACUGAGGGUUUUUACCCUUGCG
dsRNA-1 CGCACAUCGAGUUCGGGCUGUUUCACGGAUUUUUAAAUCUCACUGGAUCGGCCUAGCUUG
dsRNA-2 CGCACAUCGAGUUCGGGCUGCUUCACGGAUUUUUAAAUCCUUGUGGUGCGGCUUUGCUUA
dsRNA-1 AUGCGCGCCCCAAAAGAGAUGCAAGUCCCGUUGGUUCUUUCUUAUGUUCGCCCUUUAUAC
dsRNA-2 AUGCGCACGCCGAAUAACAUGGGA———CAAUUCAAUCAUCUAUAUAUAA————————AUAC
dsRNA-1 AAACAAAUCUGCAAAAACAGUUAAAAACAAAAAGUUUCAAAAACACGCGUAAAUUUAAAC
dsRNA-2 AAAAAA———UAUAAAAACUUUAAAUUGUGGAAAACUUCAAAAACAUAUGAAAAACAAAAA
dsRNA-1 ACUCCAAAAAACAGCAAACCAUGCGUUCGAACAGGCUAGGUUAUAAGUCACUACAUCUGU
dsRNA-2 UUUC——AAAAACAGCAAACCGUGCGCUCUAACAGGCUAGGUUAUAAGUCACUGCGAGUGU
dsRNA-1 GGUGGGCUAAGCCGAAUAGGACCUGAAGCGCAUGUUCGCCCCUGGACAGAUCCGCCGGAA
dsRNA-2 GGUGGGCUAAGCCGAAUAGGACCUGAAGUGCAUGUUCGCAUCUGGACAGAUCCGUCGGAA
dsRNA-1 ACGGCGUAGGUGUCGAGCCCUUAGUUGGGUGUGGAGUAUUCACACUUAAAUCGAUGCGUG
dsRNA-2 ACGGCGUAGGUGUUGAGCCCUUAGUUGGGUGUGAAGUAUCCACACUUAAAUCAAUGCGUG
dsRNA-1 UGGAAGCCCCAGUUCCAGCUGGUUUUGAGUGCUUCUGCAGUGGUGCAAGAUCGGAUAGCG
dsRNA-2 UGGUGGCCCCAGUUCCAGCUGGUUUUGAGUGCUGCUGCAGUGGUGCAAGAUCGGACAGCG
dsRNA-1 UGCAUGCAACACGUGACCGAGGAGAAGCUUUGGUGGCUGGUCCACCCCCCGCCUAAGGUU
dsRNA-2 UGCAUGCAACACGUGACCGAGGAGAAGCUUUGAUGGCUGGCCCAUCCCCCGCCUAAGGUU
dsRNA-1 GAGAAAAGUAAUCUAGGUAAACCAAACCCAGGGGCAUGUGGGCACUGUAACGACUGAACG
dsRNA-2 GAGAAAACUAAUCUAGGUAAACCAAACCCAGGGGAAAGUGGGCACUGUAACGACUGAACG
dsRNA-1 GCACCCGGGGCUUUUGCUCUGAAAGAUACAGUCUUCCCUAGAACGCUGGCGUUCAUUUGA
dsRNA-2 GCACCCGGGGCUUACGCUCUGAAAGAUACAGUCUUCCCUAGAACGCUGGCGUUUAUUUGA
dsRNA-1 CGUGUACGUAAGAUAUUGAAUAUAAUAACUGUUAUAGGCCAACUUCGGUAAUAGCAGCUU
dsRNA-2 CG————————————AAACAUAUUCAUUGUUAUAGGCCAGCUUAGGUAAUAGCAAUUG
dsRNA-1 CAUUAAACUUGUUUAUUCCAACUCCAAAAUUUUCAAAUUCUCUACAACGAGCCUACUCCA
dsRNA-2 UGUUA———UUAAAUCUUUAAAAUUCAAAACUAUAAGA———————AAAACG———CUG—UCCU

```
dsRNA-1    ACACUUCUCUAGCGCAUCUCGCUGAAGAACAACAUCUCGAAUCUUCUCAUCGACAGUAUU
dsRNA-2    GCAAUUCUUCGGCGCAUUAAGCUGAAGAACUUUCCAGCAAAACA-CUCAUCGACUAGAAU
            ** ****   ******   **********       * ** *  *********   * *

dsRNA-1    GUUGGUGGGCCCUCAU-UUUUUAGUUGUUAAAAACGCUAAAAACAAAAAACGAUUAAA
dsRNA-2    AUUGGCGUGUUUUUACAUUUUUAAA----------------------------------
            **** * *   * *  ******
```

Fig. 8. Sequence similarities between the 5'-UTRs of W779 L1 and L2. The 5'-UTRs of the open-reading frame-containing strand of L1 (1636 nts) and L2 (1656 nts) were aligned using the CLUSTAL W program. Conserved sites are indicated by asterisks, while gaps are shown by -. Sequence identity found between the terminal regions of the two segments is 70.2%.

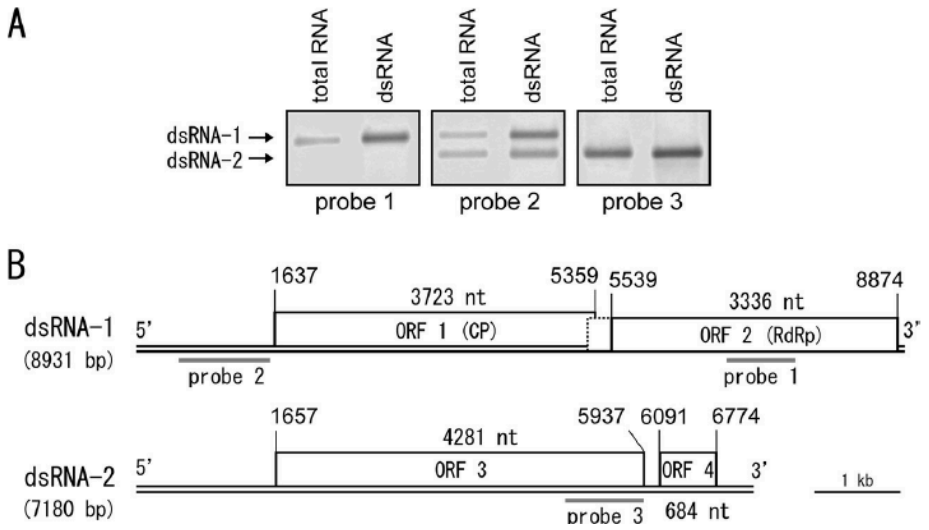

Fig. 9. Molecular characteristics of W779 dsRNA-1 and dsRNA-2. (A) Northern blot analysis of W779 dsRNA-1 and dsRNA-2. Total RNA and dsRNA prepared as stated in Materials and Methods were electrophoresed under denaturing conditions, blotted onto nylon membranes, and probed by DIG-labeled DNA fragments (probes 1 to 3). The positions of probes 1 to 3 are shown in panel B. (B) Schematic representation of the genetic organization of the strain W779 dsRNA-1 and dsRNA-2 segments. dsRNA-1 and -2 are 8,931 and 7,180 nt in length, respectively. dsRNA-1 has a 1,636-nt-long 5' UTR, two ORFs (ORF1 and ORF2), and a 57-nt-long 3' UTR, while dsRNA-2 has a 1,656-nt-long 5' UTR, two ORFs (ORF3 and ORF4), and a 406-nt-long 3' UTR. ORF1 to -4 are composed of 1,240, 1,111, 1,427, and 227 codons, respectively. Open boxes drawn with solid lines denote ORFs, while that drawn with dotted lines indicates a possible extension of ORF2 by frameshifting. Numbers above solid lines refer to map positions of initiation and termination codons of the respective ORFs.

Terminal sequences of the two segments were determined by a combination of classic 5'-RACE and 3'-RLM-RACE. Six clones gained by 5'-RACE were sequenced for each 5' end of both strands of dsRNA-1 and -2. Most of the clones (four out of six), obtained by d (C) tailing of cDNA to the 5' terminus of the plus-sense strand, had the 5'-terminal sequence 5'-(G)nGCATAAAAA, which was shared by dsRNA-1 and -2. The 5' sequence of the minus-sense strands was 5'-(G)nGCGAAAAA, which is common to the two segments. In order to determine the extreme terminal nucleotide sequence, a total of four 3'-RLM-RACE reactions were designed for the two strands each of dsRNA-1 and -2. Fragments were amplified whose sizes agreed with the ones presumed from the positions of the primers and the expected lengths of regions uncovered by the contigs (Fig. 10).

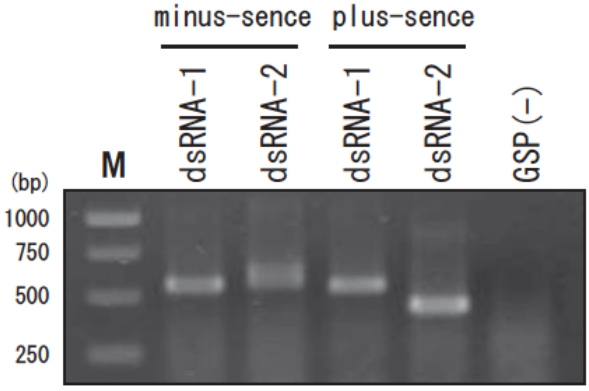

Fig. 10. RACE analysis of W779 L1 and L2 dsRNA. (A) Agarose gel electrophoresis pattern of 3' RLM-RACE clones. DNA fragments amplified by 3' RLM-RACE were electrophoresed in 1% agarose gel in 0.5X TAE. An adapter oligonucleotide 5'-PO4-CAATACCTTCTGACCATGCAGTGACAGTCAGCATG-3' was added to the 3' termini of plus-sense (+) and minus-sense strands (-) of L1 and L2. cDNA was synthesized using a complimentary primer to the ligated adapter (3RACE-1st) and amplified by PCR with the common primer (3RACE-2nd) and strand-specific primers. Strand-specific primers were CS6 for the plus-strand of L1 (lane L1, plus-sense), CS5 for the minus-strand of L1 (lane L1, minus-sense), CS8 for the plus-strand of L2 (lane L2, plus-sense), and CS7 for the minus-strand of L2 (lane L2, minus-sense). See Table 1 for sequences of those primers. GSP(-) is a PCR product with a 3RACE-2nd primer alone without any segment-specific primers). M refers to the GeneRuler 1 kb DNA ladder (Fermentas) in this and subsequent Fig. 8.

The resultant six 3'-RLM-RACE clones derived from a single RLM-RACE reaction were identical in sequence. The terminal sequences of dsRNA-1 and -2 were determined

by RLMRACE to be 5'-GCA and CGC-3' for the plus strand. As shown in Fig. 11A, the 5' 24-mer and 3' octamer are strictly conserved among RACE clones of dsRNA-1 and -2. Except for the conserved terminal heptamer, no conserved sequence stretches were detected in the 3'-terminal regions (Fig. 11A). In addition to three potential tandem stem-loop structures commonly found within the 3'-terminal 90-nt sequences of dsRNA-1 and -2 by Mfold at default settings (Fig. 11B), a 9-bp inverted repeat could be formed by the 5'- and 3'-terminal sequences of either strand of each segment (Fig. 11C).

The complete nucleotide sequences of dsRNA-1 and -2 were deposited in the GenBank/EMBL/DDBJ databases. The schematic genetic organization of the coding strands of dsRNA-1and -2 is shown in Fig. 9B. dsRNA-1 and -2 are 8,931 and 7,180 nt in length, each possessing 5' UTRs of ~1.6 kb, two tandem nonoverlapping ORFs, and relatively short 3' UTRs. dsRNA-1 ORF1 and -2 could encode polypeptides of 1,240 aa (P1) and 1,111 aa (P2), respectively, while dsRNA-2 ORF3 and -4 encode polypeptides of 1,426 aa (P3) and 227 aa (P4) (Fig. 9B). P1 was unequivocally shown by PMF analysis to be the major capsid protein of 135 kDa (Table 2). That is, the MALDI-TOF MS analysis allowed the identification of 24 specific tryptic peptides with 38.8% coverage of the 135 kDa and a highly significant MOWSE score of 262 in the Mascot program. Examples included FHNQLSGVYER (amino acid positions 130 to 140), QPLLDEAFGAG VVQPGNMDLVGAGIDFTR (amino acid positions 505 to 533), DLGDFTAGTVDAAASGYEWDNYVYR (amino acid positions 557 to 581), MLSLTFGLAGQLR (amino acid positions 711 to 723), and AAHTWDTFVQNPR (amino acid positions 1078 to 1090). No peptide sequences matched those coded for by other ORFs of dsRNA-1 and -2. Sequence heterogeneities among cDNA clones were noted. Two transitions were detected at position 8358 of dsRNA-1 (T to C) and position 3702 of dsRNA-2 (C to T) that were silent, while two transversions were found at dsRNA-2 positions 2183 (C to A) and 5275 (A to T) that would cause amino acid changes on the ORF 3-encoded protein (P3) from Pro176 to His and Ser1207 to Cys, respectively. Moreover, an interesting 40-nt deletion was detected at the 5' UTR of dsRNA-2 that extended from position 172 to position 211. The deletion was observed in RT-PCR clones, as well as RLM-RACE clones (see the slightly broader band of RLM-RACE products in Fig. 10, lane dsRNA-2 minus sense). A total of 21 independent

cDNA clones were analysed, including RACE clones, and 8 of them carried the same deletion. This suggested that two dsRNA-2 segments that differ from each other in size exist in W779, as recently found for a novel RNA mycovirus in *Phytophthora infestans* (Cai *et al*., 2009).

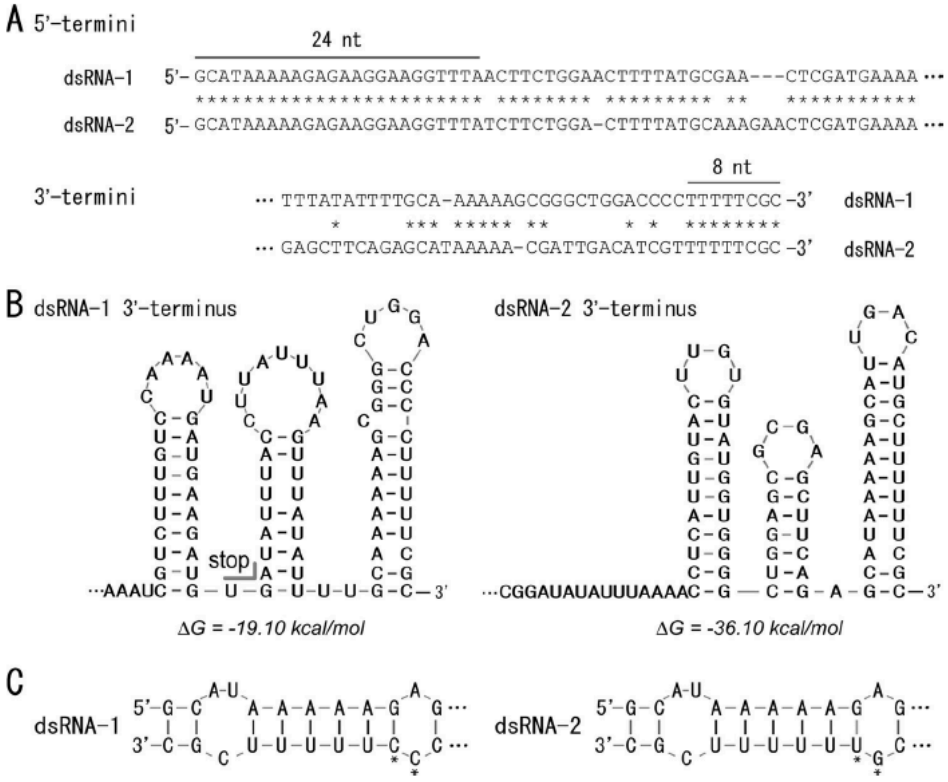

Fig. 11. Characteristics of the terminal sequence domains of dsRNA-1 and dsRNA-2. (A) Conserved terminal sequences of dsRNA-1 and dsRNA-2. The terminal sequences of the ORF-containing strands of dsRNA-1 and -2, obtained by sequencing the RACE clones, are shown. The 5' 24-mer and 3' octamer (lines above the sequences) are shared by the segments. Identical nucleotides are denoted by asterisks. Sequence similarities are found in the entire 5' UTRs. (B) Possible secondary structures of the 3'-terminal sequences of W779 dsRNA-1 and dsRNA-2. The 3'-terminal 90-nt sequences of each of the plus-sense strands of dsRNA-1 and -2 were analyzed with the Mfold program. The default settings were utilized for the analyses. Secondary structures are depicted in a modified style from the ones provided by the program. The stop codon of ORF2 is indicated. (C) Possible inverted repeats formed by the terminal sequences of W779 dsRNA-1 and dsRNA-2. Both dsRNA-1 and -2 potentially form inverted repeats between the conserved terminal sequences. Nucleotides that differ between the inverted repeat structures of dsRNA-1 and -2 are shown by asterisks.

2.3.4 Interviral amino acid sequence similarities and amino acid sequence motifs

As shown in Fig. 9B, dsRNA-1 and -2 each possess two ORFs coding for a total of four proteins. The deduced amino acid sequence of P1, P3, or P4 did not yield any significant hits, with E values below 0.01, in BLAST or FASTA3 searches. A BLAST search detected low levels of sequence similarities only between the dsRNA-1 ORF2-encoded P2 and RdRps of members of the families *Totiviridae* and *Chrysoviridae*. The highest sequence identity scores were found by a BLAST search between P2 and RdRps encoded by virus-like dsRNAs isolated from two different basidiomycetes, *Phlebiopsis gigantea* (PgV1) (30%) (Kozlakidis *et al*., 2009) and *Lentinula edodes* (LeV-HKB) (25%). The partial sequences of those dsRNAs were recently published or are publicly available only in the database. Table 3 summarizes the results of a BLAST search with dsRNA-1 P2 (RdRp), indicating sequence identities found between aligned regions, bit scores, and E values among 17 mycoviruses. FASTA3 searches with P2 yielded hits similar to those listed in Table 3.

A search of the PROSITE motif database with dsRNA-1 ORF2-encoded protein P2 detected functional sequence motifs typical of RdRps that included the SG——TS/T and GDD motifs. This domain was readily identified by a Pfam search as the RdRp_4 motif. In addition, a search of the PROSITE database revealed that ORF2-encoded P2 contains a carbamoyl phosphate synthase subdomain signature 2 motif (INECNLKV) in the terminal region (amino acid positions 927 to 934) when default settings were used to exclude common motifs. No other sequence motif was observed in the polypeptides (P1, P3, and P4) coded for by ORF1, -3, and -4, except for frequently found motifs like phosphorylation sites and glycosylation sites.

A multiple amino acid sequence alignment of RdRp motifs I to VIII and their flanking regions of P2 and those of related viruses was constructed with CLUSTAL_X (Fig. 12), which was modified manually based upon the alignments reported by Bruenn (Bruenn, 2003), Jiang and Ghabrial (Jiang, D & Ghabrial, 2004), and Hillman et al. (Hillman *et al*., 1994).

Table 3. Summary of the results of a BLASTP search with dsRNA-1 ORF2-encoded RdRp.

Mycovirus[a]	RdRp size (aa)	RdRP_4 conserved region			BLAST			Accession no.
		Motif I-VIII	Size (aa)	% Identity	Overlap	Bit score	E value	
Unassigned								
W779	1,111	378–765	388					AB512282
LeV-HKB[c]	1,245	491–878	388	25	170/664	177	4e-42	AB429554
PgV1[c]	1,414	669–1,061	393	30	183/601	201	4e-49	AM111096
Chrysovirus[e]								
PcV	1,117	453–832	380	22	120/523	96.3	2e-17	AF296339
Hv145SV	1,086	426–805	380	22	142/625	93.2	1e-16	AF297176
ACD-CV[b]	1,087	427–806	380	25	83/326	77.8	6e-12	NC_009947
CCRS-CV[b]	1,087	427–806	380	25	84/326	80.9	7e-13	AJ781397
FoV1[c]	858	360–738	379	22	76/339	64.3	6e-08	EF152346
AbV1	1,078	372–785	414	23	82/356	62.8	2e-07	X94361
Totivirus								
ScV-L-A	731	169–520	352	24	72/297	67.0	1e-08	J04692
ScV-L-BC	863	306–654	349	25	35/139	40.0	1.5	U01060
UmV-H1	1,820[d]	1,142–1,530[d]	389[d]	22	90/400	72.8	2e-10	NC_003823
Victorivirus[e]								
HmV-17	845	243–594	352	32	43/131	51.2	6e-04	AB085814
GaRV-L1	825	221–573	353	29	51/171	50.4	0.001	AF337175
BfTV1	838	242–585	344	24	58/235	43.1	0.16	AM491608
MoV1	845	227–575	349	23	62/260	42.0	0.35	AB176964
Hv190SV	835	241–585	345	27	30/111	37.4	9.3	U41345

[a] See the legend to Fig. 5 for definitions of virus name abbreviations.
[b] No evidence demonstrating the fungal origin is provided.
[c] Only the partial nucleotide sequences are available.
[d] Data are taken from the cap-pol fusion protein.
[e] Tentative and presumptive members are included.

All of the mycoviruses listed in Table 3 were subjected to phylogenetic analysis. As reported earlier (Bruenn, 2003; Jiang & Ghabrial, 2004), a few amino acid residues were strictly conserved in most of the motifs, e.g., K-E-G—R in motif III and D–DFN–H in motif IV. Motifs I and II were not found in members of the families *Partitiviridae* and *Hypoviridae*. Therefore, alignments of sequences from motifs III to VIII were employed for the construction of a phylogenetic tree in which the RdRp sequences of members of the family *Hypoviridae* were used as the outgroup. As expected from the results of a BLAST search (Table 3), the dendrogram showed that W799 RdRp clusters with dsRNA elements from *P. gigantea* and *L. edodes*. Importantly, their clade is separate from those of the other known dsRNA mycovirus families (Fig. 13). W799 RdRp is evolutionarily more closely related to members *Totiviridae* and *Partitiviridae*. Grouping of chrysoviruses and members in the W779 RdRp clade is supported by a relatively strong bootstrap value, 839 in a total of 1,000 trials.

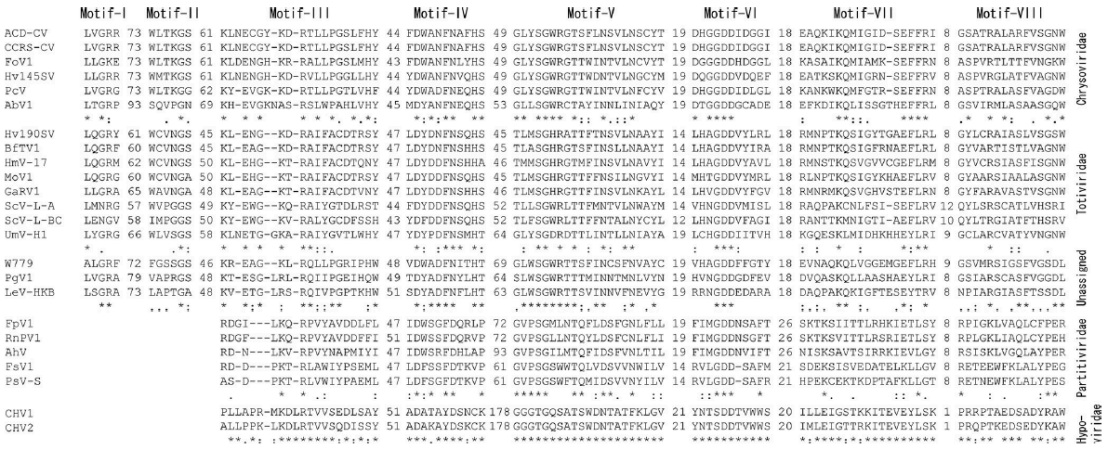

Fig. 12. Molecular evolutionary analysis of the W779 dsRNA virus. Multiple alignment of sequences of the RdRp motifs (I to VIII) encoded by W779 dsRNA-1 and other mycoviruses. The alignment was prepared by the program CLUSTAL_X and modified manually based on those reported by Bruenn (Bruenn, 2003), Jiang and Ghabrial (Jiang & Ghabrial, 2004), and Hillman et al. (Hillman *et al*., 1994). Abbreviated virus names: LeV-HKB, *Lentinula edodes mycovirus* HKB; PgV1, *Phlebiopsis gigantea* mycovirus dsRNA-1; PcV, *Penicillium chrysogenum* virus; HvV145S, *Helminthosporium victoriae* 145S virus; ACD-CV, Amasya cherry disease-associated chrysovirus; CCRS-CV, cherry chlorotic rusty spot-associated chrysovirus; FoV1, *Fusarium oxysporum* chrysovirus1; AbV1, *Agaricus bisporus* virus 1; ScV-L-A, *Saccharomyces cerevisiae* virus L-A; ScV-L-BC, *Saccharomyces cerevisiae* virus L-BC; UmV-H1, *Ustilago maydis* virus H1; HmV-17, *Helicobasidium mompa* no. 17 dsRNA virus; GaRV1, *Gremmeniella abetina* RNA virus L1; BfTV1, *Botryotinia fuckeliana* totivirus 1; MoV1, *Magnaporthe oryzae* virus 1; Hv190SV, *Helminthosporium victoriae* 190S virus; FpV1, *Fusarium poae* virus 1 (AF047013); RnPV1, *Rosellinia necatrix* partitivirus 1-W8 (NC_007537); AhV, *Atkinsonella hypoxylon* virus (L39125); FsV1, *Fusarium solani* virus1 (D55668); PsV-S, *Penicillium stoloniferum* virus S (NC_005976); CHV1, *Cryphonectria* hypovirus 1-EP713 (M57938); CHV2, *Cryphonectria* hypovirus 2-NB58 (L29010). See Table 1 for the accession numbers, except for members of the families *Partitiviridae* and *Hypoviridae*. LeV-HKB and PgV1 are partially characterized, and their entire genome sequences are not available.

2.3.5 Biological effects of transfection with purified particles

R. necatrix strain W1015, which was cured of the W779 virus, showed enhanced mycelial growth and virulence (Fig. 2), while introduction of the virus back into W1015 by anastomosis resulted in reduced virulence. These results strongly suggest that the phenotypic changes were induced by virus infection. To further examine the possibility that the W779 virus can cause phenotypic alterations in host fungal strains other than W779, transfection of purified particles into virus-free spheroplasts derived from virus-

free isolates W97 and W370T1 of *R. necatrix* was carried out. W370T1 was previously shown to be susceptible to a mycoreovirus (MyRV3) and a partitivirus (RnPV1) and to be stable phenotypically when transfected with virus particles (Kanematsu *et al*., 2004; Sasaki *et al*., 2005; Sasaki *et al*., 2007; S. Kanematsu, unpublished data). Mycelial incompatibility between W779 (MCG351) and W370T1 (MCG139) or W97 (MCG80) impeded lateral transfer of the W779 virus when the two strains were co-cultured. However, transfected colonies of W97 and W370T1 became infected with the virus and showed mycelial growth rates decreased by 55 to 65%, as well as reduced growth of aerial hyphae relative to that of the virus-free strain (Fig. 14A). Virus infection was stably maintained in transfectants during repeated subculturings. Subcultured colonies showed a phenotype identical to that shown in Fig. 14A and were found by dsRNA extraction and gel electrophoretic analysis to carry dsRNA-1 and -2. Moreover, virus particles shown in Fig. 3 were purified from these fungal colonies. Therefore, the morphological consequence of W779 virus infection is similar in three host backgrounds, W97, W370T1, and W1015 (compare Fig. 2A and 14A).

The absence of residual mycelia in the virion fractions used for transfection was confirmed by culturing them on PDA. Furthermore, transfected strains were able to transmit the virus to their virus-free counterparts W97 and W370T1 through anastomosis but not to virus-free W1015, which is isogenic to W779, which is vegetatively incompatible with strains W97 and W370T1. These results eliminated the possibility that fungal colonies transfected with W779 particles originated from presumable contaminants.

Fig. 14B shows the levels of virulence exhibited by untransfected [virus (-)] and transfected [virus (+)] strains W97 and W370T1. Representative apple plants inoculated with virus free and virus-containing strain W370T1 are shown in Fig. 14B (top). Virus-free fungal strains induced a lethal phenotype much more frequently in aerial parts of plants than did virus containing fungal strains. More-severe symptoms were also evident in roots inoculated with virus-free fungal strains. In apple rootstocks inoculated with virus-containing strains, lesions on the taproot were small and superficial, allowing vigorous growth of healthy root hairs. By contrast, lesions induced by virus-free

counterparts girdled the entire taproot, destroying most lateral roots. The mortality of apple rootstocks was much greater when they were inoculated with virus-free strains (7/10 for W97 and 10/10 for W370T1) than when they were inoculated with transfected strains (0/10 for W97 and 1/10 for W370T1) (Fig. 14B, bottom). Taken together, these results clearly show that the W779 virus is responsible for hypovirulence and repressed mycelial growth in *R. necatrix*, regardless of the fungal host strain.

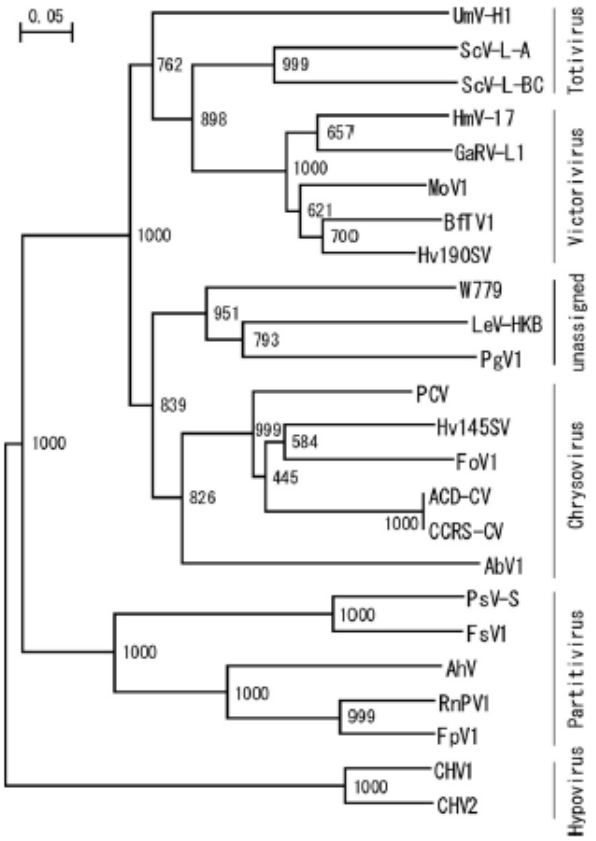

Fig. 13. Phylogenetic analysis of the W779 virus. A multiple alignment of RdRps from 24 related viruses representing the established dsRNA mycovirus families and genera and virus-like elements (Fig. 12) was used to construct a dendrogram. The neighbor-joining tree was constructed by using CLUSTAL_X in which hypoviruses with ssRNA genomes were included as an outgroup. Numbers at the nodes denote bootstrap values out of 1,000 replicates.

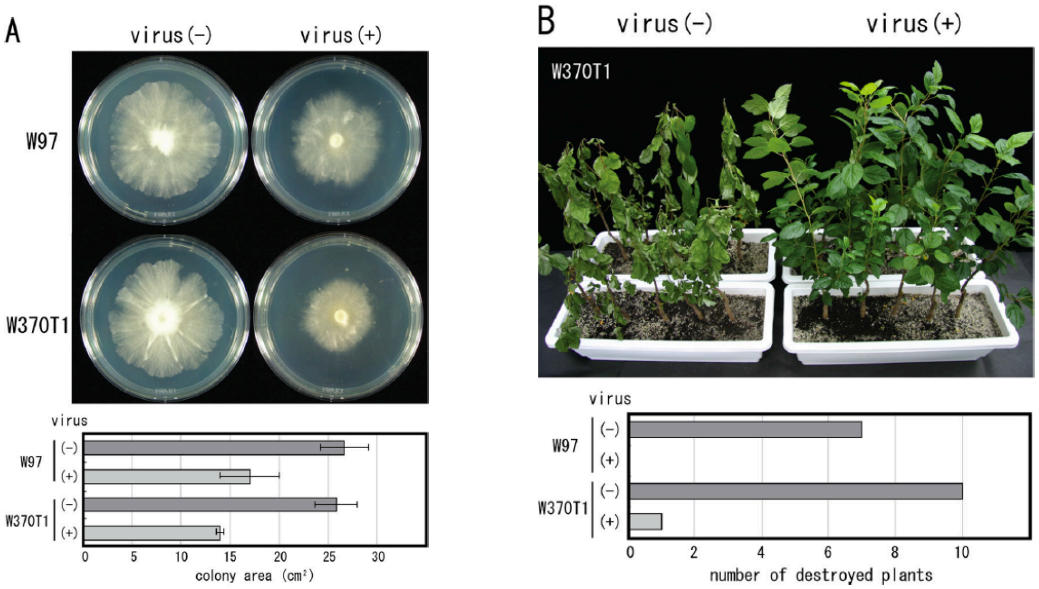

Fig. 14. Effects of W779 virus introduction on the phenotypes of viral mycelially incompatible fungal strains. (A) Colony morphology of transfected and untransfected fungal strains. Purified virus particles were introduced into spheroplasts derived from W97 and W370T1 (vegetatively incompatible with W779 and W1015). Regenerated isolates were grown on PDA for 6 days at 25°C in the dark. Representative colonies transfected with virus particles [virus (+)] are shown. Untransfected strains W97 and W370T1 were cultured in parallel [virus ()]. Mean colony sizes and standard deviations of five cultures are shown in graphic form below the colony photograph. (B) Virulence assay on apple rootstocks. Nursery rootstocks (*M. prunifolia* var. ringo) were planted in plastic containers (five rootstocks per container), cultured for approximately 1.5 months, and subsequently inoculated with fungal mycelia of each of the following fungal strains: virus-free W370T1 [virus (-)], virus-infected W370T1 [virus (+)], virus-free W97 [virus (-)], and virus-infected W97 [virus (+)]. Ten plants in two containers were inoculated with each strain. Phenotypes of apple plants 4 weeks following inoculation with virus-infected and uninfected W370T1 are shown. Virus-free W370T1 induced lethal-type symptoms in all of the plants in the two left pots, while virus-infected W370T1 is attenuated in virulence in the right two pots. The graph below the photograph shows the number of apple plants destroyed out of 10 scored at 4 weeks postinoculation.

2.4 Discussion

Fruit crops-*R. necatrix*-mycoviruses is an interesting pathosystem that attracts scientific and public attention in Japan. It is similar to the chestnut-*C. parasitica*-mycoviruses system that has contributed to a better understanding of fungal and viral pathogenesis (Dawe & Nuss, 2001; Deng *et al*., 2007; Faruk *et al*., 2008a; Faruk *at el*., 2008b; Sun *et*

al., 2009; Sun & Suzuki, 2008), including insights into RNA silencing in fungi as an antiviral response (Segers et al., 2007), viral replication (Deng & Nuss, 2008; Hillman & Suzuki, 2004; Guo *et al*., 2009), and biocontrol with mycoviruses (Anagnostakis, 1982; Heiniger & Rigling, 1994; Milgroom & Cortesi, 2004). *R. necatrix* is a destructive soilborne fungal phytopathogen of economically important fruit crops. Although most fungal viruses cause symptomless infections (Ghabrial & Suzuki, 2009), several viruses are known to induce phenotypic alterations in this fungus (Kanematsu *et al*., 2004; Sasaki *et al*., 2007). Thus, *R. necatrix* and the associated mycoviruses provide a good system with which to explore virus-host and virus-virus interactions based on established methods of host fungus transformation and artificial virus inoculation, the latter being still limited to a few viruses. Furthermore, the potential of mycoviruses infecting *R. necatrix* as biocontrol (virocontrol) agents has been suggested (Matsumoto, 1998). Biological and molecular characterization of the novel bipartite dsRNA virus infecting a field strain, W779, of *R. necatrix* is important from the perspectives of fundamental fungal virology and practical virocontrol with mycoviruses. Several lines of evidence have been presented in support of the conclusion that dsRNA-1 and -2 represent the genome of a novel virus species. Firstly, only dsRNA-1, not dsRNA-2, encodes an RdRp, suggesting that dsRNA-1 and -2 are not derived from two independent viruses. Both segments show similar sequences at the 5' and 3' ends (Fig. 11A; Fig. 8), a fact considered to be important for virus replication. The conserved terminal property is frequently observed in the genome segments of multipartite viruses. The MALDI-TOF MS analysis assigned peptide sequences in the 135-kDa capsid protein to those of dsRNA-1 ORF1-encoded P1 (Table 2) but not to those of P2, P3, or P4, indicative of the absence of capsid proteins other than the 135-kDa protein that might show a similar migration position. Thus, the two segments are encapsidated into particles ~50 nm in diameter (Fig. 3) consisting of a single major structural protein (P1) of 135 kDa. A clue to addressing whether the two segments are contained in single particles comes from inspection of Fig. 4 and Fig. 1. Variable and unequal molar ratios of dsRNA-1 and dsRNA-2 in purified virus particles particles favor the idea that the two segments are separately packaged into particles composed of a single major capsid protein. These findings led us to conclude that the two elements dsRNA-1 and -2 represent the genome of a novel virus for which we propose the name *Rosellinia*

necatrix megabirnavirus 1 strain W779 (RnMBV1/W779). Megabirna is from the much greater (mega) size (approximately 16 kbp) of its bisegmented dsRNA genome (birna for bipartite dsRNA genome) than those of members of the family Birnaviridae (approximately 6 kbp) (Delmas *et al*., 2005) or Picobirnaviridae (approximately 4 kbp) (http: //www.expasy.ch/viralzone/all_by_protein/603.html). dsRNA-1 and -2 are similar to each other in genetic organization; that is, each has an extremely long 5' UTR, two ORFs, and a relatively short 3' UTR. Their genetic organization aises an interesting question as to how the ORFs are expressed. The extremely long (~1.6 kb) 5' UTRs of dsRNA-1 and -2 are similar in sequence (Fig. 8) and contain a number of minicistrons. Those minicistrons would hamper canonical translation of 5'-proximal large ORF1 and -3, according to the scanning model (Kozak, 1980). The 5'-proximal ORFs are likely to be expressed by a noncanonical translational mechanism. A parallelism in size and the presence of mini-ORFs are found between the 5' UTRs of RnMBV1 and members of the genus Aphthovirus of the family *Picornaviridae.* Picornaviruses utilize internal ribosome entry site (IRES)-mediated translation for expression of their polyproteins, requiring different sets of initiation factors, depending on the IRES type (Bruenn, 2003). Picornavirus IRES sequences have well-defined structural and sequence motifs. Although no IRES is identified in fungal or mycoviral mRNAs, IRES activities are implicated in the 5' UTRs of genome size mRNAs of hypoviruses (Hillman and Suzuki, 2004) and totiviruses (Ghabrial and Suzuki, 2009). It will be interesting to examine whether the 5' UTRs of RnMBV1 dsRNA-1 and dsRNA-2 serve as IRES sites. Guo *et al*. (Guo, *et al*., 2009) developed a reporter assay system to assess low expression levels of a downstream gene in a dicistronic configuration in the filamentous fungus *C. parasitica*. A similar approach could be utilized to delineate the possible expression strategy for ORF1 and -3. How 3'-proximal ORF2 (P2) and ORF4 (P4) are expressed is also largely unknown. Preliminary experiments failed to identify subgenomic RNAs corresponding to the downstream ORFs, while full-length mRNAs of dsRNA-1 and -2 were detected, suggesting a polycistronic nature of those mRNAs. It should be noted that dsRNA-1 ORF2 is in 1 frame relative to ORF1 and an in-frame UGA triplet is located at map positions 5332 to 5334, which is 69 codons upstream of the start codon of ORF2 at positions 5539 to 5541 and 25 nt upstream of the stop codon of ORF1 at 5357 to 5359 (Fig. 9B). Moreover, the FSFinder program readily identified a possible

slippery sequence, 5'-A-AAA-AAC-3' (consensus sequence: X-XXN-NNZ; X, any; N, A or U; Z, any but G) and a stem-loop structure at bases 5350 to 5356 and 5368 to 5425. These two elements are situated immediately upstream and downstream of the termination codon of ORF1, respectively. These findings may suggest that ORF2 is expressed by a 1 frameshift mechanism. This strategy is widely used by many animal (e.g., members of the family *Retroviridae* and the order *Nidovirales*), plant (e.g., members of the family *Luteoviridae* and the genus *Dianthovirus*), and fungal (e.g., members of the genus *Totivirus*) viruses. In almost all of these examples, the catalytic domains (pol or RdRp), which are required for their genome replication, are expressed by -1 frameshifting. In support of this notion, a minor protein band of 250 kDa was detected (Fig. 6), although it can be a dimer form of the 135-kDa capsid protein. An immunological and/or biochemical study is needed to test this possibility. dsRNA-2 ORF4 is situated in the same frame as ORF3 without termination codons between the ORF3 stop and ORF4 start codons. A readthrough mechanism may allow expression of ORF4 as a fusion protein with P3 from the dsRNA-2 full-length mRNA if ORF4 (P4) is translated. As an alternative possibility, IRES-mediated translation of ORF4 is not ruled out. While proteins P1, P3, and P4 do not show any significant sequence similarity to known protein sequences, dsRNA-1 ORF2-encoded P2 shows low levels of sequence identity to RdRps encoded by virus-like dsRNAs and dsRNA mycoviruses belonging to the families *Totiviridae* and *Chrysoviridae* (Table 3). However, RnMBV1 is readily differentiated from these related mycoviruses in genome size, genome segment number, and/or genome organization. Moreover, RnMBV1 particles are larger than those of any other International Committee for the Taxonomy of Viruses-approved mycoviruses, except mycoreoviruses, which are known to form rigid particles (30 to 40 nm in diameter). The phylogenetic tree generated based on RdRp sequence alignment (Fig. 12) reveals that RnMBV1 RdRp clusters with the partially characterized dsRNA elements PgV1 and LeV-HKB from basidiomycetes (Fig. 13), with a high bootstrap value of 951, and is placed separately from other known dsRNA mycoviruses. The members of this cluster and members of the family *Chrysoviridae* might have diverged from an immediate ancestral virus. The grouping of these members is supported by a relatively high bootstrap value of 839. Based on these data, we propose a new virus family, *Megabirnaviridae*, containing RnMBV1/W779 as the type species. At least one

tentative member of the proposed family occurs in strain W8 of *R. necatrix* that is coinfected with a partitivirus, RnPV1.

Corresponding proteins between RnMBV1 and the tentative member exhibit moderate levels of sequence identity. Furthermore, another strain of RnMBV1 was detected at a geographically distant location from Ibaraki Prefecture where W779 was collected. These results show that members of the proposed *Megabirnaviridae* family occur widely in *R. necatrix*. It is often difficult to establish the etiology of mycovirus because of the lack of an introduction method (Ghabrial and Suzuki, 2008). One of the solutions to this problem is the construction of infectious viral cDNA clones or preparation of in vitro-synthesized transcripts derived from virus cDNA clones. Examples include plus-sense ssRNA fungal viruses like hypoviruses and narnaviruses for which virus infection can be initiated by transcripts from chromosomally integrated full-length viral cDNA or by synthetic transcripts directly introduced into the cytoplasm of host cells (Chen et al., 1994; Choi and Nuss, 1992; Esteban and Fujimura, 2003). Another approach is virion transfection using purified virus particles. However, this approach has rarely been successful. Thus, mycoviruses were once regarded as "noninfectious, endogenous, or heritable" (Ghabrial, 2001). Recently, reproducible PEG-mediated transfection methods with virus particles were developed for mycoreoviruses (Hillman and Suzuki, 2004; Hillman *et al*., 2004). Since then, the approach was applied to not only members of the genus Mycoreovirus (Sasaki *et al*., 2007) but also a member of the family *Partitiviridae* (Sasaki *et al*., 2006). This study provided the third example of such viruses that are infectious to *R. necatrix* as particles. Particles of dsRNA viruses are believed to contain all of the enzymatic activities necessary for transcription and the synthesis of viral mRNA, leading to the onset of infection. The virion transfection technique may allow examination of the experimental host range of not only RnMBV1 but also other dsRNA mycoviruses producing rigid particles like members of the families *Chrysoviridae* and *Totiviridae*. This study clearly established a virus etiology for the reduced virulence and vegetative mycelial growth of *R. necatrix*. Curing of RnMBV1 in W779 results in the generation of an isogenic fungal strain, W1015, that shows an enhanced growth rate and virulence level (Fig. 2). The virus is able to infect strains W370T1 and W97 via virion transfection and induce a similar set of phenotypic alterations, i.e., reduced mycelial growth and attenuated virulence (hypovirulence) (Fig. 14). From these RnMBV1-

infected strains, virus particles encapsidating dsRNA-1 and -2 were isolated. The transfected fungal strains, W97 and 370T1, belonging to MCG80 and MCG139 (Arakawa *et al*., 2002), are vegetatively incompatible with W779 (MCG351) (Ikeda *et al*., 2005) and unable to receive RnMBV1 when cocultured with W779. It was confirmed that the transfected strains shown in Fig. 14 carried the phenotypic markers of their parents. Thus, a possibility of contamination with the W779 fungal cells during transfection is ruled out. These combined results represent the completion of Koch's postulates for this novel virus and provide a basis for future identification of viral and host factors associated with symptom expression. This study was conducted as part of a project entitled Development of Introduction Protocols of Virocontrol Agents into Phytopathogenic Fungi toward a feasible virocontrol of primarily root rot of fruit trees in Japan (Ghabrial and Suzuki, 2009). To achieve virocontrol (one form of biological control) of the disease white root rot, breach three barriers were need to: (i) isolation of mycoviruses with virocontrol potential (virocontrol agents), (ii) transfection of fungal strains of interest with virocontrol agents, and (iii) efficient spread of virocontrol agents ideally at individual and population levels, as well as the conversion of virulent fungal strains to hypovirulent ones in the soil once they are introduced. As discussed above, the novel virus RnMBV1 is infectious as particles and able to confer hypovirulence, under laboratory conditions, on virus-free fungal strains that otherwise are virulent. Therefore, the first two constraints were overcame by developing an artificial introduction method for RnMBV1 with the ability to attenuate virulence. From the practical point of view, issue iii is critical and may be influenced by many factors, like the ecological fitness of virocontrol agents and the genetic structures of causal fungal pathogens. One crucial factor is the diversity of MCGs in a given population, since lateral transmission of mycoviruses is expected to be inversely correlated with MCG diversity (Milgroom and Cortesi, 2004). This notion is exemplified by the successful biocontrol of chestnut blight disease in Europe. An opposing example is the failure of attempts at biocontrol of the same disease in eastern North America, where complex populations of the causal pathogen are presumed to impede the spread of virulence-attenuating viruses via anastomosis in a plot. Interesting ecological studies of the white root rot fungus were carried out previously that showed simple population structures of the fungus in single infested orchards of Japanese pears (H. Nakamura, personal

communication). That is, only a few strains belonging to different MCGs dominate single infested fields. The less diverse structure of fungal populations will undoubtedly stimulate future research on the virocontrol of white root rot disease.

Chapter 3. Biological and molecular characterization of Rosellinia necatrix megabirnavirus 1 in an experimental host, *Cryphonectria parasitica*

3.1. Introduction

Rosellinia necatrix megabirnavirus 1 (RnMBV1), a member of the family *Megabirnaviridae*, was originally isolated from a field fungal isolate (W779) of the white root rot fungus (Ikeda *et al.*, 2004), which is an important soil-borne phytopathogen. Molecular characterization revealed that two 9.0-kbp and 7.4-kbp dsRNA genome segments termed dsRNA1 and dsRNA2, respectively, are encapsidated in icosahedral particles of 50 nm in diameter (Chiba *et al.*, 2009). Each segment possesses an extremely long 5' untranslated region (UTR) of approximately 1.6 kbp, two open reading frames (ORF1 and ORF2 on dsRNA1, and ORF3 and ORF4 on dsRNA2), and a relatively short 3' UTR. The 5' UTR shows high levels of overall sequence identity (70%) with highly conserved sequence stretches located between the two segments, while the remaining sequences are unrelated except for the 3' terminal conserved octamer sequence –UUUUUCGC-3'. ORF1 encodes the major 135-kDa capsid protein (CP), while ORF2, overlapping ORF1 in its 5'-terminal portion, encodes an RNA-dependent RNA polymerase (RdRp) domain (Chiba *et al.*, 2009). The long 5' UTR is believed to be involved in non-canonical translation such as that mediated by the internal ribosome entry site (IRES). DsRNA1 has ORF2 on the -1 frame with regard to ORF1 and a heptamer slippery sequence (5'-A-AAA-AAC-3') with a potential stem-loop/pseudo-knot structure immediately upstream and downstream of the CP frame stop codon. These sequence features are similar to those found near the consensus slippery sequence of viral mRNAs translated via -1 frameshift mechanisms (Dinman *et al.*, 1991; Dinman & Wickner, 1992; Li *et al.*, 2001). Therefore, Chiba et al. (2009) assumed that ORF2 is expressed via -1 ribosomal frameshifting from full-length transcripts of dsRNA1. ORF3 and ORF4 are situated in tandem on dsRNA2, and would encode proteins with no significant sequence similarity to any known protein in the

databases. However, little is known about whether the RnMBV1 ORFs, except for ORF1, are expressed in infected mycelia.

RnMBV1 causes severe reduction of both mycelial growth of *R. necatrix* in synthetic media and fungal virulence to plant hosts, irrespective of strain. (Chiba et al., 2009). This has been corroborated using a transfection protocol originally devised for a mycoreovirus (Hillman *et al.*, 2004). The virus is also transmissible horizontally between mycelially compatible fungal strains leading to conversion of a virulent to a hypovirulent strain (S. Kanematsu and N. Suzuki, unpublished data). Based on these properties and the availability of an artificial introduction method, RnMBV1 is considered to be a candidate virocontrol (biological control using viruses) agent with strong potential for controlling white root rot (Kondo *et al.*, 2013). These background circumstances allowed us to address whether RnMBV1 can infect other phytopathogenic fungi and confer hypovirulence, as tested for other viruses for which artificial introduction systems are available,e.g. hypoviruses and mycoviruses. (Chen *et al.*, 1996b; Kanematsu *et al.*, 2010; Sasaki *et al.*, 2002).

The chestnut blight fungus, *Cryphonectria parasitica*, has attracted a great deal of attention not only as a destructive plant pathogen but also as a model filamentous ascomycete for studies of virus/virus and virus/host interactions in view of the availability of its host genome sequence, a number of mutant strains, protocols for multiple transformation, transfection, and reporter assay, and its versatility for stable culture under laboratory conditions (Dawe & Nuss, 2013; Hillman & Suzuki, 2004; Nuss, 2005; Sun *et al.*, 2006). The fungus is a natural host to many different viruses (Hillman & Suzuki, 2004) and has contributed to various facets of fungal virology research. Host factors associated with virus replication and/or symptom expression have been isolated using different methods and characterized (Faruk *et al.*, 2008; Segers *et al.*, 2007; Sun *et al.*, 2008; 2009). Interestingly, *C. parasitica* also supports replication of heterologous viruses from Xylariales, an order of white root rot fungus taxonomically different from the Diaporthales accommodating *C. parasitica* (Kanematsu *et al.*, 2010), and evokes RNA silencing of these viruses.

In the present study, we carried out biological and molecular characterization of RnMBV1 using the wild type and a mutant strain (defective in anti-viral defense) of the chestnut blight fungus that is taxonomically distinct from the original host fungus, *R. necatrix*. This study represents an additional example of the usefulness of *C. parasitica* for exploring the pathogenesis and gene expression strategy of a heterologous virus.

3.2. Materials and methods

3.2.1 Fungal and virus strains

All fungal and viral strains used in this study are shown in Table 1. RnMBV1-W779 is the wild-type field strain described previously (Chiba *et al.*, 2009). The standard virus-free strain EP155 and an RNA silencing-defective *dcl-2* knock-out mutant (Δ*dcl-2*) (Segers *et al.*, 2007) of *C. parasitica,* a generous gift from Dr. Donald L Nuss served as the recipient of the virus. Both transfectants and fusants, fungal strains generated after transfection and hyphal anastomosis (lateral virus transmission), respectively carry RnMBV1-W779. Fungal strains were grown at 25-27^{o}C for 5-7 days in either Difco^{TM} potato dextrose broth (PDB) for RNA/DNA extraction and spheroplast preparations, or Difco^{TM} potato dextrose agar (PDA) or Vogel's media (Vogel, 1956) for pre-culture and phenotypic observation.

3.2.2 Transfection of *C. parasitica* spheroplasts

Transfection of *C. parasitica* was performed as described by Hillman *et al.* (2004). Spheroplasts of *C. parasitica* Δ*dcl-2* strains were prepared using the methods of Eusebio-Cope et al. (2009). RnMBV1 virions were purified according to the method of Chiba *et al.* (2009) by differential and sucrose or cesium sulfate gradient centrifugation. Purified particles were transfected into Δ*dcl-2* spheroplasts using polyethylene glycol (PEG). After regeneration of spheroplasts, mycelial plugs from multiple positions were transferred onto new PDA plates and propagated. Virus infections (transfections) were analyzed by AGE of dsRNA.

3.2.3 Transfection of *R. necatrix* W1015 spheroplast

Transfection of *R. necatrix* was performed as described by Kanematsu *et al.* (2004) with minor modifications. W1015 strain grown in PDA (Difco) culture was cut into small pieces, inoculated in PDB (Difco) and incubated in dark at 25^{o}C without shaking for 2 days. Physical breaking of mycelia was done by pipetting the PDA-containing fungal culture several times. The fragmented mycelia were transferred into the new PDB and incubated in dark at 25^{o}C without shaking for 2 days. The young mycelia were harvested by centrifugation, washed once with osmoticum (0.6M mannitol, 10mM 3-morpholinopropanesulfonic acid [MPPS], pH7.0) and centrifuged to collect the mycelia. The mycelia were resuspended in filter-sterilized enzyme osmoticum mixture containing 0.4% Zymolyase 100T and incubated at 20-22 ^{o}C for 3-5 hr with agitation. The spheroplasts were collected by filtering through two layers of gauze cloth contained in stainless steel mesh with 45 μm opening, centrifuged and washed twice with osmoticum. The pellets were suspended in MMC buffer (0.6M mannitol, 10mM 3-morpholinopropanesulfonic acid [MOPS], pH7.0 and 10mM$CaCl_2$). The spheroplasts were kept on ice and final concentration determined with a hemacytometer.

Virus particles were purified using Chiba *et al.* (2009) and introduced into spheroplasts of W1015 and Δ*dcl-2* strain using PEG as described by Sasaki et al. (2006, 2007) and Hillman et al. (2004), respectively. After regeneration of spheroplasts, mycelial plugs from multiple positions were transferred onto new PDA plates and propagated. Virus infections (transfections) were analyzed by AGE of dsRNA.

3.2.4 Phenotypic measurements of fungal colonies

Effects of virus infection on fungal colony morphology, growth, sporulation and pathogenicity were evaluated. Growth rates of fungal colonies on PDA and Vogel's minimal medium with 1 % (w/v) sucrose as the normal carbon source or 1% fructose as specified, kept on a bench-top at 25-27^{o}C for 7 days were estimated. Colony areas of 3 replicates were averaged. Phenotypic observation was carried out and recorded.

Sporulation level was evaluated using the method of Hillman et al. (Hillman *et al.*, 1990). Fungal strains were cultured on PDA plates in 60 mm diameter for 14 days, the

first 4 days on the bench-top and the last 10 days under moderate light of approximately 3000 lux using a 16-h photoperiod. Asexual spores liberated in 6 ml of 0.15% Tween-20 were counted.

Virulence levels were measured in apples (cv. Jonagold) as the areas of lesions induced by fungal strains, as described by Hillman *et al.* (2004).

3.2.5 Transmission assay

Vertical transmission through asexual spores was evaluated as described by Eusebio-Cope (Eusebio-Cope *et al.*, 2010). Spore suspensions prepared as above were plated onto PDA, incubated at 24-26^{o}C for 2 days, and the germinated spores were transferred onto new PDA. Approximately 10 single spore germlings were grown on a PDA plate (9 cm in diameter) (Sun *et al.*, 2006). Two weeks after inoculation on PDA, virus-infected colonies (visually estimated for Δ*dcl-2*) were scored. This was confirmed by dsRNA from single spore isolates showing a virus-infected phenotype. Determination of transmission rates for RnMBV1 in EP155 was done by combined Northern blot and reverse-transcription (RT)-PCR of mRNA, because virus-infected colonies showed a phenotype distinct from but similar to virus-free colonies and a low level of viral dsRNA. SsRNA fractions were bulked from three single spore germlings and subjected to Northern blot. When bulked samples tested positive, individual isolates were examined by RT-PCR using L1L2-5' (GCATAAAAAGAGAAGGAAGTT) and L1-1RV1 (GAGATTTAAAAATCCGTGAAA) primers.

Horizontal transmission through hyphal contact was performed as described by Chiba *et al.* (2013b). The virus-infected donor strains were cultured with a virus-free recipient strains at a distance of 1 cm on a PDA plate and incubated at 24-26^{o}C. After 2 weeks of hyphal contact, mycelial plugs were taken from different places in the recipient side and subcultured into PDB for 7 days for RNA preparation.

3.2.6 RNA preparation and Northern blot analysis

Total RNA was prepared from the mycelia of fungal strains cultured in 20 ml PDB or on PDA-cellophane (for small-scale preparation) in which fungal mycelia were

homogenized with a mortar and pestle in the presence of liquid nitrogen. Nucleic acid were isolated by two rounds of phenol/chloroform and one round of chloroform in extraction buffer (100mM Tris-HCl, pH8.0, 200 mMNaCl, 4 mM EDTA, 4% SDS) and precipitated by ethanol. To eliminate fungal chromosomal DNA, extracted nucleic acids were digested by RQ1 DNase I (Promega, Madison, WI) in the presence of an RNase inhibitor (40 units) (Toyobo, Tokyo) for 1 h at 37^{o}C followed by phenol/chloroform, chloroform extraction and ethanol precipitation (Eusebio-Cope *et al.*, 2010). The final concentration of the total RNA suspended in sterile distilled water was adjusted to an optical density of 25 at 260 nm (OD_{260}) (about 1 mg/ml) and electrophoresed in 1.4% agarose gel in 1XTAE buffer.

The dsRNA fractions were obtained from total RNA, which had not been treated with nucleases, but subjected to CC41-mediated column chromatography (Eusebio-Cope and Suzuki, unpublished result). The clarified RNA extracts obtained after one round of phenol/chloroform and chloroform were mixed with 0.05 g/ml of CC41 (Whatman, UK) in 1X STE (100mM NaCl, 10mM Tris-HCl, pH 6.8, 1mM EDTA) buffer adjusted to 16% (v/v) ethanol and then mix in room temperature for 2 hr. The mixture was centrifuged and washed with 16% ethanol in STE buffer at least three times. The dsRNA fraction was then eluted by 1XSTE, precipitated by ethanol and electrophoresed in 1% agarose gel in 1XTAE buffer.

For ssRNA preparation, lithium chloride (LiCl) precipitation was performed instead of ethanol precipitation. 10M LiCl was added to extracted nucleic acids at a final concentration at 2M LiCl, precipitated overnight at 4 ^{o}C and then centrifuged to obtain ssRNA.

For Northern blot analysis, ssRNA was heat-denatured (65^{o}C for 15 min) and electrophoresed under denaturing conditions. The separated RNA was capillary-transferred onto a Hybond-N+ nylon membrane (Amersham Biosciences, Buckingham, England). The membrane was treated with dioxigenin (DIG)-11-dUTP-labelled DNA probes amplified from cDNA by PCR (Roche Diagnostics, Mannheim, Germany). Pre-

hybridization, hybridization, and detection of hybridization signals were performed as described by Suzuki *et al.* (2003).

3.2.7 RT-PCR and sequence determination

RT-PCR was performed as described by Suzuki *et al.* (2004). The dsRNA fraction prepared from a mini-scale culture was denatured in the presence of DMSO (Asamizu *et al.*, 1985). Reverse transcription and subsequent PCR involved RnMBV1-specific deoxyoligonucleotide as primers (Table 2). Amplified DNA fragments were sequenced directly or indirectly after being cloned into pGEM T-easy (Promega). Three or four RT-PCR reactions were set to amplify DNA fragments spanning the 5'-terminal, central, and 3'-terminal portions of the RnMBV1 dsRNA1 or dsRNA2, respectively.

3.2.8 Antigen preparation for antibody production, purification of antibody and western blotting

(1) Subcloning into pGEX-6P-1 (Promega) and pMAL-c2X (New England Biolabs). As described by Suzuki et al. (Suzuki *et al.*, 1994), recombinant proteins encoded by N and C terminal portions from each of the ORF1-coded CP (aa 1-367 and aa 891-1240 ;Fig. 18A) and ORF3-coded large protein (aa 1-397 and aa 1,080-1,426 ;Fig. 17A) and N and C terminal portions of ORF2-coded RdRp (aa 1-381 and aa 764-1,111 ;Fig. 18A) were synthesized by PCR using sense and antisense primers (Table 2), and then ligated into pGEM-Teasy (Promega). The recombination expression plasmids were constructed by digestion of specific restriction enzyme, purification of inserted DNA segments and ligation into specific cloning site of expression vector. ORF1 and 3 were fused with GST (glutathione S-transferase) and expressed using the expression vector pGEX-6P-1 and ORF2 were expressed as fusion proteins with MBP (maltose-binding protein) using pMAL-c2X.

(2) Expression and purification. Fusion proteins were expressed from pGEX-6P-1 and pMAL-c2X constructs. Individual expression plasmid was transformed into *E. coli* BL21 strain. The overnight culture from the transformed bacteria cells were diluted to 1:1000 in rich growth medium (16 g of tryptone, 10 g of yeast extract and 5 g of NaCl in 1000 ml of distill water) containing 100 mg Ampicillin per milliliter and

cultured at 37°C with shaking until the optimal density reached 0.5 (about 3 hr). The *E. coli* cells were then induced by 0.5mM IPTG at 15°C with shaking for 20 hr. The induced cells were harvested at 5000 xg at 4°C for 15 min, resuspended in lysing buffer (100mM Tris-HCl, pH8.0, 10mM KCl, 5mM $MgSO_4$, 0.4 M sucrose, 10mM mercapthoethanol, 10% glycerol), sonicated on ice to break the cells and centrifuged at 5000 xg for 20 min at 4°C. The pellets were resuspended with minimal volume of lysing buffer, subjected to 10%SDS-PAGE, and eluted the insoluble protein from gel by electro-elution. The supernatant was then clarified by filter and purified with sepharose 4B (New England Biolabs). The mixture of soluble and insoluble protein was used as antigens in rabbits.

(3) Western blotting was performed as described by Sun and Suzuki (Sun & Suzuki, 2008). Total protein fractions were electrophoresed in 10% SDS-PAGE gel and then electro-transferred to a nitrocellulose polyvinylidene difluoride membrane (Bio-Rad) and immuno-detected as described by Suzuki et al. (1994) or using the ECL Plus system (GE Healthcare). To reduce non-specific reactions, antisera were pre-absorbed with acetone powdered mycelial (virus-free) homogenates.

(4) Purification of polyclonal antibody. The polyclonal antibody against fusion protein of ORF3 was purified by affinity sepharose (NHS-activated sepharose 4 Fast Flow) from Amersham Pharmacia Biotech. The protocol is briefly as follows, pre-cleaning the NHS-activated sepharose by distilled water and coupling buffer (50 mM $NaHCO_3$ pH 8.5) and coupling with antigen. After washing and blocking with blocking buffer (0.1 M ethanolamine, 50 mM Tris –HCl, pH 8.0), the precleaned antibody was filtered and mixed gently overnight at 4°C. After several times of washing with buffer (1M NaCl, 1% Triton X-100, 20 mM Tris-HCl, pH 7.5), the antibody was eluted with 0.1 M Gly-HCl (pH 2.5).

(5) EP155 Acetone powder preparation. *C. parasitica* EP155 was cultured in 1 L of PDB at 25 °C for 1 week. The mycelia were harvested and ground into powder form with liquid nitrogen. Forty ml of PBS buffer was added, centrifuged and supernatant discarded. The 40 ml of cold acetone was added to resuspend the pelleted mycelia,

incubated at -80^{o}C for 1 hour and centrifuged at 14,000 rpm for 15 min. The pellets were then dried at room temperature and kept at -20^{o}C. Diluted purified antibody (1:1000) was added with EP155 acetone powder, mixed at 4^{o}C overnight and centrifuged at 11,000 rpm, 4^{o}C for 5 min.

3.2.9 Pigment analysis

Pigment analysis was determined as previously described by Hillman *et al*. (1990) with a minor modification. Fungal strains were cultured in 25 ml PDB (Difco) for 12 days. Mycelia were harvested and ground into powder form using liquid nitrogen. Absolute ethanol (1:1, weight:volume) was added to the mycelial powder and homogenized. One milliliter of aliquot was transferred to new 1.5 ml eppendorf tube and incubated at room temperature for 3 hours followed by centrifugation at 12,500 rpm for 1 min. The absorbance at 454 nm was estimated with an Ultrospec 2000 (Pharmacia Biotech) spectrometer. Alternatively, pigment production was also visually estimated on PDA culture.

3.3 Results

3.3.1. Transfection of fungal spheroplasts with virus particles

In an attempt to introduce RnMBV1 into experimental host, *C. parasitica*, spheroplasts of *C. parasitica* standard strain (EP155) and a strain lacking dicer 2 gene (Δ*dcl-2*) were transfected with purified virus particles of RnMBV1. DsRNA contained in individual transfectant was analyzed after 1 week after transfection. In Δ*dcl-2*, fifteen out of twenty five fungal colonies infected with wild type RnMBV1 and containing dsRNAs of approximately 8.9 kbp and 7.2 kbp were obtained. While, nine fungal colonies harbored the other type of dsRNA genome rearrangement RnMBV1 (Fig. 1).

Therefore, in order to examine whether wild-type RnMBV1 was able to infect the standard strain, wild-type RnMBV1 was transferred to EP155 via anastomosis with Δ*dcl-2*/RnMBV1 (#10) as a virus donor. After 2 weeks of fusion RnMBV1 was able to

infect EP155 and Δ*dcl*2 recipient strains. From PDA fusion plate (Fig. 2), conversion of Δ*dcl*-2 into Δ*dcl*-2 harboring RnMBV1 can be observed easily because of the phenotype change. Meanwhile, movement of RnMBV1 into infected EP155 is difficult to observe on PDA plate due to its slightly altered phenotype. Results obtained from visual inspection were confirmed by extraction of dsRNA of RnMBV1 from recipient strains. The detected dsRNAs were similar to wild type RnMBV1 in both EP155 and Δ*dcl*-2 (Fig. 3).

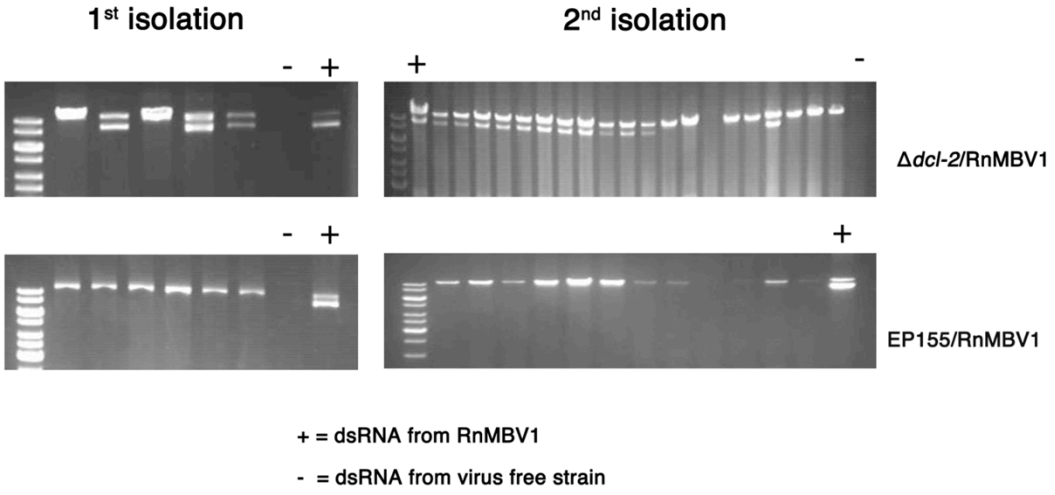

Fig. 1. Infection of a non-natural host, *C. parasitica* by RnMBV1. (a) Agarose gel electrophoretic analysis of dsRNA from transfectants. Spheroplasts of Δ*dcl-2* were transfected by purified RnMBV1 particles from the original *R. necatrix* W779. Numbers above the lanes of the 1% agarose gel refer to independent transfectants. DsRNA fractions from virus-free Δ*dcl-2*, purified RnMBV1 from W779, and DNA size standards (lane M, Fermentas) were electrophoresed in parallel.

Table1. Fungal and viral strains used in this study.

Strain	Description	Reference or Source
Fungal		
EP155	Virus-free field isolate of *C. parasitica*	ATCC 38755
EP155/RnMBV1(#3)	EP155 infected with RnMBV1	This study
EP155/RnMBV1(#1)	EP155 infected with genome rearrangement RnMBV1	This study
Δ*dcl-2*	A *dcl-2* knock-out mutant of EP155	Segers *et al*. (2007)
Δ*dc-2*/RnMBV1(#10)	Δ*dcl-2* infected with RnMBV1	This study
Δ*dc-2*/RnMBV1(#1)	Δ*dcl-2* infected with genome rearrangement RnMBV1	
W779	RnMBV1-carrying field isolate of *R. necatrix*	Chiba *et al.* (2009)
W1015	A virus-cured strain of W779	Chiba *et al.* (2009)
Viral		
RnMBV1	Prototype of the family *Megabirnaviridae*	Chiba *et al.* (2009)

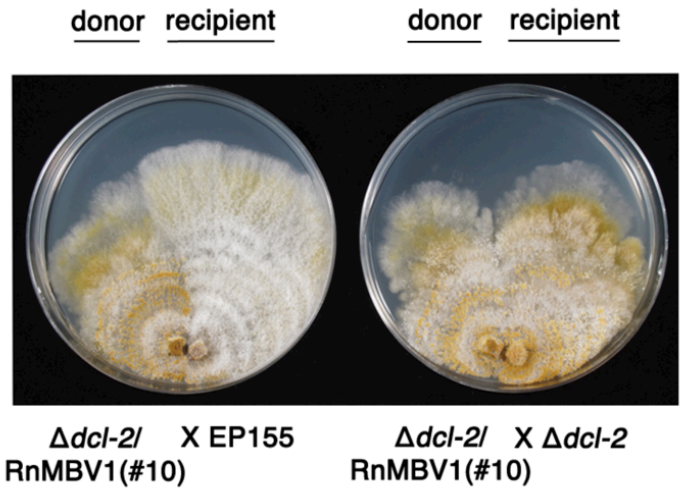

Fig. 2. Introduction of RnMBV1 to the *C. parasitica* standard strain EP155 from RnMBV1-infected Δ*dcl-2* via hyphal fusion (anastomosis). The donor strain Δ*dcl-2* infected by RnMBV1 (#10 in a) was anastomosed with either EP155 or Δ*dcl-2* as a recipient.

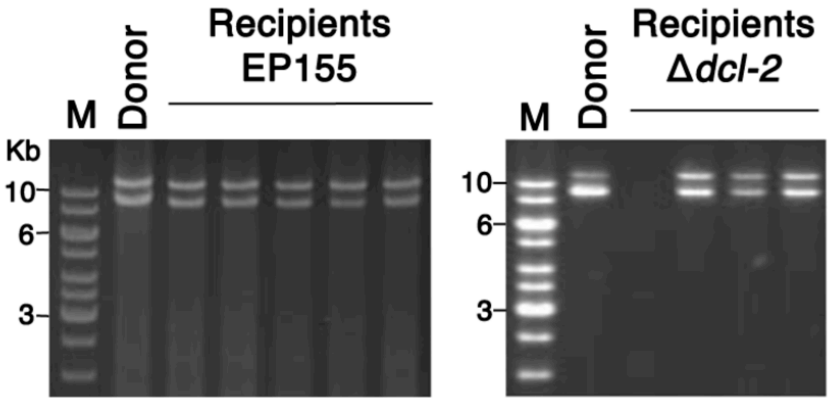

Fig. 3. Detection of viral dsRNAs from recipient strains. Fungal subcultures from the recipient sides of co-cultures as in Fig. 2 were subjected to dsRNA extraction and subsequent agarose gel electrophoresis. Each lane represents independent fusant.

Northern blot analysis was first performed using ssRNA. As shown in Fig. 4, probe1 generated from dsRNA1 allowed detection of single band of dsRNA1 in Δ*dcl-2* /RnMBV1 (#1 and #10) and EP155/RnMBV1 (#1 and #3) (Lane: 1, 2, 3 and 4) and showed the same migration position with RnMBV1 (lane 7). In the case of probe 2 which represents region similarity in dsRNA1 and 2, Δ*dcl-2*/RnMBV1 (#10) and EP155/RnMBV1 (#3) exhibited hybridization to dsRNA1 and dsRNA2 segments (lane: 2 and 4) and showed the same dsRNA pattern with RnMBV1 (lane:7). When probe3 hybridizing to dsRNA2 was used, similar migration position of single band of dsRNA2 among RnMBV1 (lane 7), Δ*dcl-2*/RnMBV1 (#10) and EP155/RnMBV1 (#3) (lane 2 and 4) were found. Surprisingly, hybridization with probe2 and probe3 of Δ*dcl*-2-RnMBV1 (#1) showed its difference to EP155/RnMBV1 (#1) in which the former harbored genome rearrangement of dsRNA patterns not found in RnMBV1 (control ;lane7). Probe2 showed only one band while probe 3 detected the distinct band of dsRNA2 in rearrangement RnMBV1 infected fungal isolates (compare lane 1 and 2 with lane 7). Whereas no dsRNA1 or dsRNA2 signals were detected in uninfected *C. parasitica* Δ*dcl-2*, EP155 and *R. necatrix* (W1015) (lane: 5, 6 and 8) when hybridized with probes1, 2 or 3.

To determine genetic organization of RnMBV1 in *C. parasitica*, RT-PCR was carried out using DNAse treated mRNA as template and primer set shown in Table 2. As shown in Fig. 5, the same expected size of all fragments were observed between Δ*dcl-2*/RnMBV1(#10) and RnMBV1.

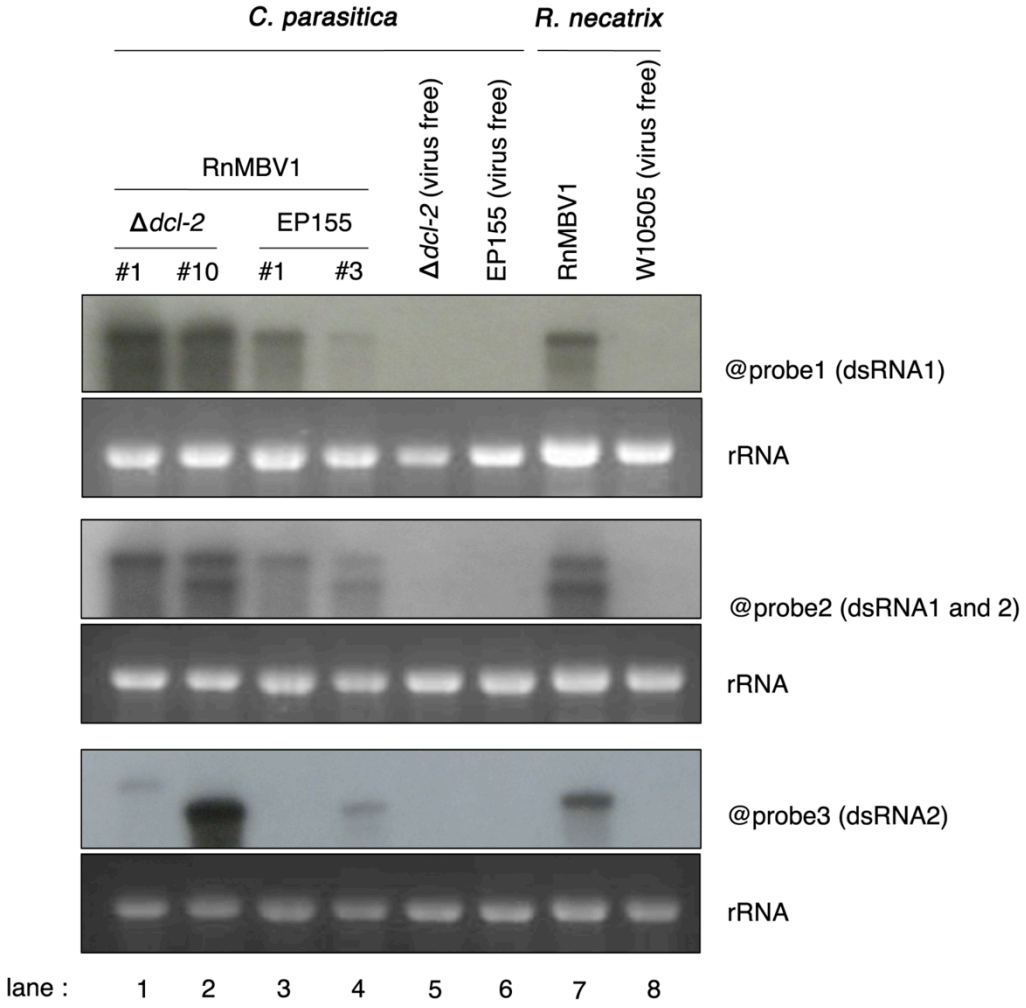

Fig. 4. Northern blot analysis of genome rearrangement and wild-type RnMBV1 infected *C. parasitica*. SsRNA isolated from virus free and virus-infected strain EP155 and Δ*dcl*2 were fractionated into 1% denatured gel in 1xMOPs buffer. After blotting onto the nylon membrane, the membrane was hybridized with DIG-11-dUTP-labelled DNA fragments of RnMBV1 probe 1 (dsRNA1), probe 2 (dsRNA1 and 2) and probe 3 (dsRNA2). SsRNA from RnMBV1 virus infected of *R. necatrix* was used as a positive control. Ribosomal RNAs (rRNA) were stained with EtBr and used as a loading reference.

Table 2. Primers used in the experiment

Primer name	Sequence 5'-3'
Primer for cDNA dsRNA-1 synthesis	
L1L2-5'	GCATAAAAAGAGAAGGAAGTT
L1CD1	TGGAGGACATTAGCGATAGC
L1CD2	TCTACAACGAGCCTACTCC
L1CD3	GCTCAGCTTGACTTTTGGG
L1CD4	GTGCACAATGTGCATTCCG
L1CD5	GTTAGCTGCGTAGTCAAGG
L1CD6	AAGGAGATCCACACTGCAG
L1-3'	GCGAAAAAGGGGTCCAGC
Primer for dsRNA1 full-length PCR	
T7L1-5'	TAATACGACTCACTATAGGCATAAAAAGAGAAGGAAGGTTT
L1-Apa-R	AATGAGGGCCCACCAACAA
L1-Apa-F	GTTGGTGGGCCCTCATTTTT
L1-Sal-R	GGAGTCGACCTGGTATCCA
L1-Sal-F	CAGGTCGACTCCAGCGAC
L1-Bam-R	CTAGGATCCGTGCACACAC
L1-Bam-F	CACGGATCCTAGCGTCATG
L1-3'-Not	GCGGCCGCGAAAAAGGGGTCCAGC
Primer for cDNA dsRNA-2 synthesis	
L1L2-5'	GCATAAAAAGAGAAGGAAGGTT
L2CD1	CTCCAAACCTCCAAACGATG
L2CD2	GCAATAACCACCTCGCATTG
L2CD3	TTCGACGTGAAATCCGTTAG
L2CD4	GCGACTTAGTAGATACGGAG
L2-3'	GCGAAAAAACGATGTCAATCG
Primer for dsRNA-2 full-length PCR	
T7L2-5'	TAATACGACTCACTATAGGCATAAAAAGAGAAGGAAGGTTT
L2-Nhe-R	ACATTGGCTAGCGCAACTTC
L2-Nhe-F	GTTGCGCTAGCCAATGTGG
L2-Apa-R	CAAGGGGCCCAGACGCAT
L2-Apa-F	GTCTGGGCCCCTTGGTG
L2-3'-Not	GCGGCCGCGAAAAAACGATGTCAATCG
Primer for antigen preparation	
ORF1-N-FW	CAAGGATCCATGTCTGGCGACAA
ORF1-N-RV	CAACTCGAGGCGAAAATCGATCA
ORF1-C-FW	CAAGGATCCGGCGGTTTCCATAT
ORF1-C-RV	CAACTCGAGTTAGTTTTTTGGTT
ORF2-N-FW	CAATCTAGAATGGATGGTAGGCA
ORF2-N-RV	CCAAAGCTTGCCCAAAGCTATGT
ORF2-C-FW	CAATCTAGATTACAAGCTCCTCA
ORF2-C-RV	CCAAAGCTTTCACATCTTCATCA
ORF3-N-FW	CAAGGATCCATGGGTATCACTTA
ORF3-N-RV	CAACTCGAGGTCTGCGGGTAGTGT
ORF3-C-FW	CAAGGATCCTATGGTGAGTTGTG
ORF3-C-RV	CAACTCGAGCTATTGCATGGTCC

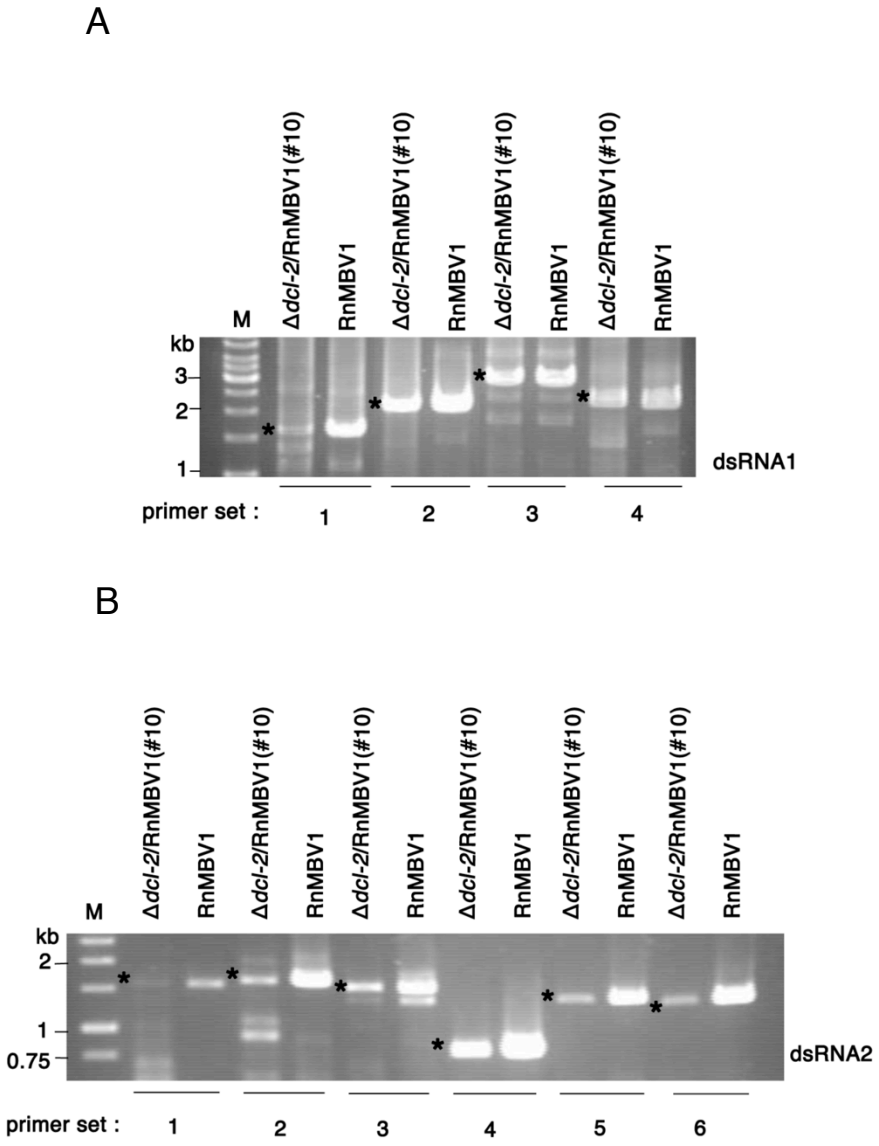

Fig. 5. Agarose gel electrophoresis of RT-PCR on the RnMBV1. RnMBV1 and Δ*dcl*2/RnMBV1 (#10) was used as template in cDNA synthesis and subsequent PCR using primer sets shown in Table 2. (A) Amplified products of dsRNA1 and (B) dsRNA2 was electrophoresed in agarose 1% gel in 0.5XTAE buffer. Size standard were electrophoresed in parallel (lane M) in each gel. Asterisks in A and B refer to expected bands.

cDNA fragments of dsRNA1, 2 and effect of RnMBV1 genome rearrangement to *C. parasitica* will be discussed on the next chapter.

3.3.2. Biological properties of RnMBV1 in *C. parasitica*

Colony morphology of the virus infected strains and virus free parental strains grown under the same conditions were compared. As shown in Fig. 7A, infection of Δ*dcl-2* with RnMBV1 showed a distinct phenotype from virus-free Δ*dcl-2*, which was characterized by irregular margin with less dense mycelia, reduced growth rate and enhanced pigmentation. No drastic effects of RnMBV1 infection on colony morphology of EP155 were apparently observed when cultured on PDA. However, a slight reduction of growth rate and a slight increase of pigmentation were detected (Fig. 6). The morphological differences in the two host strains infected and uninfected with RnMBV1 were more pronounced more on nutrient-limited media (Vogel's) than on PDA (Fig. 7B).

For fungal virulence, above 4 strains were inoculated to apples and their virulence level was evaluated by measuring lesion areas. Virus-free EP155 and Δ*dcl-2* induced large lesion area of 42.63 and 38.85 cm^2, respectively. Whereas, hypovirulence conferred similarly to EP155 and Δ*dcl-2* upon infection by RnMBV1 and showed lesion area of 16.14 cm^2 and 13.42 cm^2, respectively. Those values are significantly smaller than those virus free strains *($p<0.01$)* (Fig. 8).

Effect of virus infection on fungal sporulation is not applicable to assess in *R. necatrix* (original host) because it rarely produce spores under laboratory conditions (Nakamura, 2002). Evaluation in *C. parasitica* showed that RnMBV1-infected colonies sporulated to a level comparable to virus-free in both EP155 and Δ*dcl-2* (Table 3).

Combined results suggested that RnMBV1 is able to infect both *C. parasitica* strains and induce phenotypic changes and virulence attenuation in both the wild-type and RNA silencing-defective strains of the experimental host.

Table 3. Levels of asexual sporulation.

Fungal strain/Virus strain	Number of conidia/ml
Δ*dcl-2*/RnMBV1 #10	$1.31 \times 10^8 \pm 3.01 \times 10^{7a}$
Δ*dcl-2* (virus free)	$2.89 \times 10^8 \pm 5.0 \times 10^{7ab}$
EP155/RnMBV1 #3	$3.58 \times 10^8 \pm 2.7 \times 10^{7bc}$
EP155 (virus free)	$4.70 \times 10^8 \pm 8.03 \times 10^{7c}$

Data (mean±SD.) with different letters are significantly different *(p<0.01)* among treatments (*n*=3).

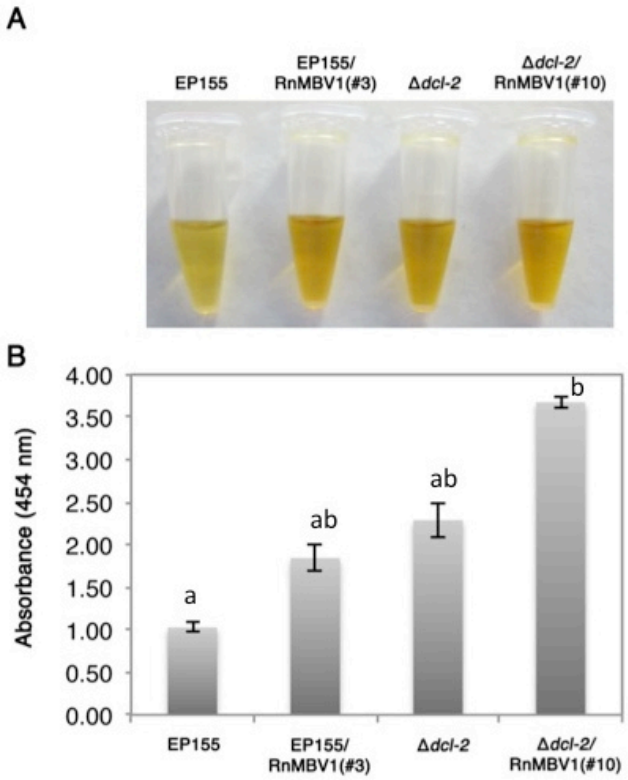

Fig. 6. Comparison of pigment production of RnMBV1 infected EP155 and Δ*dcl-2* compared to virus free strains. (A) The relative levels of pigmentation in different fungal strains in ethanol. (B) Graphical representation of relative level of pigmentation of different strains. Pigmentation was measured as absorbance at 454 nm. Measurement were done in 3 replicates for each strain were used for the measurement to calculate average and standard deviation. Data (mean±SD.) with different letters are significantly different *(p<0.01)* among treatments (*n*=3).

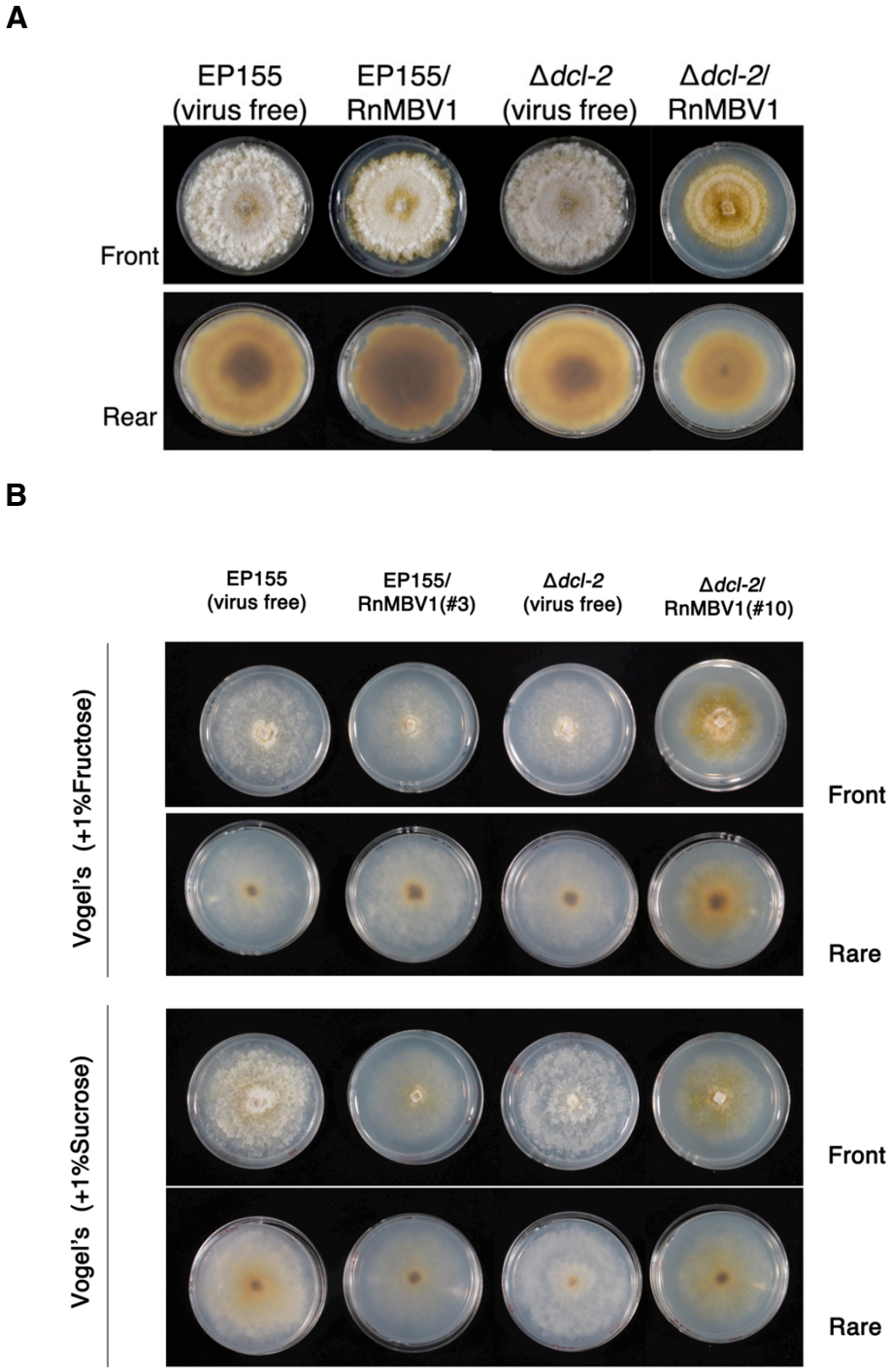

Fig. 7. Colony morphology of *C. parasitica* EP155 and Δ*dcl*-2 infected or uninfected with RnMBV1. (A) Fungal colonies were grown on PDA for 6 days on a bench top and then photographed. (B) Fungal colonies were grown on Vogel's agar supplemented with either 1% sucrose or fructose for 2 weeks at 24°C on a bench top and then photographed.

A

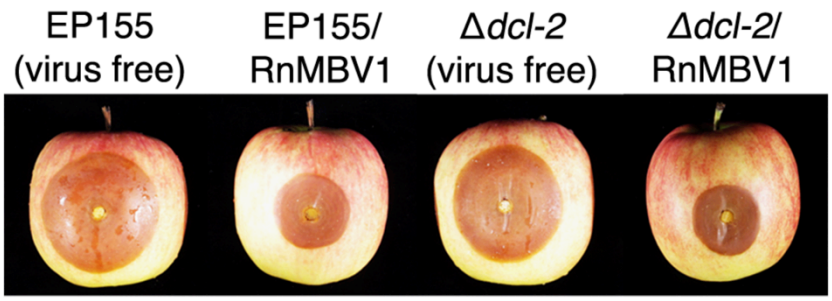

B

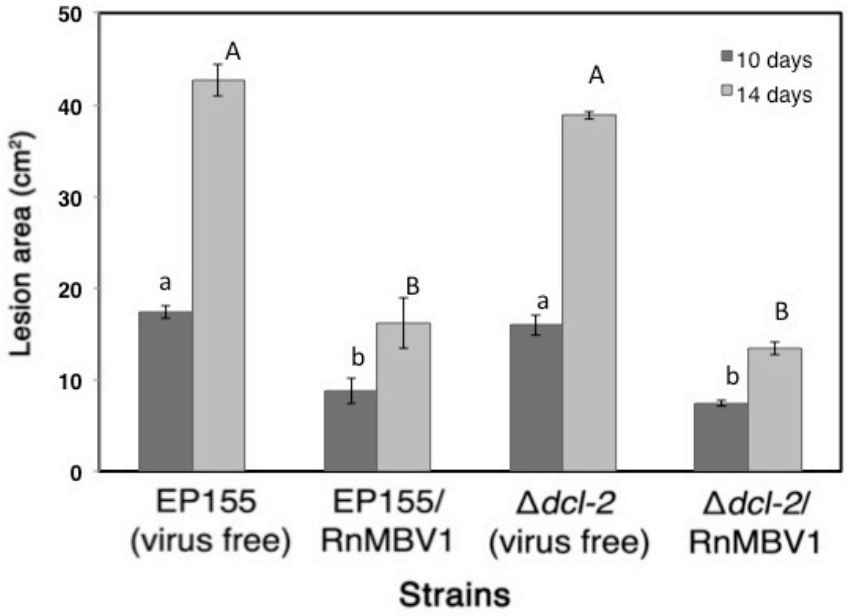

Fig. 8. Virulence levels were measured for 4 fungal strains; EP155 and Δ*dcl-2* infected or uninfected with RnMBV1 in apple assay. (A) Representative lesions induced by the fungal strains at 12 days after inoculation are shown. (B) Graphic representation of virulence levels. Virulence is expressed as the average of lesion area on day 10 and 14 post inoculation from 3 replicates for each strain with standard deviations. Data (mean±SD.) with different letters are significantly different *($p<0.01$)* among treatments (n=3).

3.3.3 Transmission of RnMBV1

3.3.3.1 Hyphae anastomosis (Horizontal transmission)

As mentioned before (Fig. 2), RnMBV1 can be moved and stably maintained in *C. parasitica*. RnMBV1-infected fungal strains were sub-cultured continuously and at 4th subculture (about 1 month after fusion) RnMBV1 seem to be lost from EP155. That is no dsRNAs were detected from the samples. Nevertheless, sub-culturing was continued for all the samples and found out that RnMBV1 is still present in EP155 even after 9th subculture. Difference in RNA level was evident in these strains in independent subsamples in which the same amount (wet weight) of infected mycelia were used for AGE analysis. This may be due to the uneven distribution and accumulation of the virus throughout fungal colony. Northern blot analysis of RnMBV1 infected *C. parasitica* EP155 from different positions showed varied concentration of dsRNA1 signal (Fig. 10). Although, dsRNA from some samples could not be detected on AGE analysis, northern blot analysis using probe1 confirmed the presence of RnMBV1 in *C. parasitica* EP155 from subculture 1-9 (Fig. 9B).

The same observation is true for Δ*dcl-2*. However, concentration of dsRNA in RnMBV1 infected EP155 was extremely low than in RnMBV1 infected Δ*dcl*-2 (Fig. 9A). This may be due to the presence of RNAi component, dicer 2 in EP155, that functions as anti-viral defense.

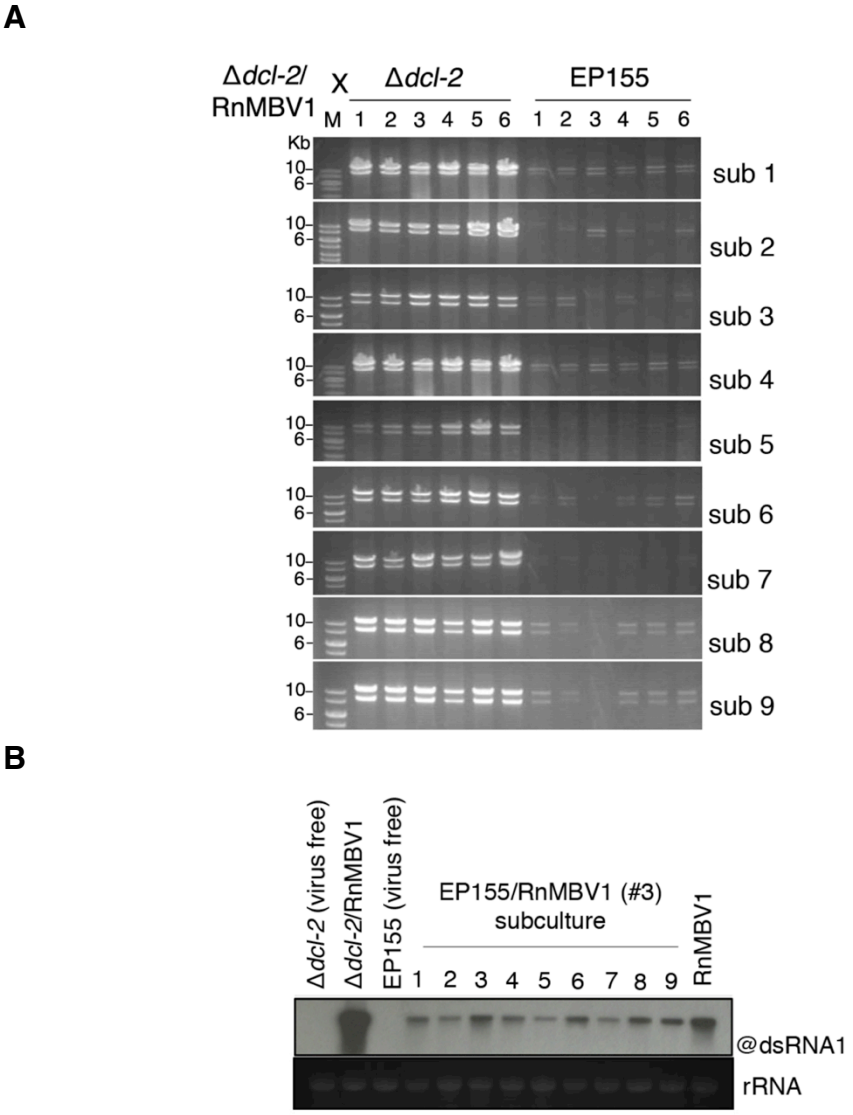

Fig. 9. DsRNA profiles of RnMBV1-infected fungal strains obtained from different sub-culturing. (A) DsRNA patterns of RnMBV1-infected EP155 and Δ*dcl-2*. DsRNAs were purified from nearly the same amount (0.05 g, wet weight) of mycelia from 9 independent subcultures (1^{st}-9^{th} round) and analyzed in AGE. (B) Northern blotting of EP155/RnMBV1 (#3). SsRNA fractions were prepared from RnMBV1-infected *C. parasitica* strain EP155. The same amounts (2 μg) of RNA from subculture 1^{st}-9^{th} were applied to 1% denatured agarose gel. Specific cDNA probe for dsRNA1 was used. EtBr-stained rRNAs were shown as loading control.

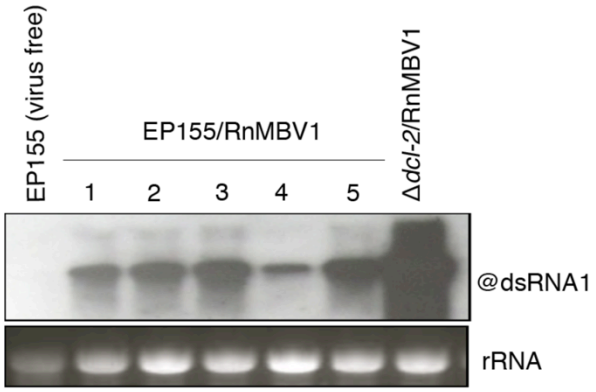

Fig. 10. Expression level of RnMBV1 detected by northern blot analysis of RnMBV1 infected *C. parasitica* strain EP155 obtained from different positions. EP155/RnMBV1 (#3) was grown on PDA (90 mm plate) then mycelia were cut from 5 different positions in PDA. SsRNA fractions were prepared from RnMBV1-infected *C. parasitica* strain EP155. The same amounts (2 μg) of RNA from position 1-5 were applied to 1% denatured agarose gel. Specific cDNA probe for dsRNA1 was used. EtBr-stained rRNAs were shown as loading control.

3.3.3.2 Vertical transmission

To assess the movement of RnMBV1 into the reproductive units of *C. parasitica* and check its frequency in the next generation, single spore isolation was performed. Infection of *C. parasitica* by RnMBV1 provided an opportunity to address whether the virus is transmitted vertically through conidia, which cannot be assessed in the original host fungus because it rarely produce spores under laboratory conditions (Nakamura, 2002). First, approximately 50 germlings with the normal virus-free phenotype were confirmed to be dsRNA-free. Therefore, we tested all single conidial isolates with symptoms for the presence of RnMBV1 dsRNA and confirmed that the vertical transmission rate in Δ*dcl-2* was 0.48% (Table. 4, Fig. 11). Since RnMBV1 did not induce obvious phenotypic alterations in EP155, northern blot and subsequent RT-PCR analyses were used to examine virus infection employing bulked RNA fractions for all single conidial isolates (see Materials and Methods). From 725 single spore germlings tested 2 samples exhibited the signal of dsRNA1 (Fig. 12A). In the same time 10% of the germlings (about 8 samples) were subjected to RT-PCR to confirm the northern blot result. Figure 12B showed that no expected band was found in the samples tested. Since, each sample for northern blot was bulked from three single spore germlings,

ssRNAs from the six individual germlings that gave positive results to northern blot analysis were subjected to RT-PCR. Two single spore isolates (No. 106 and 341) from 6 samples showed the expected PCR product of 600 base pairs and had the same migration position with positive control (RnMBV1 infected EP155 and Δ*dcl-2*). No expected band was found in Δ*dcl-2* virus free strain (Fig. 12C). From northern blot and RT-PCR results, its was concluded that the virus was vertically transmitted at 0.27% in EP155 (Table. 4).

Table 4. Vertical transmission of RnMBV1 through conidia in *C. parasitica*.

Fungal strain/ Virus strain	Experiments (number of infected / tested germlings)				Total	Efficiency (%)
Δ*dcl-2*/RnMBV1 #10	3/643	2/583	2/534	4/493	11/2253	0.48
EP155/RnMBV1 #3	1/512	0/120	1/120	-	2/725	0.27

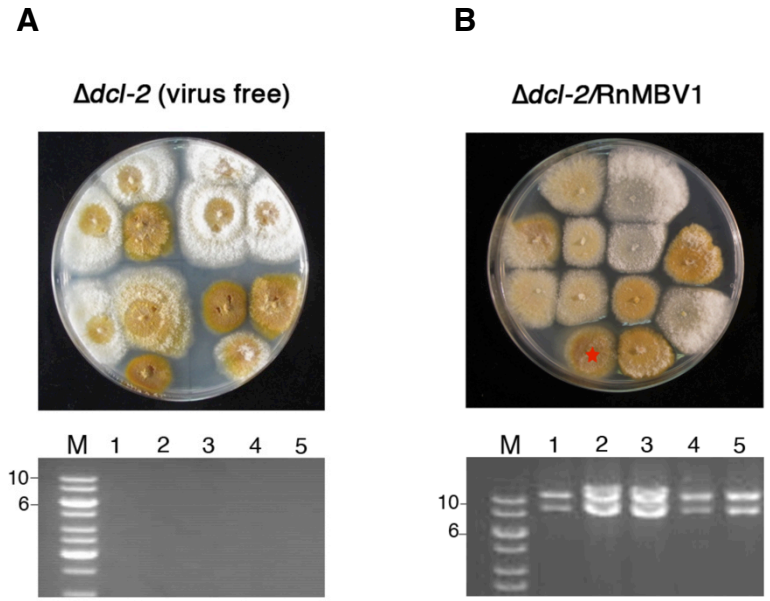

Fig. 11. Germling from single spore isolation. (A) Top; colony morphology of germlings of Δ*dcl-2* with the normal virus-free phenotype. Below; AGE analysis were confirmed to be dsRNA-free. (B) Top; colony morphology of germlings of Δ*dcl-2* infected with RnMBV1. The red mark represents the colony morphology of infected fungal. Below; AGE analysis of dsRNA profiles confirming virus infection.

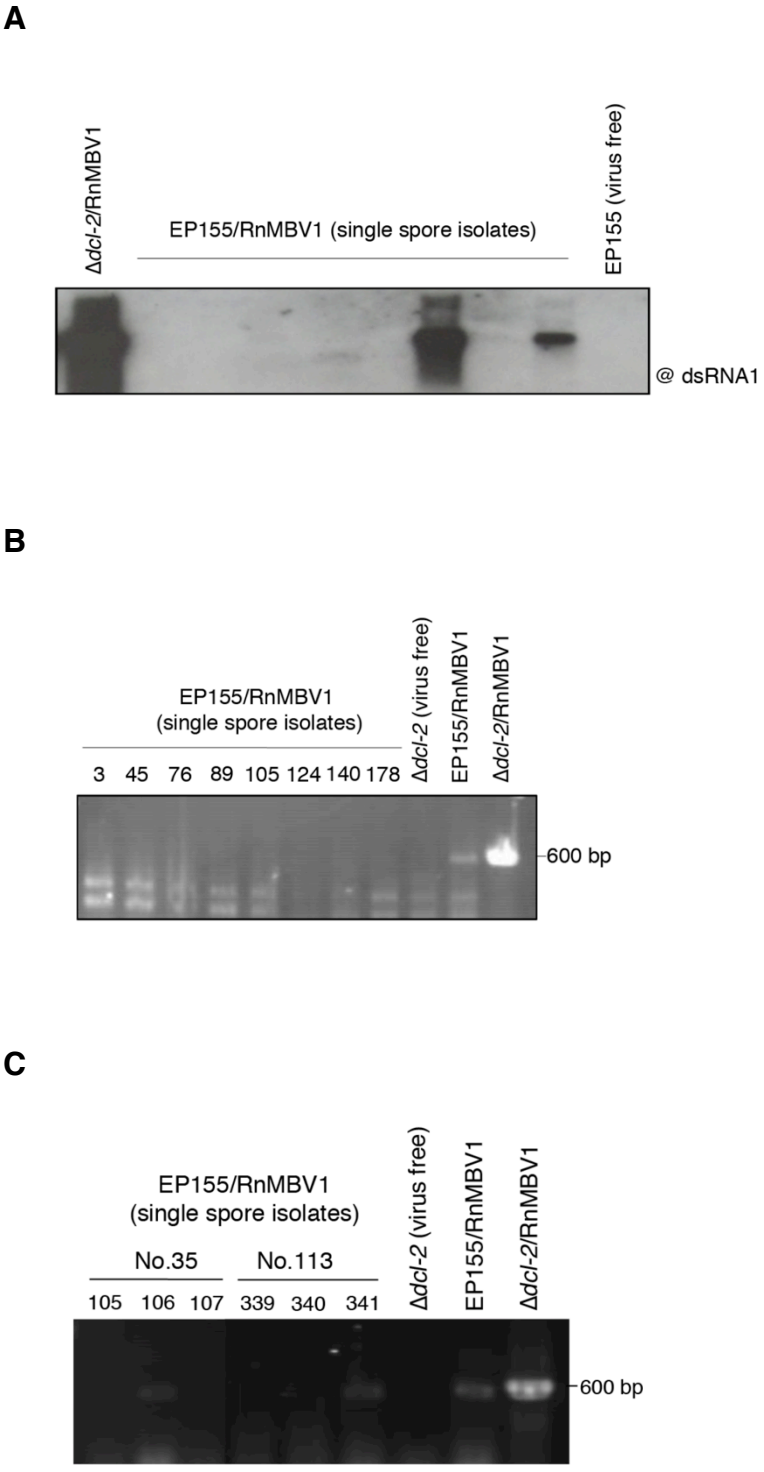

Fig. 12. Vertical transmission of RnMBV1 infected *C. parasitica* EP155. (A) Northern blot of bulked sample representing three single spore germlings. Eighty ssRNA fractions were prepared and applied to 1% denatured agarose gel. Specific cDNA probe for dsRNA1 was used. (B) RT-PCR using dsRNA1 primers of 10% randomly sampling. (C) The six individual ssRNAs from 2 positive results were subjected to RT-PCR using dsRNA1 primers.

In addition, colony morphology of RnMBV1 infected EP155 and Δ*dcl-2* from hyphal fusion and single spore isolation is the same with fungal transfectants (Fig. 13).

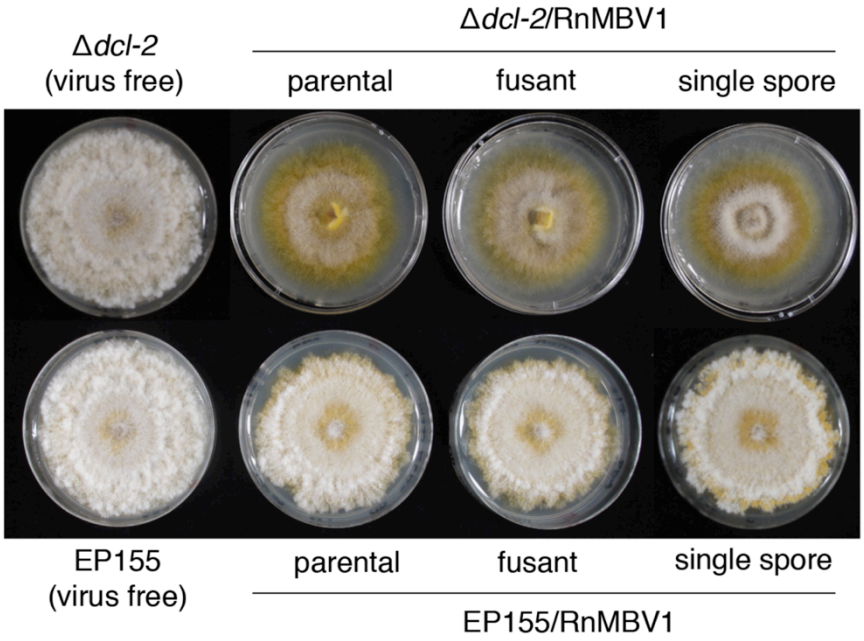

Fig. 13. Colony morphology of RnMBV1 infected EP155 and Δ*dcl-2* from hyphal and vertical transmission compared with parental strains. Fungal colonies were grown on PDA for 6 days on a bench top and then photographed.

3.3.4 Replication level of RnMBV1 in RNA-silencing-defective is higher than in RNA silencing-competent strains

In order to determine whether RnMBV1 is targeted by RNA silencing in the experimental host, *C. parasitica*, the levels of viral RNA accumulation between EP155 and Δ*dcl-2* were compared. As shown in Fig. 14A, the accumulation level of RnMBV1 in Δ*dcl-2* was markedly higher than in standard EP155 fungal colony. In addition, Northern analysis of serial RNA dilutions from Δ*dcl-2*/RnMBV1 revealed approximately 20-fold higher accumulation of the virus in Δ*dcl-2* (Fig. 14B). These clearly indicate that RNA silencing targets RnMBV1 in this experimental host. It was noteworthy that RnMBV1 accumulation levels in Δ*dcl-2* were comparable to that in the natural host, *R. necatrix*, when normalized against rRNAs (Fig. 14A).

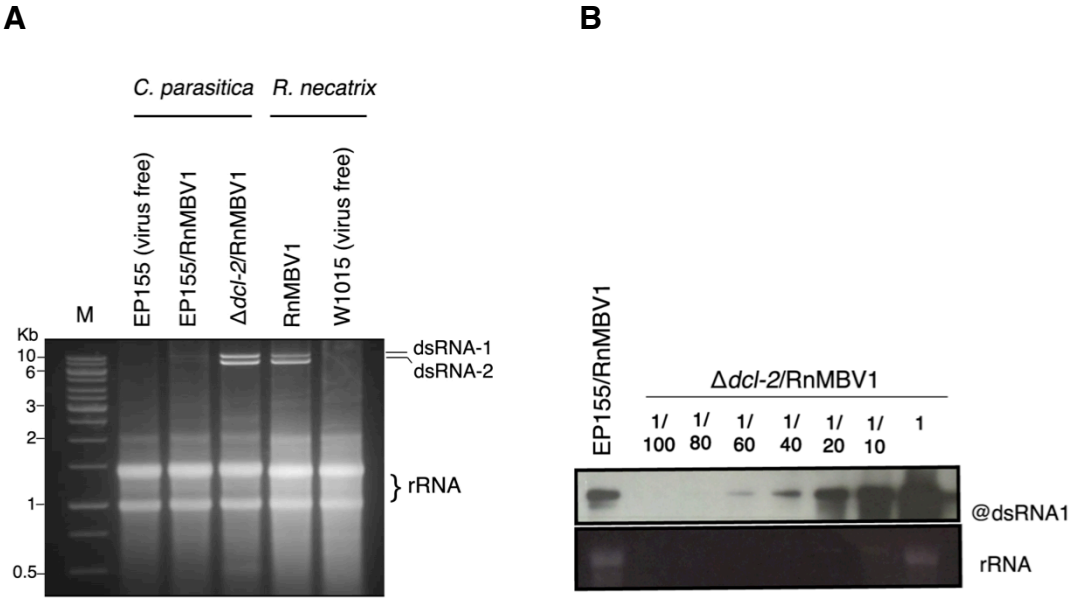

Fig. 14. Comparison of viral accumulation in RNA silencing-defective and -competent strains. (a) Agarose gel electrophoresis (AGE) profiles of total RNA fractions. RNAs were isolated from RnMBV1-free and -infected EP155 and Δ*dcl-2* and applied to 1.4% agarose gel. (b) Northern blotting of serial dilutions of RnMBV1 mRNA. SsRNA fractions were prepared from RnMBV1-infected *C. parasitica* strains Δ*dcl*-2 and EP155. The same amounts (10 μg) of RNA from the strains were applied to the left- and right-most lanes of 1% denatured agarose gel, while the middle lanes were loaded with serial dilutions derived from RnMBV1-infected Δ*dcl-2*, as shown on the top of the blot. Specific cDNA probe for dsRNA1 was used. EtBr-stained rRNAs were shown as loading control.

3.3.5 Virus particles purified from Δ*dcl-2*/RnMBV1

Samples collected from *C. parasitica* Δ*dcl-2* infected with RnMBV1 were used for isolation of virus particles. Virus particles were isolated in a similar manner using ultracentrifugation and cesium sulphate gradients. After ultracentrifugation, three distinctive layers were observed (Fig. 15A). Those three layers were collected carefully and checked by AGE and SDS-PAGE analyses to confirm presence of dsRNA and the protein of the samples, respectively (Fig. 15B). DsRNA was absent and protein of 135 kDa was present from fraction 1, indicated that RnMBV1 infected Δ*dcl-2* fraction 1 contained empty capsid. While, virus particles purified from Δ*dcl-2*/RnMBV1 fractions 2 and 3 accommodates two dsRNA segments with the same sizes to dsRNA1 and dsRNA2 extracted from RnMBV1. It is noteworthy to observe that dsRNA profiles of

fractions 2 and 3 from Δ*dcl-2*/RnMBV1 exhibited different concentrations of dsRNA1 and 2. DsRNA from Δ*dcl-2*/RnMBV1 fraction 2 showed the same concentration between dsRNA1 and 2. While, dsRNA from fraction 3 displayed higher intensity of dsRNA1 than dsRNA2. In addition, the dsRNA2 of from Δ*dcl-2* /RnMBV1 fraction 2 and 3 showed lower density than in RnMBV1.

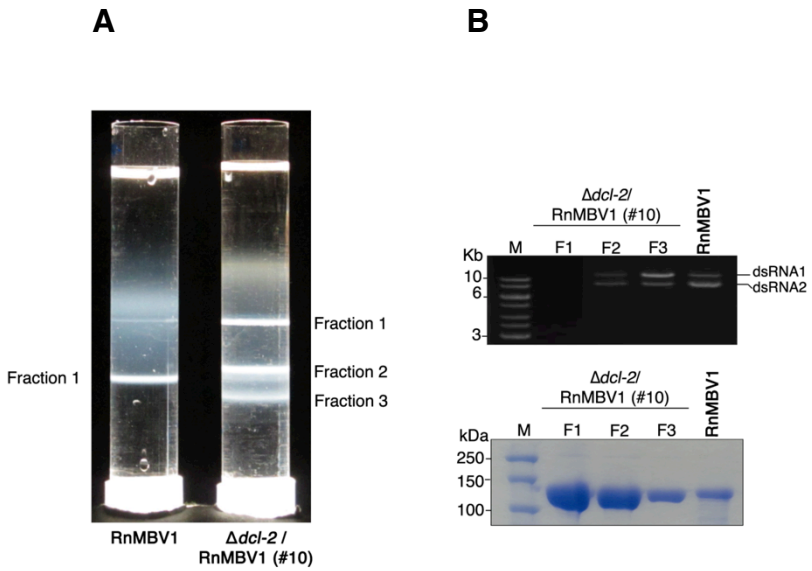

Fig. 15. Virus particles purified from Δ*dcl-2* infected with RnMBV1. (A) Photographs of the 20-50% cesium sulfate gradient tubes, RnMBV1 (left tube) and Δ*dcl-2*/RnMBV1 (right tube). Crude lysate from a virus preparation was layered on tubes containing a cesium sulphate gradient. After 15 hr at 28,000 rpm in a SW41Ti swing out rotor, virus band was clearly visible in the cesium sulphate gradient. The particle bands and other minor containing nonfully mature or empty capsids appear white with a light shadow. (B) Top; agarose gel electrophoresis analysis shows the dsRNA patterns of the viral particles present in the bands detected in the gradients shown in (A). DsRNA from 10 µl of virus particle suspension were obtained after phenol/chloroform and chloroform extraction. DsRNA fractions were loaded into each well of 1% agarose gel and electrophoresed in 1X TAE buffer. Below; analysis of the virus particles preparation by 8% SDS-PAGE. Protein from virus particles was prepared as described in method. The migration of the viral structural proteins in the gel is indicated.

Virus particles were transfected to spheroplasts of *R. necatrix* W1015 (original host), EP155 and Δ*dcl-2* to check the transfection ability. After 1 week of transfection, fungal mycelia from regeneration plate were moved to new PDA plate and then dsRNA from individual colony was checked by AGE analysis. The virus particles from all fractions

(except RnMBV1 infected Δ*dcl-2* fraction 1) were shown to be infectious. AGE analysis showed detection of dsRNA from Δ*dcl-2* and W1015 transfectants (Fig.16A). In Δ*dcl-2,* the individual RnMBV1 transfectants exhibited 2 type of dsRNA pattern which were similar to the previous results. Virus particles from Δ*dcl-2* harboring RnMBV1 showed wild type dsRNA pattern containing dsRNA1 and 2. In *R. necatrix* W1015, those three fractions were transfectable and showed only wild type dsRNA pattern. The fungal colony from transfection showed the same phenotype with parental strain (Fig. 16B).

3.3.6 Predicted non-canonical translation for RnMBV1 downstream ORFs

The expression strategies for RnMBV1-encoded genes are largely unknown. Using peptide mass fingerprinting (PMF), Chiba et al. (2009) showed that the 135-kDa protein in purified RnMBV1 preparations is encoded by ORF1. In that preparation, SDS-PAGE analysis demonstrated a faint 250-kDa band, which was assumed to be a fusion product of CP and ORF2-encoded RdRp. Although a putative slippery sequence and a stem-loop structure implicated in -1 frameshift were found, the possibility of sub-genomic RNA-mediated expression of downstream ORFs was tested. A single stranded RNA (ssRNA) fraction of virus-infected *C. parasitica* Δ*dcl-2* was analyzed by Northern blotting using cDNA probes specific for ORF2 and ORF4 (Fig. 17B; see Fig. 17A for the positions of cDNA probes), and the detected bands were considered to be mRNAs of RnMBV1 dsRNA1 and 2. Notably, these migrated at the same positions as those of *in vitro*-synthesized transcripts of full-length viral cDNAs, and no other smaller bands were detected. This clearly indicated that sub-genomic RNA is not involved in the expression of ORF2 or ORF4, and that genome-length mRNA would be the template for these proteins.

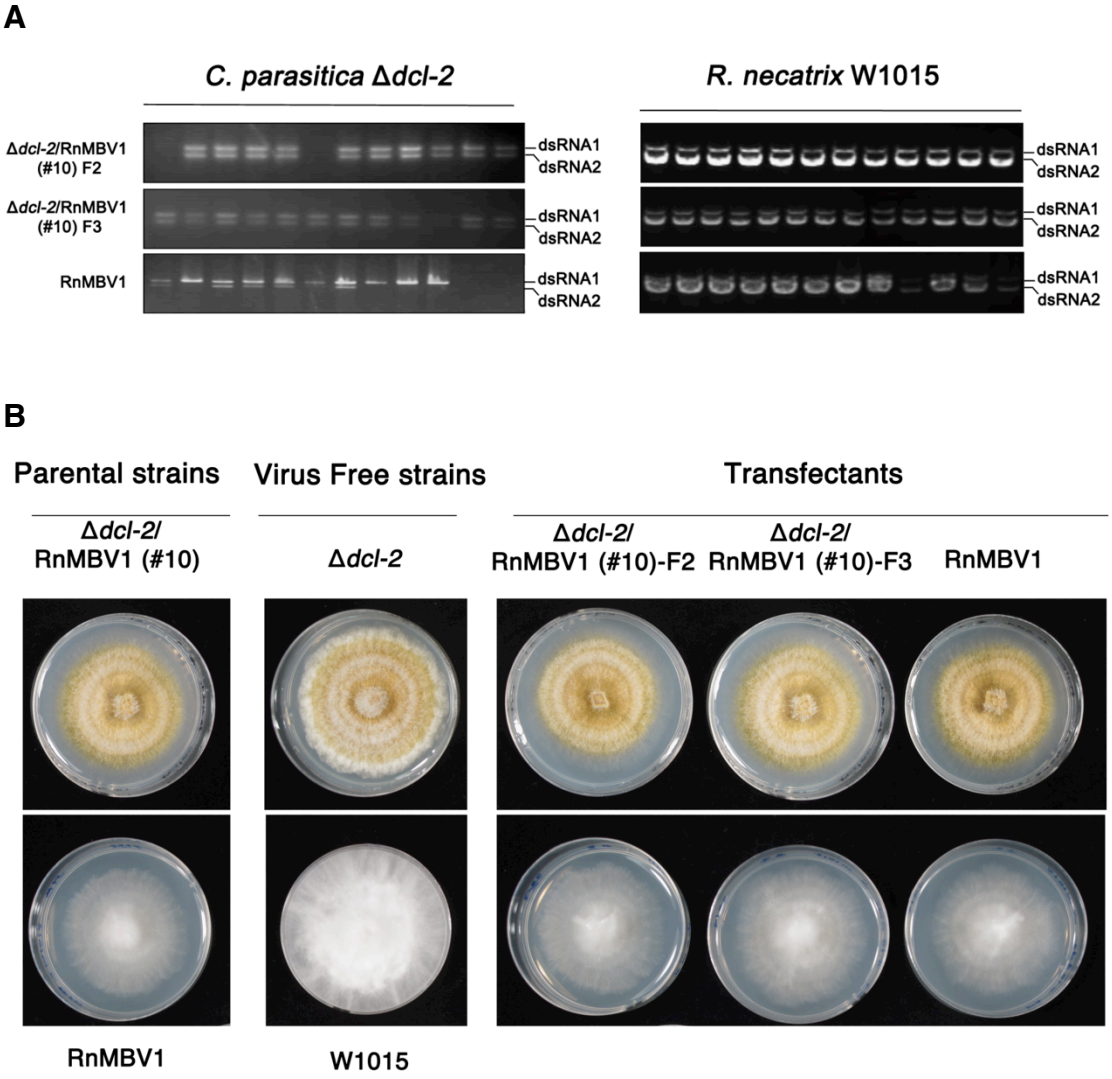

Fig. 16. Infection of RnMBV1 purified from *C. parasitica*. (A) Agarose gel electrophoretic analysis of dsRNA from transfectants. Spheroplasts of Δ*dcl-2* (Left) and W1015 (right) were transfected by purified RnMBV1 particles from *C. parasitica* and *R. necatrix* W1015. (B) Top; colony morphology of RnMBV1-infected *C. parasitica*. Δ*dcl*-2, uninfected and parental strain were grown on PDA for 6 days on a bench top and then photographed. Below; colony morphology of RnMBV1-infected *R. necatrix* W1015, uninfected and parental strain were grown on PDA for 7 days in dark at 25 ^{o}C and then photographed.

3.3.7 Expression of CP and RdRp as a CP-RdRp fusion protein and multiple protein products which derived from ORF3

Virus particles from *C. parasitica* harboring RnMBV1 were purified and subjected to western blot analysis. Antibodies against recombinant ORF1-encoded protein detected the major 135-kDa CP as well as a minor 250-kDa protein in purified virus preparations from Δ*dcl-2* infected by RnMBV1 (Fig. 18A, @ORF1). Antibodies against recombinant ORF2-encoded protein produced in *E. coli* detected the 250-kDa protein as the major protein, but not the CP, in the same virus-purified preparations as those used for detection of the CP (Fig. 18A, @ORF2). These results indicated that the RdRp domain is expressed as a CP-RdRp fusion product in infected cells, and that the domain is incorporated into the virions. RnMBV1 CP was readily detectable in total protein fractions from RnMBV1-infected EP155 and Δ*dcl-2*, but not those from virus-free EP155 (Fig. 18B). The CP was detectable in RnMBV1-infected Δ*dcl-2* even by Coomassie Brilliant Blue (CBB) staining of the SDS-PAGE gel.

Western blotting of RnMBV1-infected mycelia with an antiserum against ORF3-encoded polypeptides demonstrated a complex detection pattern. At least three protein bands corresponding to molecular masses of 150 kDa, 30 kDa, and 23 kDa were observed, the smallest one being the major protein, specifically in RnMBV1-infected Δ*dcl-2* (Fig. 18C, @ORF3). In addition, polypeptides of approximately 100 kDa, 45 kDa, and 27 kDa (marked by asterisks) were readily detectable in RnMBV1-infected Δ*dcl-2*. Note that these three protein bands were also observed in virus-free EP155 after longer exposure of film to the blot. Although their band intensity was much lower, a similar detection profile was obtained with EP155 mycelia infected by RnMBV1 (Fig. 18C).

All of these results confirmed RnMBV1 replication in *C. parasitica* and expression of all RnMBV1-possessing ORFs except for ORF4.

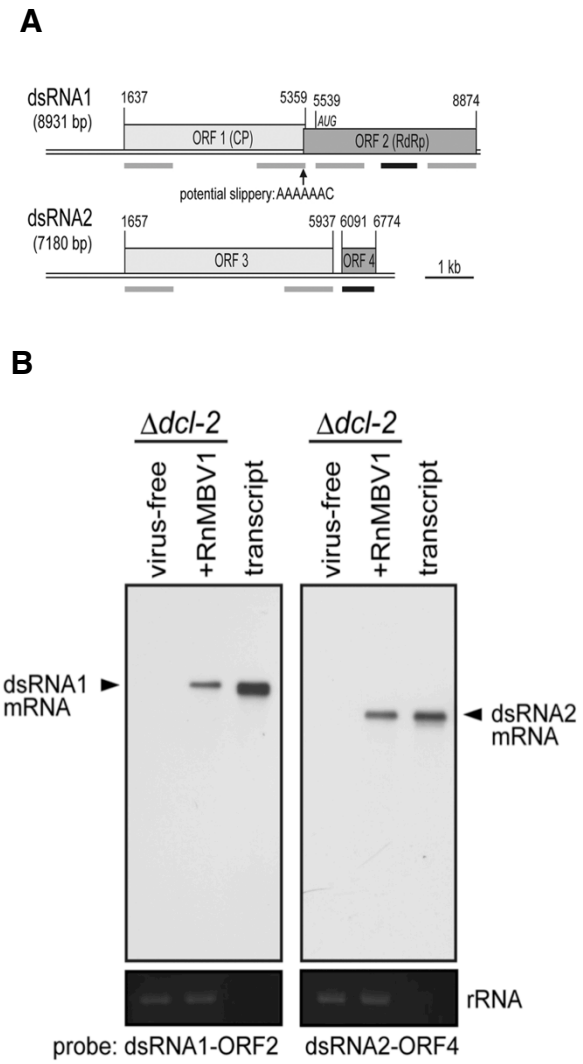

Fig. 17. Genetic organization of the RnMBV1. (A) RnMBV1 dsRNA1 and 2 are 8931 bp and 7189 bp, respectively each having two ORFs. ORF1 and ORF2 on dsRNA1 encode the CP and RdRp domains, while ORF3 and ORF4 on dsRNA2 encode polypeptides with unknown functions. Positions of the start and stop codons are shown above each ORF. Grey and black bars denote regions used as antigens and cDNA probes (see Fig. 17B and 18), respectively. The potential slippery sequence that would facilitate -1 frameshifting on dsRNA1 is also shown. (B) RnMBV1 gene expression in *C. parasitica*. (a) Northern analysis of RnMBV1-infected Δ*dcl*-2. SsRNAs isolated from RnMBV1-free and -infected Δ*dcl*-2 were fractionated using 1% denatured agarose gel. After blotting on a nylon membrane, the membrane was hybridized with cDNA probes for dsRNA1 and dsRNA2 (see Fig. 17A for the positions of the probes). Full-length transcripts synthesized by T7 RNA polymerase from full-length cDNA clones to dsRNA1 and dsRNA2 were applied in parallel.

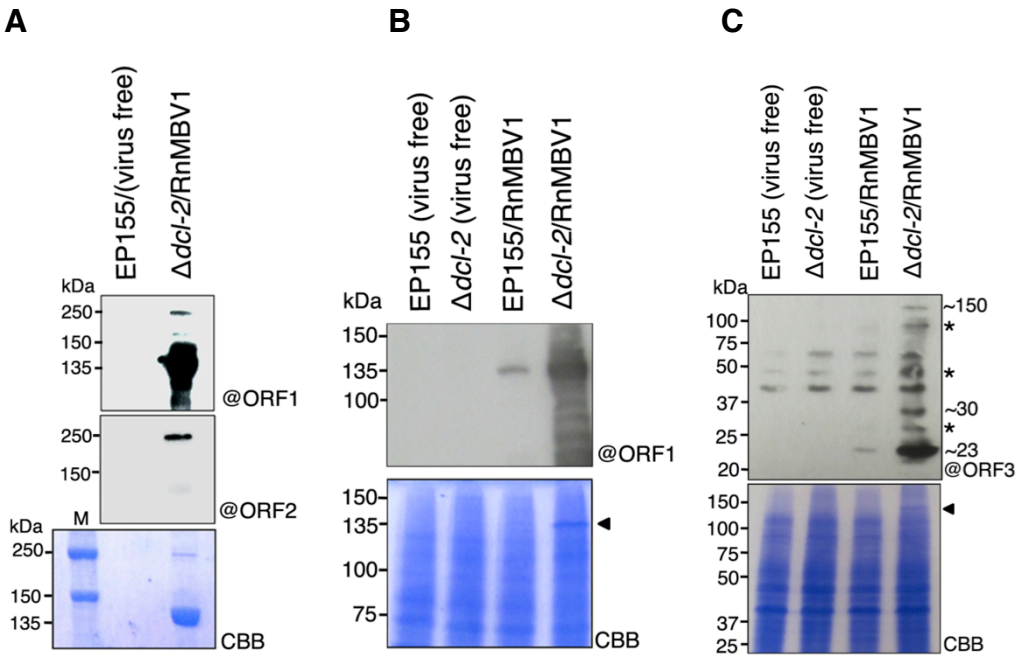

Fig. 18. Immuno-detection of RnMBV1-coded proteins. Specific viral proteins were detected by Western blotting using antibodies against *E. coli*-expressed polypeptides encoded by ORF1 (A,B), ORF2 (C), and ORF3 (C). Total proteins (B, C) or purified virion preparations (A) were obtained from EP155 or Δ*dcl*-2 uninfected (-) or infected by RnMBV1 (+). The same protein fractions as those used for Western analysis are shown in SDS-PAGE stained by CBB as loading controls (A-C). In (A), a fraction was prepared from virus-free EP155 by the same method as that for the virion fraction from RnMBV1-infected Δ*dcl*-2. Specific proteins were detected using an ECL Plus kit (GE Healthcare). The major CP of 135 kDa (marked by arrowheads) was detectable even in SDS-PAGE gel directly stained by CBB (B, C). The protein bands indicated by asterisks in (C) refer to those detected as more intense bands in RnMBV1-infected Δ*dcl*-2, although they were also detectable in virus-free and -infected EP155.

3.4 Discussion

This study addressed whether RnMBV1 is able to replicate in and confer hypovirulence to another phytopathogenic fungus, *C. parasitica*. Furthermore, the virus was also characterized molecularly to clarify the protein products and how they are expressed in *C. parasitica* after confirming its susceptibility. These objectives were achieved using

dependable, reproducible transfection protocols with purified virus particles that had been developed previously for several other mycoviruses with dsRNA (Sasaki *et al.*, 2007; Sasaki *et al.*, 2006) and ssDNA genomes (Yu *et al.*, 2010). *C. parasitica* was previously shown to support replication of heterologous viruses such as Rosellinia necatrix partitivirus 1 (RnPV1) (Kanematsu *et al.*, 2010), RnPV2 (Chiba *et al.*, 2013b; Kanematsu *et al.*, 2010), Rosellinia necatrix victorivirus 1 (RnVV1) (Chiba *et al.*, 2013a), MyRV3 (Kanematsu *et al.*, 2010), and Fusarium graminearum virus 1 (Lee *et al.*, 2011). This study provides another such example.

C. parasitica as a viral host has certain advantages over other filamentous fungi including *R. necatrix* for studies of virus/host and virus/virus interactions (Kondo *et al.*, 2013). Among them is the availability of various mutants of this experimental host that include an RNA silencing-defective strain, Δ*dcl-2* (Segers et al., 2007), which was used in this study. The two fungal strains, standard RNA silencing-competent EP155 and RNA silencing-defective Δ*dcl-2* showed different responses to RnMBV1 infection. RnMBV1 replicated at a much higher level (20-fold) in Δ*dcl-2* than in EP155 (Fig. 14B) as in the case for RnVV1 (victorivirus) and RnPV2 (partitivirus) (Chiba *et al.*, 2013a; b). This indicates that RNA silencing targets the megabirnavirus in *C. parasitica*. Viruses are known to deploy a counter-defense mechanism using RNA silencing suppressors (Burgyan & Havelda, 2011; Wu *et al.*, 2010). It remains unknown whether RnMBV1 encodes an RNA silencing suppressor. In this context, Kanematsu et al. have reported that RnMBV1 rearrangement events occasionally occur after transfection (Kanematsu *et al.*, 2013). Molecular analysis of its variants have shown that dsRNA2, while dispensable for virus viability, is required for efficient replication and full transfer of hypovirulence to the natural host. This suggests that ORF3 may be associated with counter-host defense (RNA silencing) or involved directly in RnMBV1 replication. The same group have also shown that RNA silencing operates in *R. necatrix* (Yaegashi *et al.*, 2013). The comparable content of RnMBV1 genomic dsRNA in Δ*dcl-2* and in RNA silencing-competent *R. necatrix* (Fig. 14A) suggests that RnMBV1 is adapted better to the natural host than to the experimental host.

As expected from the different replication levels, RnMBV1 induced distinct phenotypic alteration in the strains; only a mild alteration of colony morphology in the standard RNA silencing-competent EP155, and a reduced growth rate with an irregular colony margin in Δ*dcl-2* (Fig. 7). Both infected fungal strains retained similar levels of sporulation (Table 3), relative to virus-free Δ*dcl-2* or EP155. This symptom expression remained phenotypically stable after horizontal and vertical transmission. It was surprising that RnMBV1 conferred hypovirulence to the *C. parasitica* wild-type strain, as in the case of Δ*dcl-2*, in spite of the limited effects on colony morphology. Some mycoviruses, for which artificial introduction protocols have been developed, are reported to reduce virulence in heterologous fungi. For example, the prototype hypovirus CHV1, the best studied of mycoviruses infecting filamentous fungi, has been shown to replicate in non-natural hosts within or outside *Diaporthales*, which accommodates the natural host *C. parasitica* and confers hypovirulence (Chen *et al.*, 1996a; Sasaki *et al.*, 2002). While there are an increasing number of well-characterized *R. necatrix* viruses (Chiba *et al.*, 2011; Chiba *et al.*, 2013a; Lin *et al.*, 2012; Lin *et al.*, 2013; Sasaki *et al.*, 2005), only two of them are known to confer hypovirulence to the host: MyRV3 and RnMBV1 (Chiba *et al.*, 2009; Kanematsu *et al.*, 2004). MyRV3 is able to attenuate the virulence of experimental hosts such as *Valsa ceratosperma*, *C. parasitica*, and *Diaporthe* spp (Kanematsu *et al.*, 2010). Therefore, RnMBV1 is the second reported example of a heterologous virus that is able to attenuate the virulence of *C. parasitica*.

Vertical transmission of mycoviruses is one of the key factors influencing their ecological fitness, and this is also true for those infecting *C. parasitica*, spreading through conidia as well as ascospores in nature (Anagnostakis, 1987). This phenomenon is governed by multiple virus and host factors, and its rate depends on specific virus/host combinations. For example, in *C. parasitica*, CHV1-EP713 is transmitted through conidia at a rate of nearly 100%, whereas MyRV1 is transmitted at a rate of approximately 10% (Eusebio-Cope *et al.*, 2010; Suzuki *et al.*, 2003). Little is known about host factors involved in vertical transmission, although there are some reports about viral factors. A multifunctional protein p29 encoded by CHV1 is known to

enhance replication and transmission of homologous and heterologous viruses (Sun *et al.*, 2006; Suzuki *et al.*, 2003). MyRV1 lacking the S4 domain encoding a non-structural protein (VP4) shows impaired vertical transmission (Eusebio-Cope *et al.*, 2010). In the present study, an extremely low frequency of RnMBV1 transmission was observed regardless of host background or replication level. This suggests that the virus has low ecological fitness potential in this heterologous host. It is interesting to speculate that the low rate of vertical transmission is associated with the soil-borne nature of the natural host fungus, which extends in soil in the form of mycelial strands, and not spores, and rarely sporulates asexually (Nakamura, 2002).

Using PMF, Chiba et al. (2009) showed that the major 135-kDa CP of RnMBV1 is encoded by ORF1. However, it remained unclear how the upstream ORF1, preceded by extremely long UTRs, and the downstream ORF2 are expressed. This study succeeded to provide a clue to the nature of the expression of the downstream ORF2 on dsRNA1. Antibodies against ORF1-encoded proteins detected the CP as well as a minor protein of 250 kDa in purified virus preparations, confirming the previous conclusion that the RnMBV1 CP is encoded by ORF1 (Chiba *et al.*, 2009). The observation that the minor 250-kDa protein reacted specifically with an antibody against ORF2-coded protein (Fig. 17B) indicate that the RdRp domain encoded by ORF2 is expressed as a CP-fusion product. As described by Chiba et al. (2009), the presence of the consensus slippery sequence and subsequent stem-loop/pseudo-knot structure implies that RnMBV1 RdRp is expressed via -1 frameshifting.

It is considered that ribosomal -1 frameshift is used by various fungal, plant and animal viruses. Several unassigned and/or unclassified RNA fungal and insect viruses are phylogenetically related to RnMBV1 and have similar ORF configurations to RnMBV1 dsRNA1. Examples include hopper viruses such as Spissistilus festinus virus 1 and Circulifer tenellus virus 1 (Spear *et al.*, 2010) of insect origin, Phlebiopsis gigantea viruses 1 and 2 (Kozlakidis *et al.*, 2009), Fusarium graminearum virus 3 (Yu *et al.*, 2009), and Fusarium virguliforme RNA viruses 1 and 2 of fungal origin, and Phytophthora infestans RNA virus 3 of oomycetes (kingdom Chromalveolata) (Cai *et al.*, 2013). All of these viruses have undivided genome segments with 2-ORF structures,

and unlike RnMBV1, are assumed not to form particles. On the basis of their sequences, their downstream ORFs are predicted to be translated via -1 frameshifting. However, no RdRp product has yet been identified for these viruses, and RnMBV1 is the first of these viruses for which the RdRp has been shown to be translated as a CP-fusion protein. In this regard, RnMBV1 dsRNA1 is similar in genetic organization to some members of the family *Totiviridae* such as totiviruses and giardiaviruses (Ghabrial, 2008; Wickner *et al.*, 2011), although it is phylogenetically more distant from the above viruses. For the prototype totivirus, Saccharomyces cerevisiae virus L-A (ScV-L-A), effects of mutations in the slippery sequence on -1 frame-shifting and its satellite RNA replication have been reported (Dinman *et al.*, 1991; Dinman & Wickner, 1992).

The identity of the mature proteins of ORF3 is still unclear. As shown in Fig. 17D the 150-kDa, 30-kDa, and 23-kDa products were detectable specifically in infected RnMBV1-infected *C. parasitica* cells. A 40-kDa protein was identified in RnMBV1-infected *R. necatrix* cells (Kanematsu et al., 2013) using different antiserum independently prepared against the recombinant full-length product of 150 kDa. This may correspond to the 40-kDa polypeptide marked by an asterisk in Fig. 17D. On the basis of its coding capacity, it seems likely that the 150-kDa protein is the full-length product encoded by ORF3. The smaller products observed in this study may be derived from the N- and/or C- terminal portions after programmed catalytic cleavage or site-specific degradation. This notion is based on the fact that the antiserum used in this study was directed against the N and C terminal portions of the ORF3 product. Further investigation is required for unraveling the ORF3-protein function.

Chapter 4. RnMBV1 genome rearrangement occurs in both experimental host, *C. parasitica* and natural host, *R. necatrix*

4.1 Introduction

An ascomycetous fungus *Rosellinia necatrix* is a soil-borne pathogen which destroys plant roots of more than 400 species and difficult to control (Pliego *et al*., 2012). An extensive survey of RNA mycoviruses in *R. necatrix* has been conducted under the prospect of virocontrol (biological control using viruses) (Kondo *et al*. 2013) and revealed the presence of potential RNA viruses at a frequency of about 20% *(Ikeda et al*., 2004). Molecular characterization of these viruses revealed that *R. necatrix* hosts a number of mycoviruses belonging to at least 5 families: *Partitiviridae* (Chiba *et al*., 2013a; Sasaki *et al*., 2005)*, Quadriviridae* (Lin *et al*., 2012)*, Reoviridae* (Wei *et al*., 2003)*, Totiviridae* (Chiba *et al*. 2013b)*,* and *Megabirnaviridae* (Chiba *et al*., 2009).
Rosellinia necatrix megabirnavirus1 (RnMBV1) is a recently identified virus from a field strain (W779) of *R. necatrix* isolated from infested orchard by bait twig method (Chiba *et al*., 2009). RnMBV1 has spherical virus particles (~50 nm in diameter) and consists of two dsRNA segments, dsRNA1 (8,931 bp) and dsRNA2 (7,180 bp). DsRNA1 is composed of ORF1 and ORF2 that encodes capsid protein (CP) and RNA-dependent RNA polymerase (RdRp), respectively, while dsRNA2 has two ORFs that could code for two proteins with unknown function. RdRp is expressed as a CP-RdRp fusion product probably via -1 ribosomal frameshifting (Salaipeth *et al*., 2013). A distinguishing feature of RnMBV1 is the long 5' UTR (ca 1.6 kb) in both dsRNA1 and 2 segments. Phylogenetic analysis based on the conserved region of RdRp has placed RnMBV1 into a distinct clade, distantly related to the species in *Totiviridae* and *Chrysoviridae*. In addition, genome organization were clearly distinct from the above two families. Therefore, a novel virus family, *Megabirnaviridae*, were proposed with RnMBV1 as the type species, and approved by the International Committee of Virus Taxonomy in 2012.

A variety of members in the fungal kingdom have been shown to harbor mycoviruses. Most of them have dsRNA genomes and seem to have no obvious effect on host

phenotypes during their replication in the host fungal cells (Ghabrial and Suzuki, 2009). However, RnMBV1 was shown clearly to confer hypovirulence to the host fungus using a recently developed transfection protocol with purified virions (Hillman *et al*., 2004; Kanematsu et al., 2010; Sasaki et al., 2006). That is, transfection of RnMBV1-cured strain W1015, W370T1 and the standard strain W97 results in severe virulence attenuation (Chiba *et al*., 2009). The latter two strains are genetically different from W779 and belong to a different mycelial compatibility group (MCG) than W779 which impairs lateral viral transmission. Thus RnMBV1 is regarded as a potential virocontrol agent of *R. necatrix*.

Reverse genetics is generally useful to analyze functional roles in replication cycles of an RNA virus. However, reverse genetic systems have not been developed for many dsRNA viruses, except for some vertebrate reoviruses (Komoto *et al*., 2006; Boyce *et al*., 2008; Kobayashi *et al*., 2007) and birnaviruses (Mundt and Vakharia, 1996). Alternatively, variant viruses generated from RNA recombination events have long been contributed to the functional analysis of viral genomes (Nuss and Summers, 1984; Taniguchi *et al*., 1996; Sun and Suzuki, 2008; Eusebio-Cope *et al*., 2010). Genomic rearrangements are commonly found in members of the major dsRNA virus family *Reoviridae*, which is distributed in the animal, plant, and also fungal kingdoms (Desselberger, 1996; Taniguchi and Urasawa, 1995; Nuss, 1984; Sun and Suzuki, 2008; Eusebio-Cope *et al*., 2010). In most cases, a normal RNA segment is replaced by a rearranged RNA segment, which is derived from its standard segment by duplications, and/or internal deletions of genomic segment often with nucleotide substitutions. Rearrangements were also found in members of the other families such as the *Parititviridae* (Chiba *et al*., 2013a) and *Totivirdae* (Suzuki, unpublished data). The conserved terminal sequences at the 5' and 3' ends of the rearranged segments are retained because they are thought to be essential for RNA replication and packaging into the virion.

Genomic rearrangements were found in RnMBV1 at low frequency after transfection of RnMBV1 particles to both *R. necatrix* and *C. parasitica*. The RnMBV1 strains with rearranged genomes may provide clues to understand the molecular mechanism of

RnMBV1 replication and symptom expression. In *R. necatrix*, the genome structure of rearrangement strains of RnMBV1 were showed, which lost dsRNA2 but carried a rearranged dsRNA segment, termed dsRNA RS1, resulting from internal deletion and duplication of dsRNA1. At the same time, infection of *C. parasitica* with RnMBV1 particles showed the genome structure of rearrangement strains with expansion of dsRNA2, termed dsRNA RL2, and authentic dsRNA2. A robust transfection system of *R. necatrix* with virions of RnMBV1 allowed us to investigate a process of establishment of the rearranged segments and compare the host phenotype of colonies infected with the wild-type and rearrangement virus. These results provide an intriguing insight into cis-acting signals in long 5' UTR for the virus replication and packaging of RnMBV1, and clues to elucidate the mechanism of hypovirulence conferred by RnMBV1.

4.2 Material and Methods

4.2.1 Fungal and virus strains used in this study and their maintenance

All fungal and viral strains used in this study are shown in Table 1. RnMBV1-W779 is the wild-type field strain described previously (Chiba *et al.*, 2009). Virus-free *R. necatrix* isolates, W1015 (an isogenic virus-free strain was prepared from spheroplasts of W779), W97 and W370T1 (Kanematsu *et al*., 2004), were used to transfect virions. All the three fungal isolates W779, W97 and W370T1 were genetically different and belong to the different mycelial compatibility groups MCG351, MCG80 and MCG139, respectively.

The standard virus-free strain EP155 and an RNA silencing-defective *dcl-2* knock-out mutant (Δ*dcl-2*) (Segers *et al.*, 2007) of *C. parasitica,* a generous gift from Dr. Donald L Nuss served as the recipient of the virus. Both transfectants and fusants, fungal strains generated after transfection and hyphal anastomosis (lateral virus transmission), respectively carry RnMBV1-W779. Fungal strains were grown at 25-27^{o}C for 5-7 days in either Difco^{TM} potato dextrose broth (PDB) for RNA/DNA extraction and

spheroplast preparations, or Difco™ potato dextrose agar (PDA) or Vogel's media (Vogel, 1956) for pre-culture and phenotypic observation.

4.2.2 Transfection of *C. parasitica* spheroplasts

Transfection of *C. parasitica* was performed as described by Hillman *et al.* (2004). Spheroplasts of *C. parasitica* Δ*dcl-2* strains were prepared using the methods of Eusebio-Cope *et al*. (2009). RnMBV1 virions were purified according to the method of Chiba *et al.* (2009) by differential and sucrose or cesium sulphate gradient centrifugation. Purified particles were transfected into Δ*dcl-2* spheroplasts using polyethylene glycol (PEG). After regeneration of spheroplasts, mycelial plugs from multiple positions were transferred onto new PDA plates and propagated. Virus infections (transfections) were analyzed by AGE of dsRNA.

4.2.3 Transfection of *R. necatrix* spheroplast

Purification of virus particles and protoplast transfection followed the procedure of Chiba *et al*. (Chiba *et al*., 2009). Fungal mycelia were cultured on cellophane-PDA for 10 days, and harvested mycelia (ca. 10 g, wet weight) were ground to fine powder with a mortar and pestle in the presence of liquid nitrogen. Powdered mycelia were suspended in 60 ml of 0.1M sodium phosphate buffer (PB, pH7.0) containing 0.1% of 2-mercaptoethanol and homogenized, then clarified with two rounds of 15% vertrel XF. After low speed centrifugation at 5,000 x *g* for 5 min, the supernatant was centrifuged at 119,000 x *g* for 2 h. The pellet was suspended in 0.05M PB (pH7.0) and fractionated through 20-50% sucrose gradient by centrifugation at 103,900 x *g* for 1.5 h. Fractions from 35 to 25% sucrose were dispensed and checked the presence of the virus by extraction of dsRNA from each fraction. The highest two to three fractions were combined and centrifuged at 130,000 x *g* for 1.5 h. The resultant pellet was suspended in 30 μl of 0.05M PB.

Purified virions were transfected into *R. necatrix* protoplasts with the aid of PEG-$CaCl_2$ and infected strains were obtained from regenerated colonies following the procedure as described previously (Sasaki *et al*., 2006).

4.2.4 cDNA construction and sequence analysis

Total dsRNA were extracted from the fungal mycelia of W370T1/ RnMBV1-R3a and -R3b (Fig. 1. Lane 7 and 8). Each segment of dsRNA3a and 3b were excised from agarose gel, and extracted by using MagExtractor -PCR and gel clean up- (TOYOBO, Osaka, Japan). The cDNA libraries of dsRNA3a and 3b were constructed independently by using cDNA synthesis Kit, M-MLV Version (Takara, Ohtsu, Japan) based on a classic non-PCR-based method as described previously (Yaegashi *et al*., 2013a). Sequence was analyzed using ABI 3730xl sequencer at Macrogen Japan (Tokyo, Japan). Both the 5' and 3' terminal sequences of dsRNA3a and 3b segments were determined by the linker-ligation mediated method (3'-RLM-RACE).

4.2.5 Northern blot analysis and Reverse-Transcription PCR

Northern analysis of total RNA isolated from fungal mycelia as described above was done following the procedure of Chiba *et al*. (2009). Total RNA (1.5 µg) was separated by electrophoresis in 1.0% agarose gels under denaturing conditions and capillary transferred onto Hybond-N+ nylon membrane (Amersham Biosciences, Buckingham, England). The digoxigenin (DIG)-11-dUTP labeled probes were amplified from cDNA of RnMBV1 by PCR according to the manufacture's recommendation (Roche Diagnostics, Mannheim, Germany). Chemiluminescent signals of probe-RNA hybrids were detected by the aid of DIG detection kit and CDP star (Roche). Reverse-transcription (RT) - PCR was done as follows. Double-stranded RNA was denatured in 90% DMSO for 15 min. at 65 ºC. cDNA was synthesized with AMV reverse transcriptase (TAKARA) and targeted fragments were amplified with EX taq polymerase (Takara) according to the manufacture's recommendation. Primers used in this study are listed in Table 2.

4.2.6 Western blot analysis

Rabbit polyclonal antibodies against ORF1 (coat protein), ORF3 and ORF4 of RnMBV1 were used. For ORF1 protein detection, antibody generated against N-terminal (367 aa) and C-terminal (349 aa) of ORF1 was used. For ORF3 and 4 protein detection, antibodies were generated as follows. The nucleotides of the total ORF3 and ORF4 region were cloned into pET41a (Novagen, Darmstadt, Germany), and the

resulting vectors were transformed individually into *E. coli* BL21 (DE3) (Novagen). Protein extraction was performed with BugBuster Protein Extraction Reagent (Novagen) following the manufacturer's instruction. The soluble and insoluble protein fractions were separated by SDS-PAGE and the expected size of the band in insoluble protein was excised from the gel. The excised samples were sent to SIGMA ALDRICH (Ishikari, Japan) and used to raise the antiserum in rabbit.

In order to detect ORF1, ORF3 and ORF4 proteins, *R. necatrix* strains were cultured on cellophane overlaid PDA plate. The mycelia were striped with cellophane, and then homogenized with mortar and pestle under liquid nitrogen. Soluble fractions were extracted from powdered mycelia in PBS buffer, precipitated with 10% trichloroacetic acid, and then separated on 10% SDS-PAGE analysis. The proteins were transferred to immobilon-P transfer membrane (Millipore, Billerica, MA, USA) using electroblotting apparatus (Nihon Eido, Tokyo, Japan). The signals were detected by Supersignal WestDura Extended Duration substrate (Thermo SCIENTIFIC, Rockford, IL, USA).

4.2.7 Virulence assay

Virus-free strains W97 and W370T1 and their derivative strains infected with wt RnMBV1 or RnMBV1-R were inoculated on roots of apple nursery plants (*Malus pruniforia* var. ringo) as described in Chiba *et al*. (2009).

4.3 Results

4.3.1 RnMBV1 rearranged genome segment (RnMBV1-RL2) in *C. parasitica*

Virus particles from purified fraction of RnMBV1 were transfected to spheroplasts of experimental host *Cryphonectria parasitica*, standard isolate (EP155) and a strain lacking dicer gene (Δ*dcl-2*), other fungal host causing chestnut blight disease. As shown in Chapter 3, at least two type of dsRNA banding patterns were observed, one that contains 2 bands, similar to wild type RnMBV1 and one with a single band. Of the 25 total transfectants in Δ*dcl*-2, 15 isolates showed possibly the same pattern of dsRNA with wild type RnMBV1. While the remaining 9 harbored the other type of RnMBV1 rearranged genome segment (RnMBV1-RL2). RL2 refers to rearranged large segments

derived from dsRNA2. Infection of RnMBV1 to EP155 showed only one pattern of RnMBV1 genome rearrangement (Fig.1, Chapter 3).

To confirm the rearrangement result, northern blot analysis was carried out. The result was mentioned before in Fig. 4, Chapter 3.

4.3.1.1 Genome organization of RnMBV1-RL2 in *C. parasitica*

To determine genetic organization of RnMBV1 in *C. parasitica*, RT-PCR was carried out using DNase treated mRNA as template and primer set for dsRNA1 and 2 that are shown in Table 2 (this chapter and Chapter 3). As shown in Fig. 1, the same expected size of dsRNA1 fragments were observed to both RnMBV1 and Δ*dcl*-2/RnMBV1-RL2 (#1).

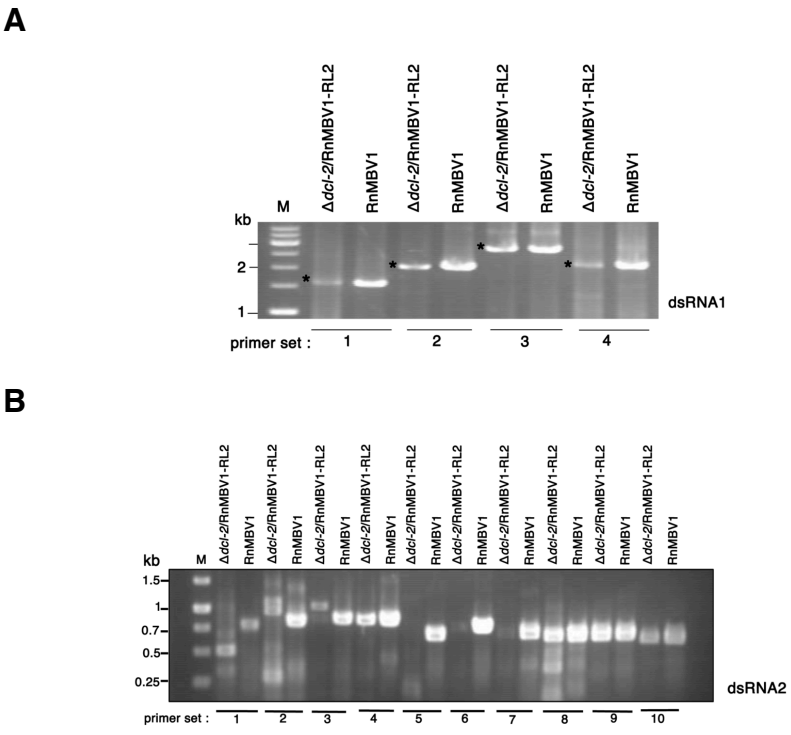

Fig. 1. Agarose gel electrophoresis of RT-PCR on the RnMBV1-RL2. DNase treated mRNA of RnMBV1 and Δ*dcl*2/RnMBV1-RL2 (#1) were used as templates in cDNA synthesis and subsequent PCR using gene specific primer sets (Table 2). (A) Amplified products of dsRNA1 and (B) amplified products of dsRNA2 were electrophoresed in 1% agarose gel in 0.5XTAE buffer. Size standard was electrophoresed in parallel (lane M). Asterisks in A refer to expected bands.

Table1. Fungal and viral strains used in this study.

Strain	Description	Reference or Source
Fungal		
EP155/RnMBV1-RL2(#1)	EP155 infected with genome rearrangement RnMBV1	This study
Δ*dc-2*/RnMBV1-RL2(#1)	Δ*dcl-2* infected with genome rearrangement RnMBV1	This study
W1015	A virus-cured strain of W779	Chiba *et al.* (2009)
W97	*R. necatrix* virus free strain belongs to group MCG80	This study
W370T1	*R. necatrix* virus free strain belongs to group MCG8139	This study
W779	RnMBV1-carrying field isolate of *R. necatrix*	Chiba *et al.* (2009)
Viral		
RnMBV1	Prototype of the family *Megabirnaviridae*	Chiba *et al.* (2009)
RnMBV1-RL2	RnMBV1 rearranged large segments derived from dsRNA2	This study
RnMBV1-RS1	RnMBV1 rearranged small segments derived from dsRNA1	This study

Table 2 Primers used for full length dsRNA2

Primer set	Primer name	Sequence 5'-3'
1	L1L2-5'	GCATAAAAAGAGAAGGAAGTT
	L2-1Rv-1	GGCTGTTTAAACACAGCATCT
2	L2-1Fw-1	TGTGAGGTACGGTGTAGCTGG
	L2-1 Rv-2	AAGAATTGCAGGACAGCGTTT
3	L2-1Fw-2	AGGCCAGCTTAGGTAATAGCA
	L2CD1	CTCCAAACCTCCAAACGATG
4	L2CD2	GCAATAACCACCTCGCATTG
	L2-2Rv-1	CAGCAGGCATATCTGAGTACT
5	L2-2 Fw-1	GCAATGAGCGGCAATGCT
	L2-2 Rv-2	CATGGCAATGACACCATT
6	L2-2 Fw-2	GGTAACTACGCCGAATGG
	L2CD3	TTCGACGTGAAATCCGTTAG
7	L2CD4	GCGACTTAGTAGATACGGAG
	L2-3Rv-1	TGTTGTGTGCACAGCAAA
8	L2-3 Fw-1	AGCTTGGTTGCAGCACGTA
	L2-3Rv-2	TGCCGGTTCTGCACCATA
9	L2-3Fw-2	TGGCGTAGATCTTAAGATCCA
	L2-3Rv-3	TCCCTTGTACCAGCACGA
10	L2-3Fw-3	CCATCGTGAAGCTGTGGA
	L2-3'	GCGAAAAAACGATGTCAATCG

Among the 10 primer sets designed from dsRNA2, the first 3 primer sets gave different RT-PCR products between RnMBV1 and Δ*dcl*-2/RnMBV1-RL2 (#1). After excising those specific bands and processed for sequencing, results indicated that those sequences are complementary to dsRNA1. While the remaining samples (using primer sets 4-10) gave sequences which originated from dsRNA2. Several attempts were made to identify the junction position where sequences of dsRNA1 and dsRNA2 are located, unfortunately, they all failed. Due to this reason, it was difficult to assemble the sequences of the rearranged virus. Mostly, sequences that were obtained here are fragmented sequences from both dsRNA1 and dsRNA2. Hence, no definitive sequence

can be reported here. Also, it is noteworthy that given the same amount of starting cDNA for RT-PCR, it seems that concentration of dsRNA1 is less in Δ*dcl*-2/RnMBV1-RL2 (#1) compared to RnMBV1.

To add to the confusion, when both samples were run long time (7h at 0.7% AGE), clear separation of dsRNA1 and dsRNA2 were achieved. Figure 2 clearly shows that concentration of dsRNA1 seems high, which contradicts with the result in Fig. 1A using RT-PCR. Interestingly, a new band in-between dsRNA1 and dsRNA2 was found, albeit at very low concentration, which is almost similar to the intensity of dsRNA2. This band is neither present in RnMBV1 nor in Δ*dcl*-2/RnMBV1-RL2 (#10).

In the previous dsRNA preparation (see Fig. 1 of Chapter 3 and Fig. 2 this Chapter), different banding pattern was observed. That is, only an apparent single band which is slightly higher than the authentic dsRNA1 was observed. That observation might have been due to 1.) Difference in AGE running condition , 2.) DsRNA of Δ*dcl*-2/RnMBV1-RL2 (#1) is still undergoing rearrangement and the dsRNA profile observed before is not yet in its stable form.

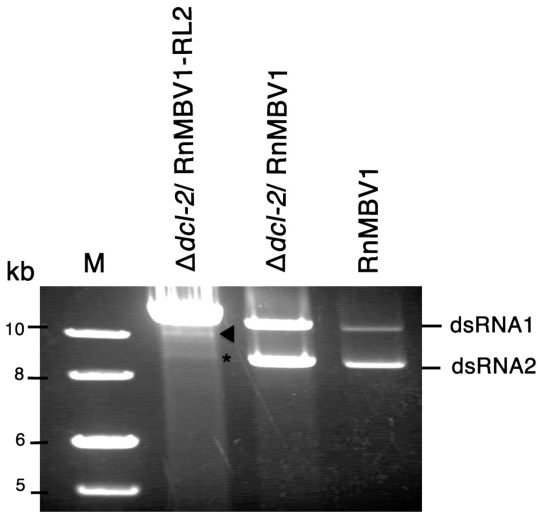

Fig. 2. DsRNA patterns of RnMBV1-R (#1) -infected Δ*dcl-2* compared with wild-type RnMBV1 -infected Δ*dcl-2* and *R. necatrix*. AGE analysis of dsRNAs. DsRNAs were isolated from fungal mycelia and applied to 0.7 % agarose gel in 1XTAE for 7 hr. Asterisks refer to authentic dsRNA2 and arrow refers to extended dsRNA2.

4.3.1.2 Biological properties of RnMBV1-RL2 in *C. parasitica*

Colony morphology of the virus infected strains and virus free parental strains grown under the same conditions were compared (Fig. 3A). Infection of Δ*dcl-2* with RnMBV1-RL2 showed a distinct phenotype from virus-free Δ*dcl-2*, which was characterized by irregular margin with less dense mycelia, reduced growth rate and enhanced pigmentation. Infection of EP155 with RnMBV1-R showed a smaller colony size than virus-free EP155 and enhanced pigmentation (Fig. 3A and Table 3). The morphological differences in the two host strains infected and uninfected with RnMBV1-R were pronounced more on nutrient-limited media (Vogel's) than on PDA (Fig. 3B).

For fungal virulence, those 4 strains were inoculated to apples and their virulence was evaluated by measuring lesion areas. Virus-free EP155 and Δ*dcl-2* induced large lesion area of 49.80 and 46.53 cm^2, respectively. Whereas, hypovirulence was conferred similarly to EP155 and Δ*dcl-2* upon infection by RnMBV1-RL2 and showed lesion area of 20.23 cm^2 and 18.10 cm^2, respectively. Those values are significantly smaller than those of virus free strains *($p<0.01$)* (Fig. 4). For sporulation level, RnMBV1-R infected colonies sporulated to a level comparable to virus-free (~10^8 spores/ml vs. ~10^8 spores/ml) in both EP155 and Δ*dcl-2* (Table 4).

Combined results suggested that RnMBV1-RL2 is able to infect both *C. parasitica* strains and induce phenotypic changes and virulence attenuation in both the wild-type and RNA silencing-defective strains of the experimental host.

4.3.1.3 Viral transmission

In order to examine whether RnMBV1-RL2 can infect the standard strain EP155, RnMBV1-RL2 was transferred to EP155 via anastomosis with Δ*dcl-2*/RnMBV1-RL2 (#1) as a virus donor. After 2 weeks of fusion, RnMBV1-RL2 was able to infect EP155 and Δ*dcl-2* recipient strains. From PDA fusion plate (Fig. 5A), conversion of Δ*dcl-2* into Δ*dcl-2* harboring RnMBV1-RL2 can be observed easily because of the phenotype change. Meanwhile, movement of RnMBV1-RL2 into infected EP155 is difficult to

observe on PDA plate due to its slightly altered phenotype. Results obtained from visual inspection were confirmed by extraction of dsRNA of RnMBV1-RL2 from recipient strains. The detected dsRNAs were similar to RnMBV1-RL2 in both EP155 and Δ*dcl-2* (Fig. 5B).

Table 3. Comparison of pigment production of RnMBV1-RL2 infected EP155 and Δ*dcl-2* compared to virus free strains.

Fungal strain/Virus strain	Absorbance (454 nm)
Δ*dcl-2*/RnMBV1-RL2 (#1)	4.19 ± 0.083^{a}
Δ*dcl-2* (virus free)	2.48 ± 0.076^{b}
EP155/RnMBV1-RL2 (#1)	2.00 ± 0.076^{c}
EP155 (virus free)	1.33 ± 0.063^{d}

Data (mean±SD.) with different letters are significantly different *(p<0.01)* among treatments (*n*=3).

Table 4. Level of asexual sporulation.

Fungal strain/Virus strain	Number of conidia/ml
Δ*dcl-2*/RnMBV1-RL2 (#1)	$1.92 \times 10^{8} \pm 4.57 \times 10^{7a}$
Δ*dcl-2* (virus free)	$3.02 \times 10^{8} \pm 5.67 \times 10^{7abc}$
EP155/RnMBV1-RL2 (#1)	$3.29 \times 10^{8} \pm 2.18 \times 10^{7abc}$
EP155 (virus free)	$4.10 \times 10^{8} \pm 5.12 \times 10^{7c}$

Data (mean±SD.) with different letters are significantly different *(p<0.01)* among treatments (*n*=3).

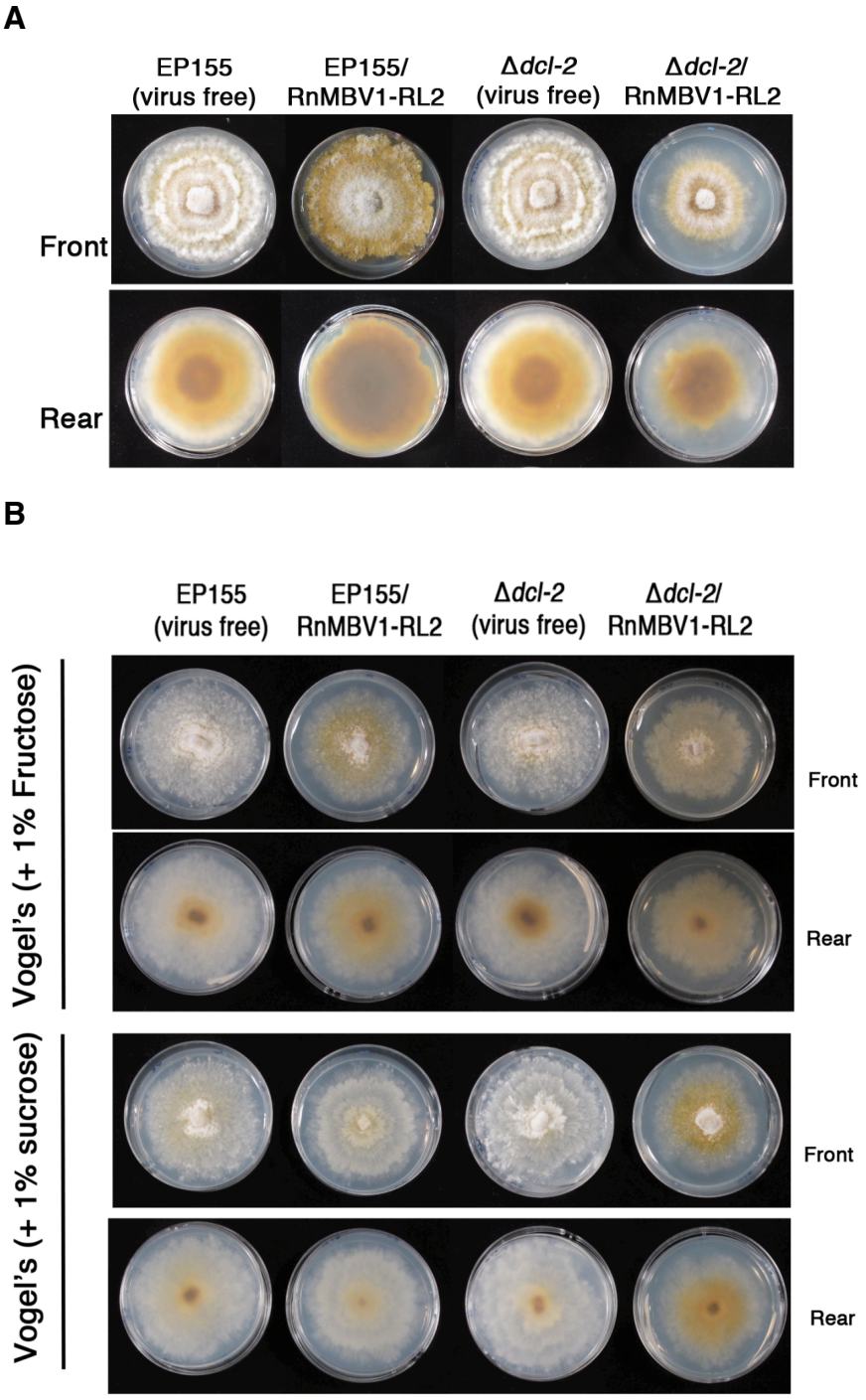

Fig. 3. Colony morphology of *C. parasitica* EP155 and Δ*dcl*-2 infected or uninfected with RnMBV1-RL2. (A) Fungal colonies were grown on PDA for 6 days on a bench top and then photographed. (B) Fungal colonies were grown on Vogel's agar supplemented with 1% of either sucrose or fructose and incubated for 2 weeks at 24°C on a bench top and then photographed.

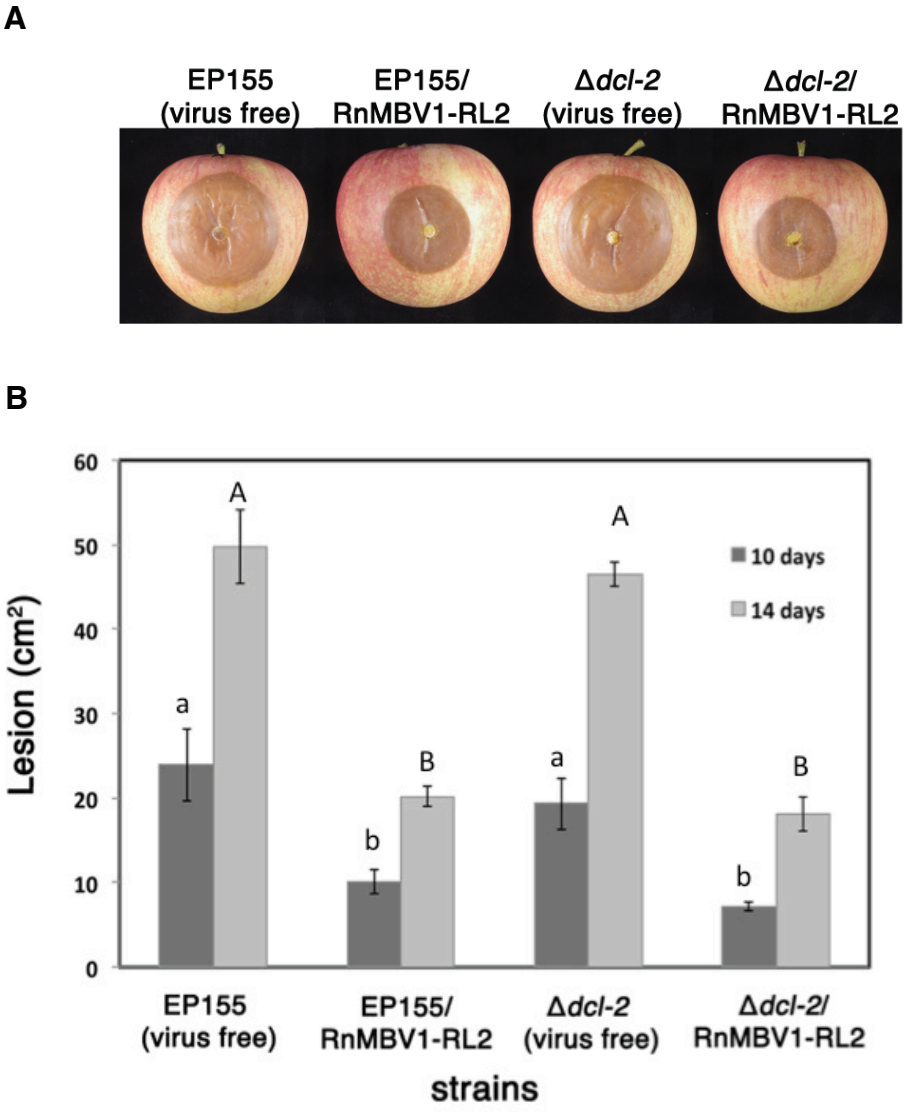

Fig. 4. Virulence levels were measured for 4 fungal strains; EP155 and Δ*dcl-2* infected or uninfected with RnMBV1-RL2 in apple assay. (A) Representative lesions induced by the fungal strains at 12 days after inoculation are shown. (B) Graphical representation of virulence levels. Virulence is expressed as the average of lesion area on day 10 and 14 post inoculation from 3 replicates for each strain with standard deviations. Data (mean±SD.) with different letters are significantly different *($p<0.01$)* among treatments (n=3).

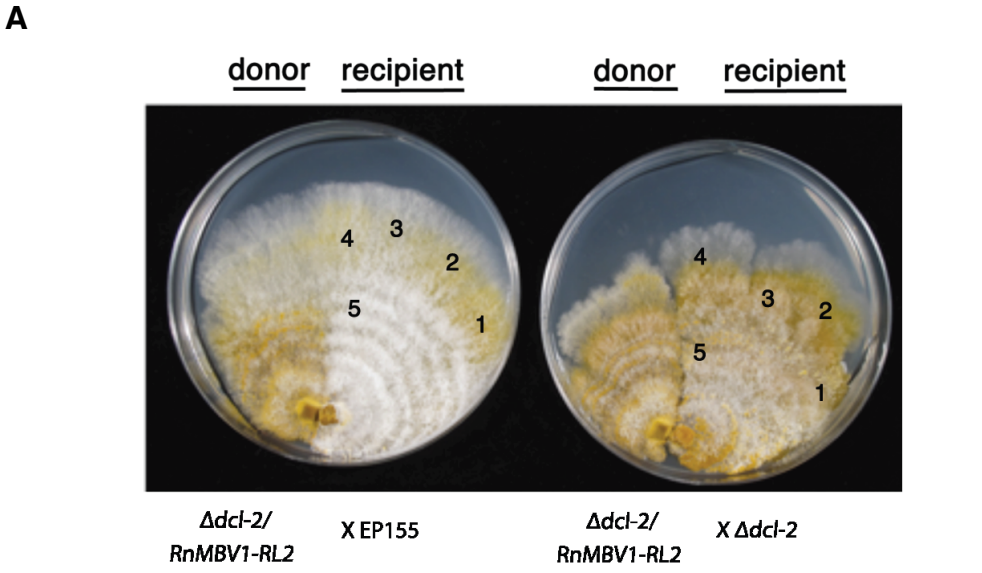

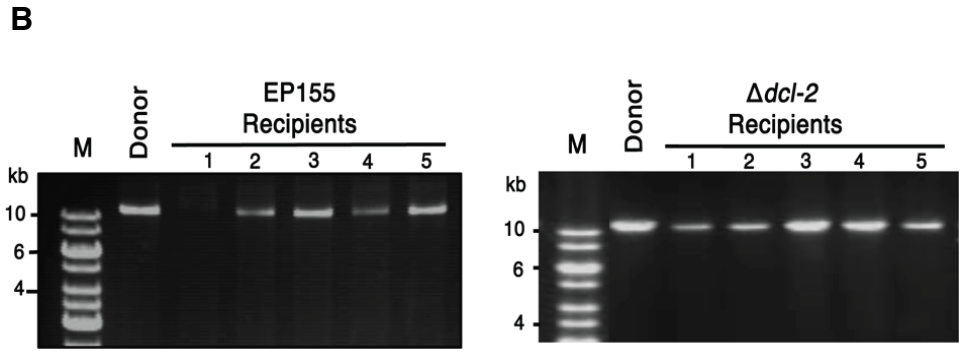

Fig. 5. Hyphal anastomosis of RnMBV1-R. (A) Introduction of RnMBV1-RL2 to the *C. parasitica* standard strain EP155 from RnMBV1-RL2-infected Δ*dcl-2* via hyphal fusion (anastomosis). The donor strain Δ*dcl-2* infected by RnMBV1-RL2 (#1) was anastomosed with either EP155 or Δ*dcl-2* as a recipient. (B) Detection of viral dsRNAs from recipient strains. Fungal subcultures from the recipient sides of co-cultures as in Fig. 2 were subjected to dsRNA extraction and subsequent agarose gel electrophoresis. Each lane represents independent fusant.

Sub-culturing was continued for all the samples and found out that RnMBV1-RL2 is still present in EP155 even after 9th subculture. Difference in RNA level was evident in these strains even in independent subsamples despite the same amount (wet weight) of infected mycelia were used for AGE analyses (Fig. 6).

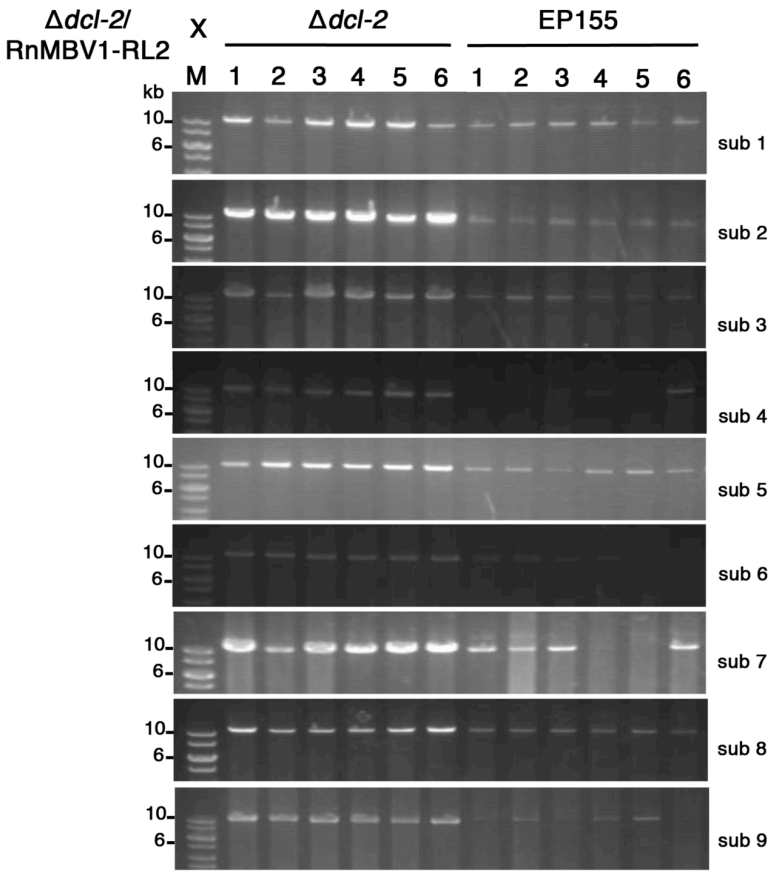

Fig. 6. Hyphal anastomosis. (A) DsRNA patterns of RnMBV1-RL2-infected EP155 and Δ*dcl-2*. DsRNAs were purified from nearly the same amount (0.05 g, wet weight) of 6 independent subcultures (1^{st}-9^{th} round) and analyzed in AGE.

Vertical transmission refers to the movement of virus into the reproductive units (conidia or ascospores) of the fungus, to be expressed in the next generation. All single conidial isolates with symptoms were checked for the presence of RnMBV1-RL2.
Visual observation and dsRNA determination were done to check the infection of RnMBV1-RL2 via spore. Thirty three samples from total 1,687 single spore germlings tested were confirmed to be infected with RnMBV1-RL2. So, vertical transmission rate in Δ*dcl-2* was confirmed to be 1.98% (Fig. 7).

Since RnMBV1-RL2 did not induce obvious phenotypic alterations in EP155 and the result of vertical transmission rate from RnMBV1-infected EP155 showed low transmission rate (0.27%). So, it was decided not to check transmission rate of

RnMBV1-RL2-infected EP155 but presumed that the transmission rate of RnMBV1-RL2-infected EP155 should be lower than RnMBV1-RL2-infected Δ*dcl-2*.

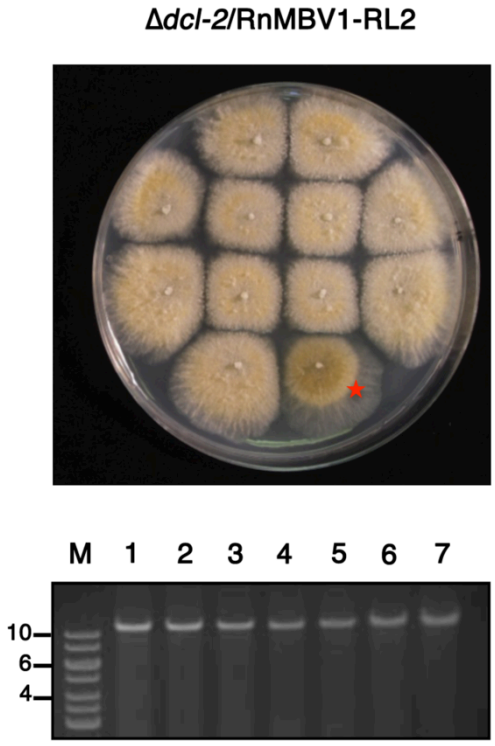

Fig. 7. Germlings grown from isolated single spore. Top; colony morphology of germlings of Δ*dcl-2* infected with RnMBV1-RL2. The red mark represents the colony morphology of infected fungal isolate. Below; AGE analysis of dsRNA from germlings confirming virus infection.

4.3.1.4 Replication level of RnMBV1-RL2 in RNA-silencing-defective strain is higher than in RNA silencing-competent strain

To find out the effect of the rearrangement in the replication of RnMBV1 in *C. parasitica,* total RNA fractions isolated from EP155 and Δ*dcl-2* infected with RnMBV1 and RnMBV1-RL2 were analyzed by agarose gel electrophoresis (Fig. 8). Increment genomic RNA accumulation was observed between RnMBV1-RL2 infected Δ*dcl-2* and

standard EP155. Between viruses, RnMBV1-RL2 showed higher accumulation level than RnMBV1 in both EP155 and Δ*dcl-2* (Fig. 8).

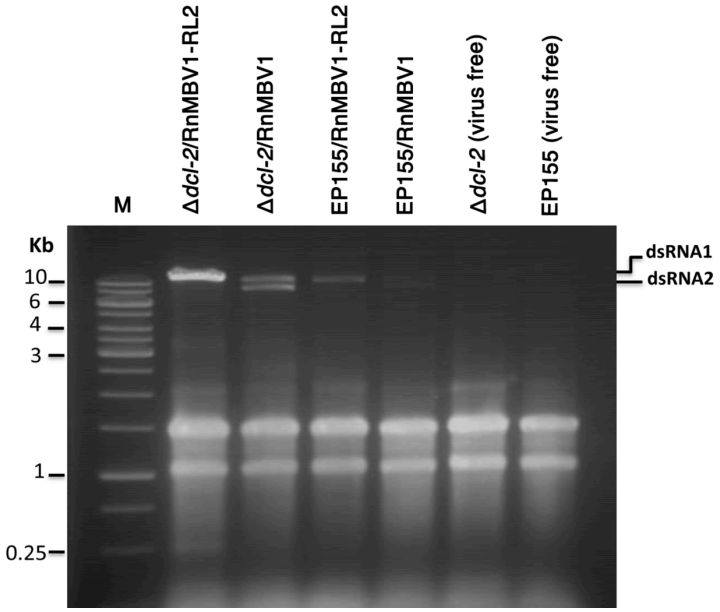

Fig. 8. Comparison of viral accumulation in RNA silencing-defective and -competent strains. Agarose gel electrophoresis (AGE) profiles of total RNA fractions. RNAs were isolated from RnMBV1-RL2-free and -infected EP155 and Δ*dcl-2* and applied to 1.4% agarose gel.

4.3.1.5 Virus particles purified from Δ*dcl-2*/RnMBV1-RL2

To verify the transfection capability of RnMBV1-RL2, its particles were purified and transfected to *C. parasitica* (Δ*dcl-2*) and *R. necatrix* W1015 (original host of RnMBV1). After ultracentrifigation, three distinct bands were observed (Fig. 9A). DsRNA of those fractions were extracted and analyzed by agarose gel electrophoresis. As shown in Fig. 9B, the amount of nucleic acids were presented in fraction 2 and 3. The viral protein in each fraction was detected by SDS-PAGE. The virus particles in those 3 fractions contained major protein band corresponding to viral capsid protein (135 kDa), indicating that fraction 1 of RnMBV1-RL2-infected Δ*dcl-2* contained empty capsid. Fractions 2 and 3 were successfully transfected to spheroplasts of Δ*dcl*-2. As shown in Fig. 10A, the colony morphology of virus infected strains (F2 and F3) were similar to the parental virus infected strain (Δ*dcl-2*/RnMBV1-RL2 #1). DsRNA profile

from virus infected fungal strains migrated in the same size with dsRNA from parental (Fig. 10B).

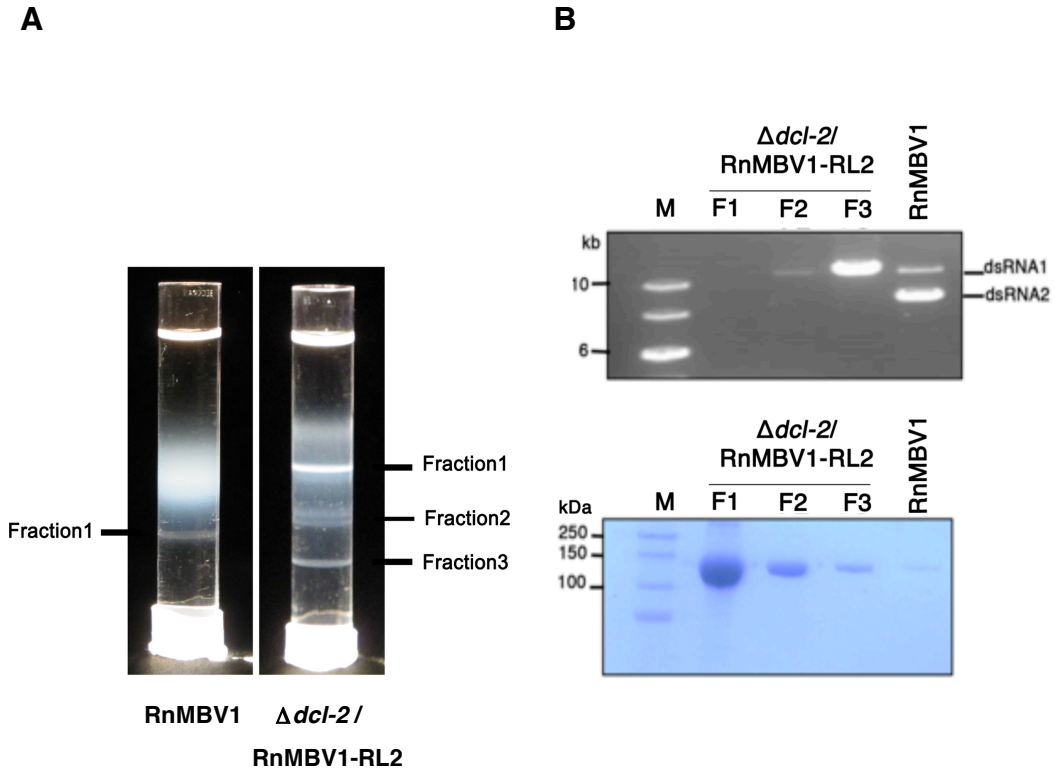

Fig. 9. Virus particles purified from Δ*dcl-2* infected with RnMBV1-RL2. (A) Photographs of the 20-50% cesium sulfate gradient tubes, RnMBV1 (left tube) and Δ*dcl-2*/RnMBV1-RL2 (right tube). Crude lysate from a virus preparation was layered on top of the tubes containing a cesium sulfate step gradient. After 15 hr centrifugation at 28,000 rpm in a SW41Ti swing out rotor, clear bands were visible in the cesium sulphate phase. The particle bands and other minor bands containing non fully mature or empty capsids appear white with a light shadow. (B) Top; agarose gel electrophoresis analysis shows the dsRNA patterns of the viral particles present in the bands detected in the gradients shown in (A). DsRNA from 10 µl of virus particle suspension were obtained after treatment with phenol/chloroform and chloroform. DsRNA fractions were loaded into each well of 1% agarose gel and electrophoresed in 1X TAE buffer. Below; analysis of the virus particles preparation by 8% SDS-PAGE. Protein from virus particles was prepared as described in method. The migration of the viral structural proteins in the gel is indicated.

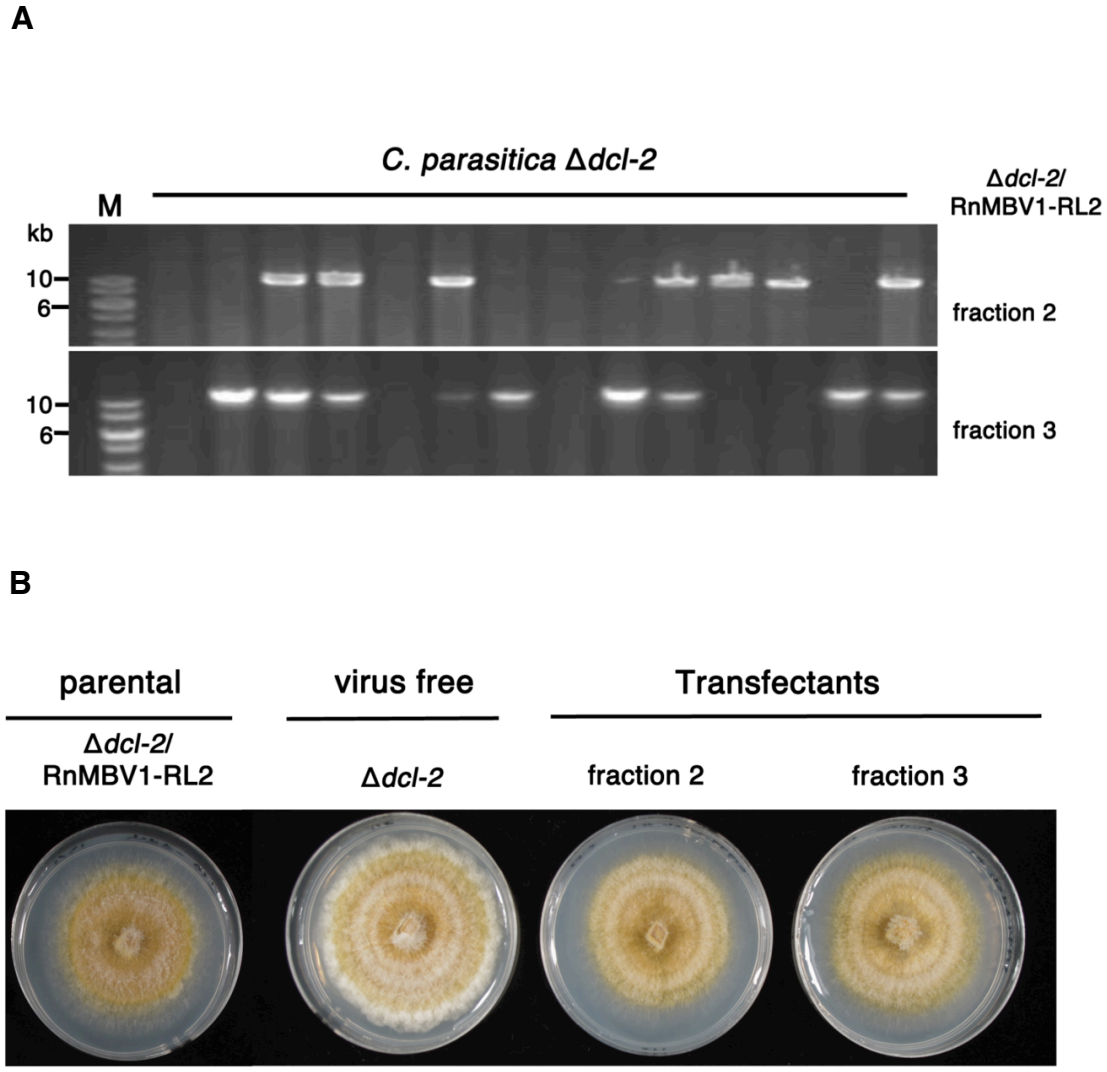

Fig. 10. Infection of RnMBV1-RL2 purified from *C. parasitica*. (A) Agarose gel electrophoretic analysis of dsRNA from transfectants. Spheroplasts of Δ*dcl-2* were transfected with purified RnMBV1-RL2 particles from *C. parasitica*. (B) Colony morphology of RnMBV1-RL2-infected *C. parasitica* Δ*dcl*-2, uninfected and parental strains were grown on PDA for 6 days on a bench top and then photographed.

4.3.2 RnMBV1 rearranged genome segment (RnMBV1-RS1) in *R. necatrix*

4.3.2.1 Isolation of RnMBV1-RS1 from RnMBV1 transfectants

During repeated transfections of virus-free isolates of *R. necatrix* with purified virions obtained from isolate W779, as described in Chiba *et al*., (2009), dsRNA profiles that differed from wild-type RnMBV1 were noticed. Agarose gel electrophoresis of

extracted dsRNA from these strains revealed two dsRNA segments, dsRNA1 and a new smaller segment. The smaller segment migrated between RnMBV1 dsRNA2 (7180bp) and the dsRNA genome of Helicobasidium mompa totivirus1 (HmTV1-V17; 5207bp), yielding an estimated size of 6.5kbp (Fig. 11). To understand the appearance of the 6.5-kbp segment, *R. necatrix* isolate W97 was transfected with dilutions of purified particles, making isolation of a relatively minor virus population more likely, with monitoring during sub culturing. Consequently, primary transfectants frequently carried the wild type RnMBV1 genome, and, much less frequently but reproducible an unusual genometype (dsRNA1 alone). After three rounds of sub-culturing every 10 days, most fungal isolates infected by the virus variant underwent further alteration from single dsRNA to double dsRNA segment profiles, comprised of dsRNA1 and dsRNAS1 (6 out of 8 isolates, Fig. 12), with one exception having a smaller segment than dsRNAS1 (lane6). After five rounds of subculturing, all the fungal isolates harbored two dsRNA segments (dsRNA1 and dsRNAS1, 7 out of 8 isolates) or dsRNA1 and a small segment (approximately 4 kbp).

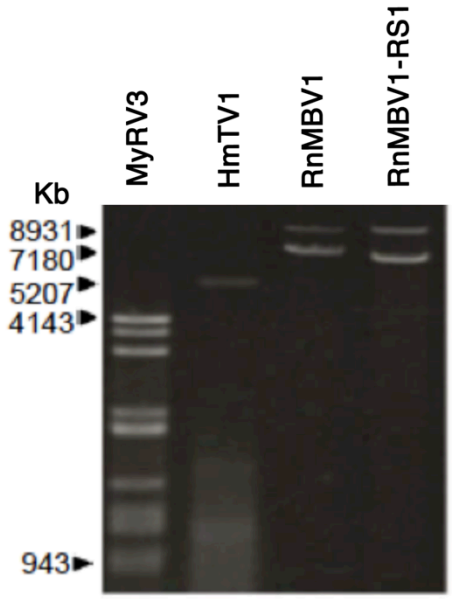

Fig. 11. DsRNA profile of the genome of wild-type RnMBV1 and RnMBV1-RS1 on agarose gel in comparison with the electrophoretic mobility of the dsRNA genomes of Rosellinia necatrix mycovirus 3 (MyRV3) and Helicobasidium mompa totivirus1 (HmTV1). The size of each dsRNA identified was shown in the left (kb).

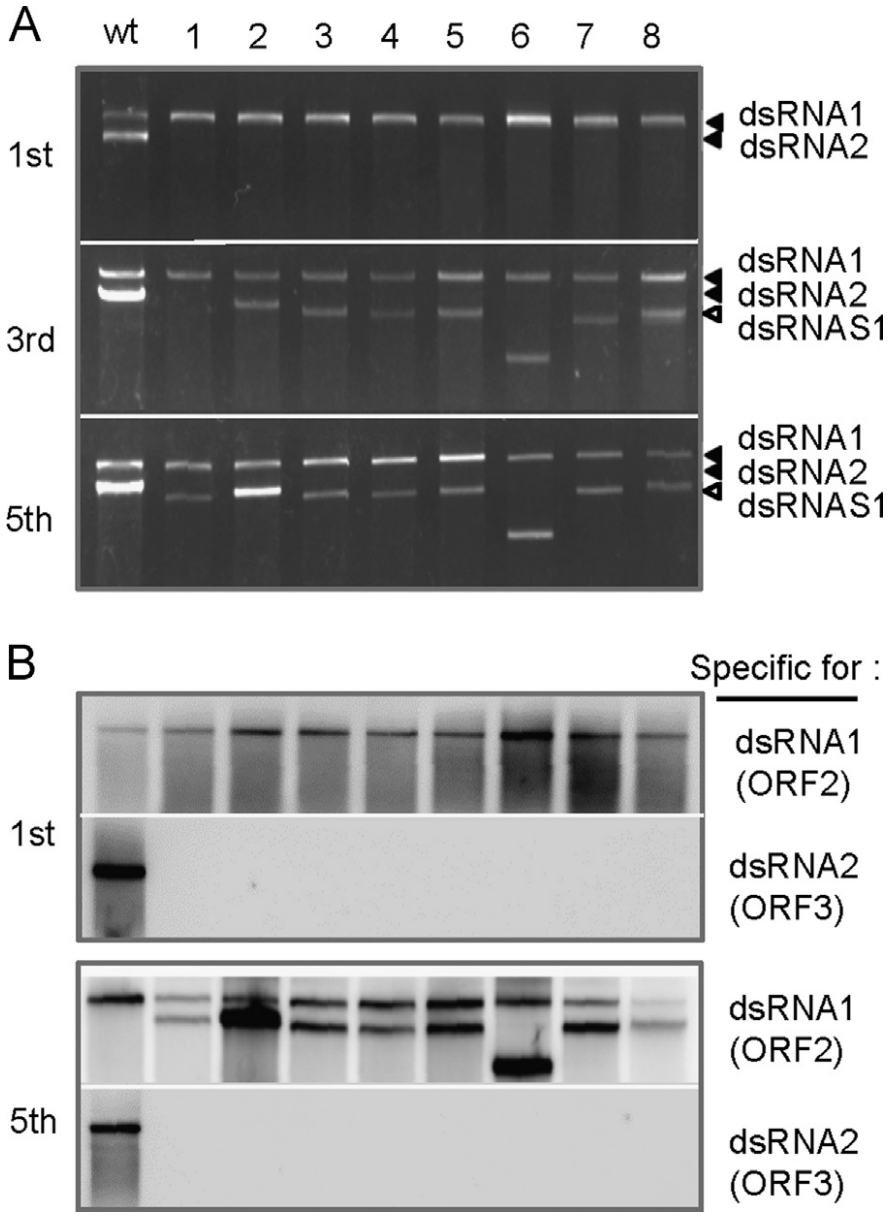

Fig. 12. Appearance of RnMBV1-RS1 in *Rosellinia necatrix* strain W97 after transfection with RnMBV1 virions. Lanes 1 to 8 are viral variants consisting of dsRNA1 only from the first culture after transfection. Third and fifth indicates the number of subcultures of each isolate every 10 days on PDA. (A) Agarose gel electrophoresis of extracted dsRNA from each mycelium. (B) Northern blot analyses of extracted dsRNA hybridized with probes specific for dsRNA1 and dsRNA2 in the position shown in Fig. 16.

4.3.2.2 RnMBV1-RS1 infectivity

Particles were purified from mycelia of the standard fungal strain (W97) infected with RnMBV1-RS1 (W97/RnMBV1-RS1). RnMBV1-RS1 particles were ~50 nm in

diameter and indistinguishable in size and shape from those of wild-type RnMBV1 when observed under transmission electron microscopy. Extracted dsRNA from purified RnMBV1-RS1 virions composed two dsRNAs which has the same mobility with dsRNA1 and dsRNARS1 from mycelia (Fig. 13). Virus-free *R. necatrix* isolates, W97 and W370T1 were successfully transfected with RnMBV1-RS1 virions in similar infectivity with wild-type RnMBV1. It is noteworthy that polyacrylamide-gel electrophoresis of dsRNA by the aid of silver staining revealed that dsRNA RS1 in this fungus comprised of two segments with slightly different mobility, dsRNAS1a and -S1b (Fig. 14, lane 3). Therefore, the transfectants with the particles showed varied dsRNAS1 profiles, including dsRNAS1a alone (lane 7), dsRNAS1b alone (lane 4 and 8), and a mixture (lane 5). No isolates showed a dsRNA profile of the wild type.

To confirm the stability and infectivity of RnMBV1-RS1, particles of RnMBV1-RS1 from two fungal strains of W370T1/RnMBV1-RS1a and –RS1b, which harbored either dsRNAS1a or -S1b beside dsRNA1 (Fig. 14., lane 7 and 8) were purified and confirmed their infectivity to W97.

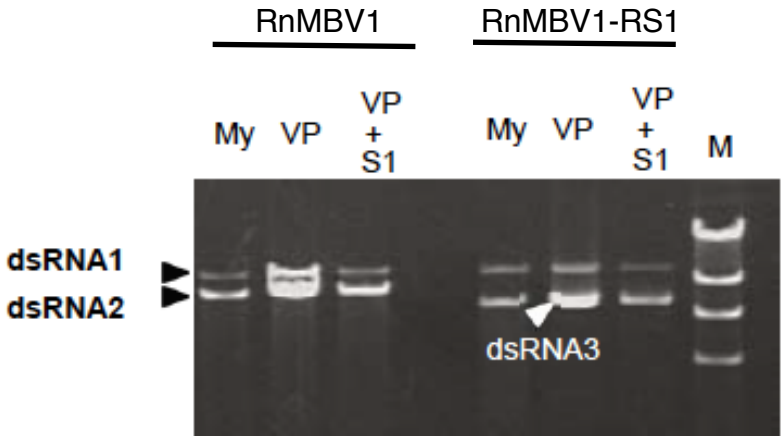

Fig. 13. DsRNA profile of wild-type RnMBV1 and RnMBV1-RS1 obtained from *Rosellinia necatrix* W779 and W97/RnMBV1-RS1a+S1b, respectively. Agarose gel (1%) electrophoresis stained with ethidium bromide. My: dsRNA extracted from mycelia, VP; total RNA extracted from purified virions, and VP+S1; dsRNA from purified virions by treating S1 nuclease. M represents λ/Hind III as a DNA marker.

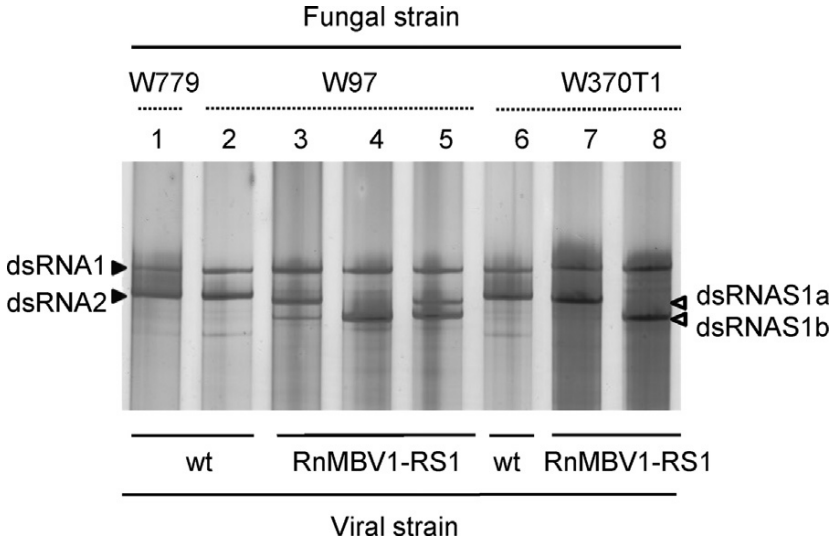

Fig. 14. Ds RNA profile of wild type RnMBV1 and its variant, RnMBV1-RS1, from mycelia of fungal strains W779 (lane1), W97/RnMBV1 (lane2), W97/RnMBV1-RS1a+S1b, -RS1b and-RS1a+S1b (lanes 3 to 5, respectively), W370T1/RnMBV1 (lane 6), and W370T1/RnMBV1-RS1a and -RS1b (lanes 7, 8) on 5% polyacrylamide gels followed by silver staining.

4.3.2.3 Genome organization of RnMBV1-RS1

RNA isolated from W370T1 infected with RnMBV1- RS1a or-RS1b were used to determine the sequence of dsRNAS1a and -S1b, because these contained only one type of dsRNAS1 segment (Fig. 15). DsRNAS1a and -S1b segments were used to prepare cDNA libraries. A total of 54 and 62 cDNAs ranging from 1 to 1.5 kbp were cloned and sequenced for dsRNAS1a and -S1b, respectively. All the cDNA clones corresponded to dsRNA1. There were no clones identical to ORF1; the majority were derived from ORF2. All the contigs from dsRNAS1a and -S1b were assembled and the 50 and 30 terminal sequences determined by RLM-RACE.

The genome organization of dsRNAS1a and -S1b are shown in Fig. 15. DsRNAS1a and -S1b are 6789 and 6290 bp in length; both are derived from rearrangements of dsRNA1. Wild type dsRNA1 and dsRNA2 each have 5' UTRs of approximately 1.6 kb with high levels of sequence similarity. The 5' 24 bp of dsRNA1 and -2 are strictly conserved. However, both of the S1a and S1b segments contained only the 5' 565 bp of 5' UTR of dsRNA1, identical to the corresponding sequence of the wild type dsRNA1. Therefore, the 5' UTR of dsRNAS1a and -S1b originated from dsRNA1 but not dsRNA2.

Commonly, dsRNAS1a and -S1b consisted of two ORF2s arranged in a head to tail orientation, lacking ORF1. DsRNAS1b had smaller portions of ORF2 than those on dsRNAS1a, explaining the length discrepancy. A mismatch mutation occurred at the ORF2 duplication junction of S1a (C to U) and one nucleotide substitution was detected: G (map positions 6678) to A (S1b, map position 648). In addition, a nucleotide substitution U to C at map position 6648 was detected in dsRNA1 from the published sequence (Chiba *et al*.,2009). This substitution was retained at the corresponding positions of S1a (map positions 717 and 4506) and S1b (map positions 618 and 4007). The 3' terminal sequences of dsRNAS1a and -S1b were conserved, as was dsRNA1. The RdRp motifs (Motif I to VIII) conserved among related dsRNA mycoviruses were encoded in the positions 6673 to 7834 of dsRNA1(Chiba etal., 2009), and these nucleotides were retained in the truncated ORF2 of dsRNAS1a and -S1b. The genome organization of dsRNAS1a and -S1b was confirmed by RT-PCR using extracted dsRNA fractions from dsRNAS1a and -S1b as templates (Fig. 16). The three sets of primers were designed to amplify fragments collectively covering the rearranged segments (L1L2-F1andL1-R3,L1-F14andL1-R11,L1-F13and L1-R1, Fig. 16 and Table 5). The expected sizes of cDNA fragments were amplified including two junction points between UTR to ORF2 and ORF2 to ORF2.

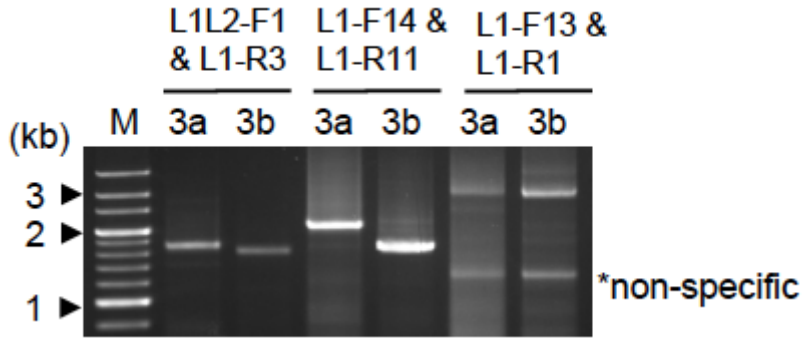

Fig. 15. RT-PCR analysis of dsRNA3a and 3b. Extracted dsRNA from mycelia of W370T1/RnMBV1-RS1a and –RS1b (lane 7 and 8 in Fig. 4) were separated on agarose gel in TAE buffer, and excised the band of dsRNAS1a and -S1b from the gel. Eluted dsRNA was used as template. Primers used for RT-PCR are denoted above line, and their positions are indicated in Fig. 3. Primer sequences are listed in Table 5.

Table 5. Oligonucleotide primers used in this study

Primer name	Sequence (5' to 3')	Map position	Used in
L1L2-F1	GCATAAAAAGAGAAGGAAGG	dsRNA1, dsRNA2, 1-20	RT-PCR
L1-R3	CCGCATAGCATCAATTTCCT	dsRNA1, 7674-7655	RT-PCR
L1-F14	AGGAAATTGATGCTATGCGG	dsRNA1, 7655-7674	RT-PCR
L1-R11	CCGTTCAAGCATCTCCATCT	dsRNA1, 5977-5957	RT-PCR
L1-F13	AGATGGAGATGCTTGAACGG	dsRNA1, 5957-5977	RT-PCR
L1-R1	GCGAAAAAGGGGTCCAGCCC	dsRNA1, 8931-8912	RT-PCR
L1-F5	CAATGTTCGACACGAGTGCT	dsRNA1, 4233-4252	RT-PCR
L1-R5	GCTGTCCCGACGTAAATCAT	dsRNA1, 5112-5093	RT-PCR
L2-F2	AGTTTGGGCTCGATGATTTG	dsRNA2, 3572-3591	RT-PCR
R2-R3	CCACGAGAACCACTCCGTAT	dsRNA2, 4524-4505	RT-PCR

4.3.2.4 Absence of dsRNA2-derived segments in RnMBV1-RS1

As shown in Fig. 12B, no portion of dsRNA2 was detected in RnMBV1-RS1. This was confirmed by a variety of techniques. Northern blotting with a probe specific for the ORF3 from dsRNA2 detected wild type RnMBV1 but not RnMBV1-RS1, as expected from the genome sequences (Fig. 17A). When RNA preparations were probed by DIG-labeled dsRNA1 cDNA, dsRNA1 and dsRNAS1 bands were observed in RnMBV1-RS1. Finally, RT-PCR analysis confirmed the absence of the ORF3 sequence in RnMBV1-RS1 (Fig. 17B). No fragments could be amplified using different sets of primers specific fordsRNA2.

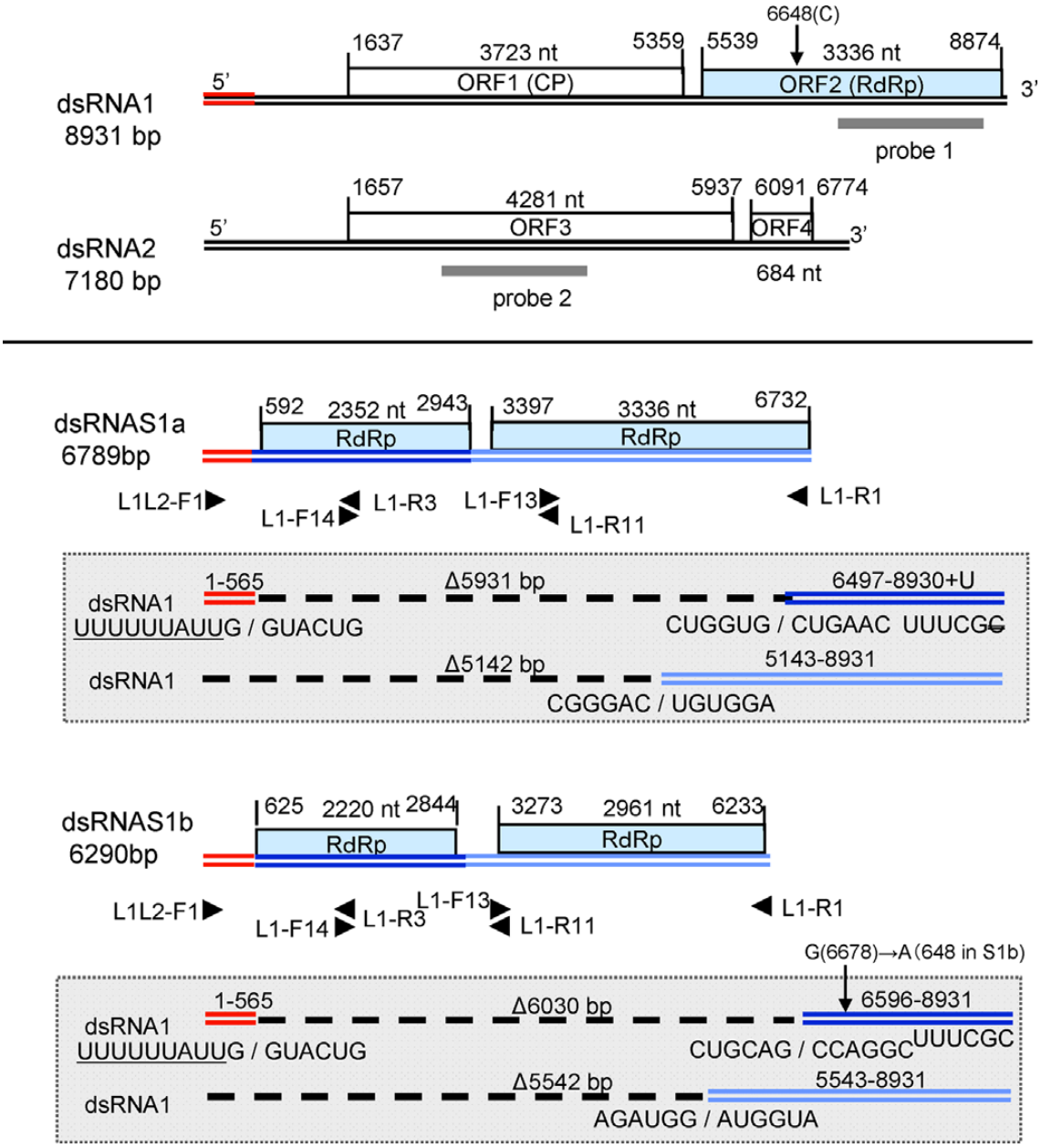

Fig. 16. Genome organization of dsRNAS1a and -S1b compared with the genome of wild type RnMBV1. Open boxes indicate ORFs, and the numbers above refer to map positions of the initiation and terminal codons of the respective ORFs. Red and blue double lines indicate the rearranged segments of dsRNAS1a and -S1b, and dotted lines indicate deletions in the rearranged segments. The sequences around the junction sites are at the bottom. Arrow heads indicate the RT-PCR primer positions in Fig. 16 and the probe position for the northern analyses in Fig. 12 and Fig. 17.

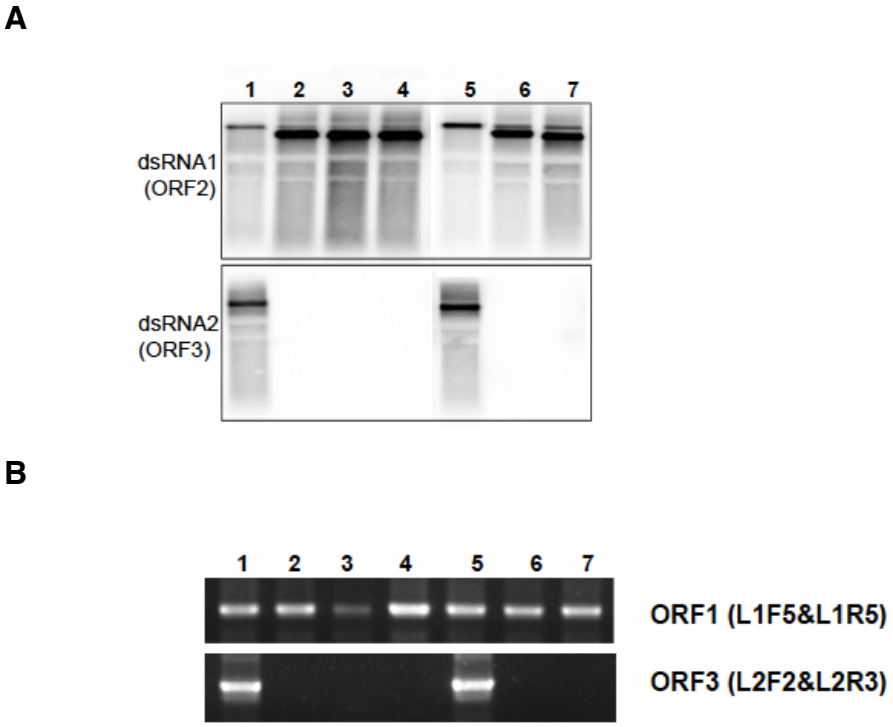

Fig. 17. Fungal strains used in the analyses were: lane1, W97/RnMBV1; lane2, W97/RnMBV1-RS1a+RS1b; lane3, W97/RnMBV1-RS1b; lane4, W97/RnMBV1-RS1a+RS1b, lane5, W370T1/RnMBV1; Lane6, W370T1/RnMBV1-RS1a; lane7, W370T1/RnMBV1-RS1b. (A) Northern blot analyses of the genome segments in RnMBV1-R. The same amount of genomic dsRNA segments as shown in Fig. 8. were separated in denatured agarose gel and capillary transferred to Hybond N+ membrane. The membrane was probed with the DIG-labeled probes specific to ORF2 (RDRP) in dsRNA1 (the upper picture) and ORF3 in dsRNA2 (the below picture). The position of the probes was denoted in the Fig. 17. (B) RT-PCR analysis of dsRNAs extracted from mycelia. Specific primers for ORF1 and ORF3 were used for RT-PCR. Primer sequences are listed in Table 5.

4.3.2.5 Decreased accumulation of RnMBV1-RS1 in *R. necatrix*

Accumulation of RnMBV1-RS1 in mycelia of *R. necatrix* was compared with RnMBV1 by measuring dsRNA concentration using agarose gel electrophoresis. (Fig. 18A). Furthermore, visual estimates of capsid protein band intensity via Western blotting showed decreased concentration in RnMBV1-RS1 compared with wild type RnMBV1 (Fig. 18B).

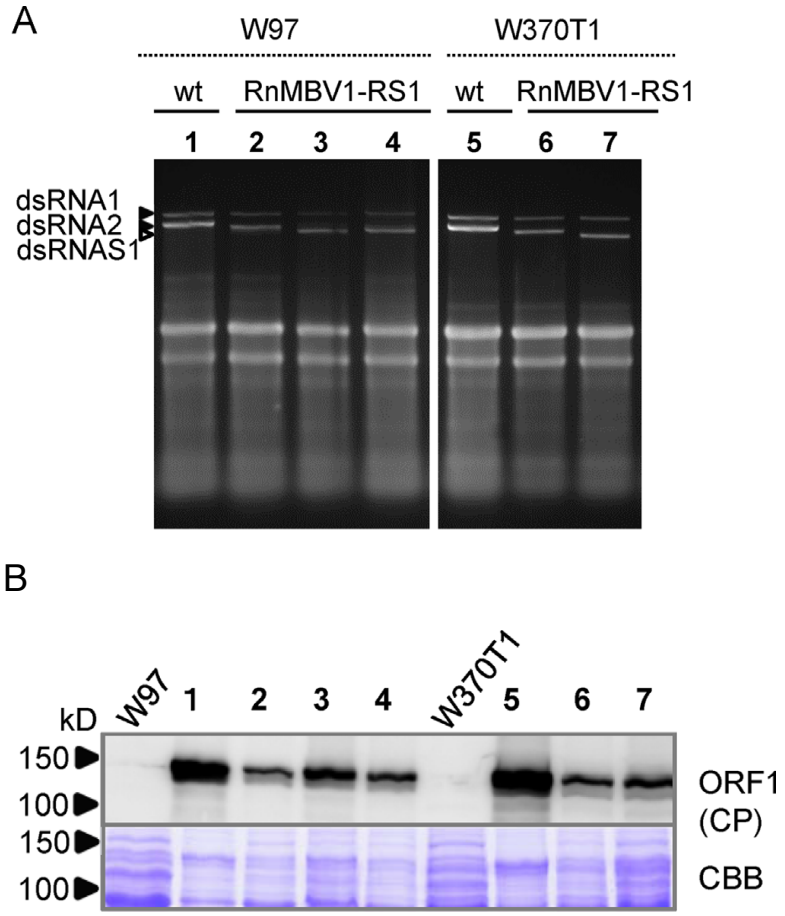

Fig. 18. Detection of genome and protein products of wild-type RnMBV1 and RnMBV1-RS1 in mycelia of *R. necatrix*. The fungal strains used were W97/RnMBV1 (lane 1), W97/RnMBV1-RS1a+S1b, -RS1b, RS1a+S1b (lanes 2 to 4), W370T1/ RnMBV1 (lane5), W370T1/RnMBV1-RS1a, -RS1b, (lanes 6, 7), and virus-free strains W97 and W370T1. (A) Agarose gel electrophoresis of 1.5 mg total RNA in 8 days mycelial culture on PDA with cellophane. (C) Western blot analyses of soluble proteins from mycelia infected with wild type RnMBV1 and RnMBV1-RS1. Proteins were separated on 10% SDS-PAGE gel and visualized with anti-ORF1 antibody or with CBB staining.

4.3.2.6 RnMBV1-RS1 infection phenotype in *R. necatrix*

Colony growth rate and formation of aerial hyphae of *R. necatrix* was considerably reduced by infection with wild type RnMBV1 regardless of the host fungal strain (Chiba *et al*.,2009). Infection with RnMBV1-RS1 resulted in different phenotypes depending on the fungal strain. The colony morphology of W370T1 infected with RnMBV1-RS1 was essentially unchanged when compared with uninfected colonies (Fig. 19A). Infection of W97 by RnMBV1-RS1 resulted in smaller colony size;

however, these are still larger than those of the wild-type-infected fungus. Growth speed in W370T1 infected with RnMBV1-RS1 was similar to virus-free W370T1 and greater than RnMBV1-RS1-infected W97 (Fig. 19B). In addition, melanization in mycelial colonies of *R. necatrix* was reduced by wild-type RnMBV1 infection (Fig. 19C). This effect was readily observed in strain W97; uninfected white colonies grown under dark conditions for 7 days and the nunder fluorescent light for a further 3 weeks turned completely black but stayed white when infected with wild-type virus. In fungal strainW370T1 uninfected colonies had some white patches which were enlarged by wild-type virus infection. Regardless of the fungal strain examined, melanization was partially restored with infected by RnMBV1-RS1. The effects of genome rearrangement on host virulence attenuation were compared by inoculating *R. necatrix* strains infected by wild-type RnMBV1 and RnMBV1-RS1 onto apple roots (Fig. 20). Similar to previous studies, the upper part of root stocks inoculated with virus-free W97 and 370T1 rapidly wilted, while those inoculated with wild-type RnMBV1-infected fungal colonies appeared healthy (Fig. 20A). RnMBV1-RS1 infected fungi were more virulent compared with those infected by the wild-type virus and leaf chlorosis was observed lower on apple plants. Root symptom severity agreed with that of the upper part of apple seedlings. All plants infected with W97 and 9 out of 10 infected with W370T1 showed no invasion of mycelia harboring wild-type RnMBV1 into the root epidermis that would lead to necrotic lesions, even after 3 months incubation (Fig. 20B). In contrast, RnMBV1-RS1 infected fungi produced extended necrotic lesions on all roots with numerous mycelia invading the root epidermis, eventhough the invasion speed of strains infected with RnMBV1-RS1 was slower than their parental virus-free strains (Fig. 20B).

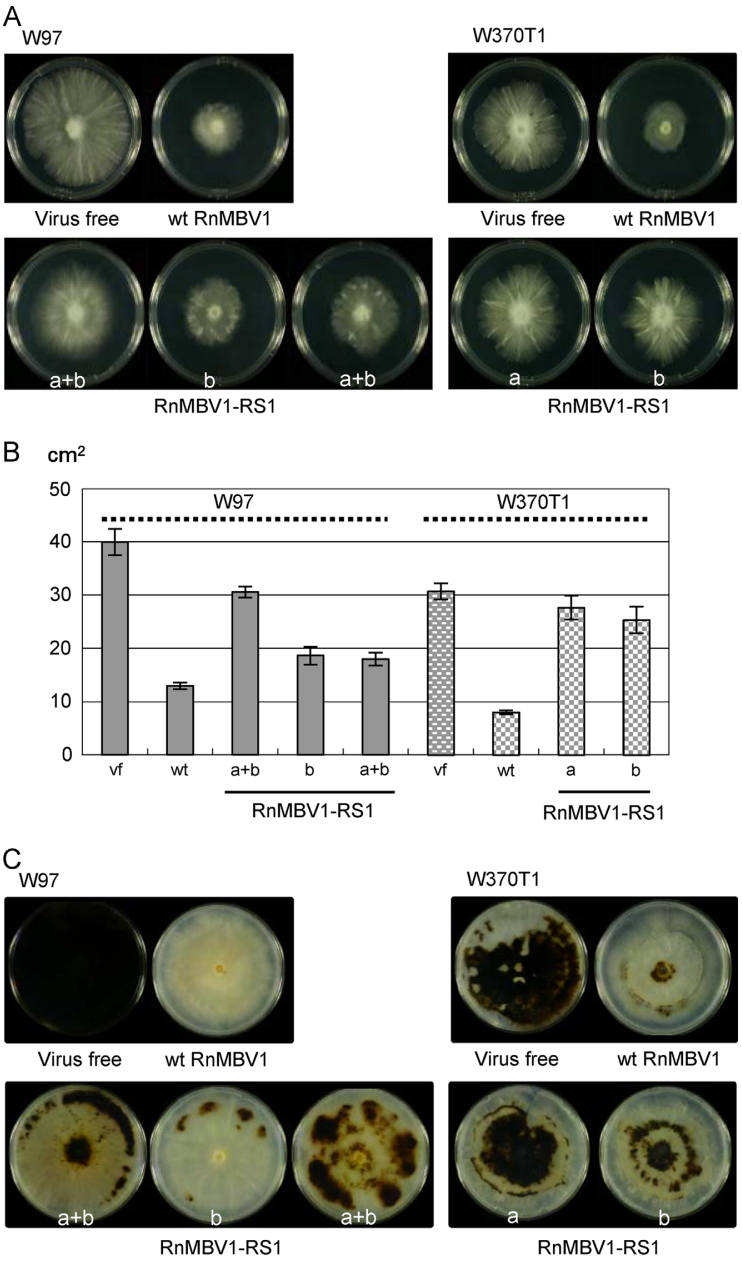

Fig. 19. Effect of wild-type RnMBV1 and RnMBV1-RS1 infection on the colony morphology of *R. necatrix*. (A) Morphology of fungal strains W97 and W370T1 infected with wild-type RnMBV1 or RnMBV1-RS1; W97/RnMBV1-RS1a+S1b, -RS1b, RS1a+S1b, W370T1/RnMBV1-RS1a,-RS1b. Each fungal strain was cultured on PDA for 6 days at 25 ^{o}C in the dark. (B) Colony area of each strain after 6 days cultivation. The bars represent the mean size of five replicates with standard errors. (C) Examination of colony melanization. Each fungal strain was cultured on PDA at 25 ^{o}C for 7 days in the dark, then further cultured for 3 weeks under continuous fluorescent light.

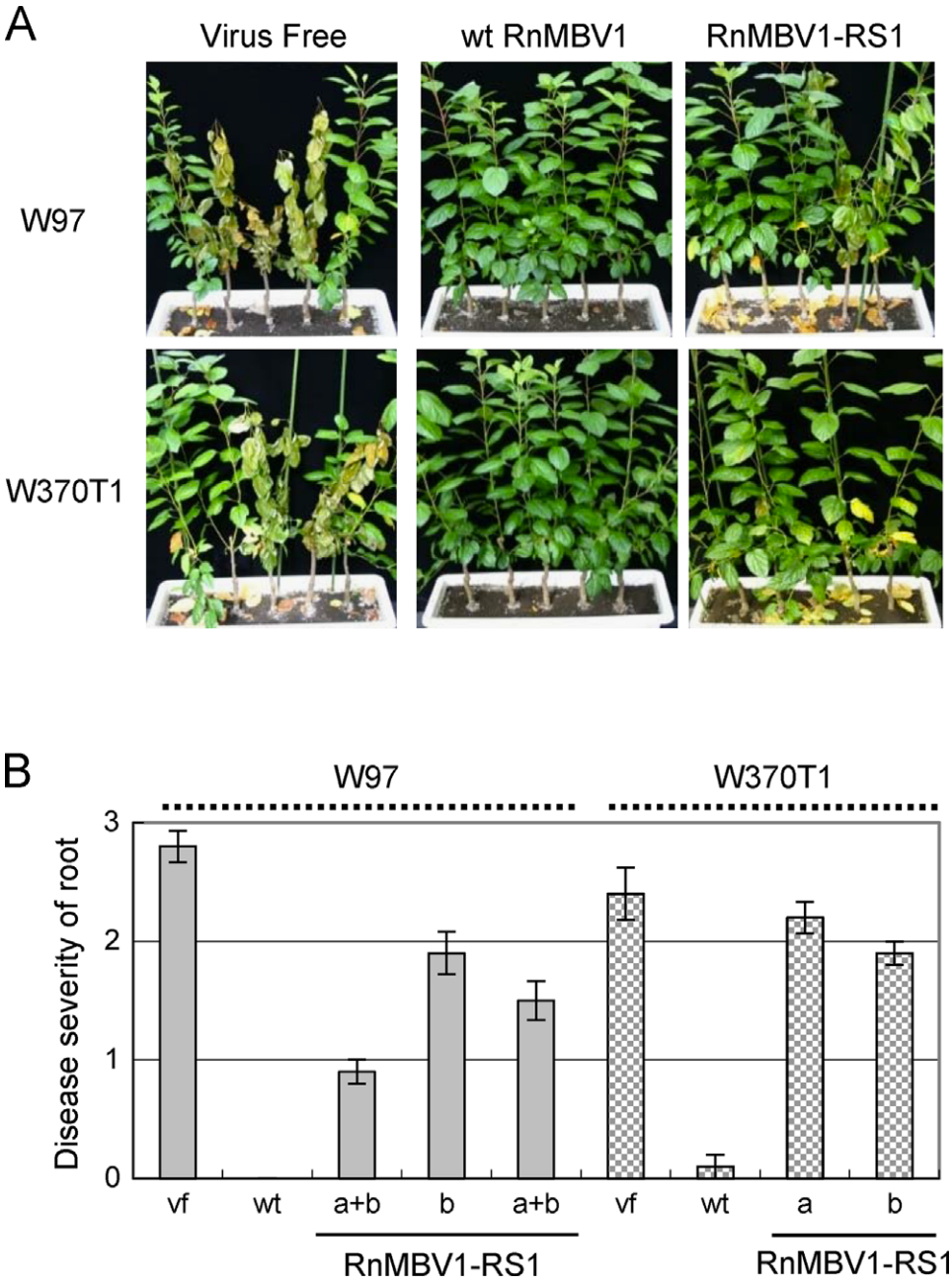

Fig. 20. Effect of wild-type RnMBV1 and RnMBV1-RS1 infection on the virulence of *R. necatrix*. (A) Symptoms of aerial part of apple nursery trees (*Malus prunifolia* var. ringo) in 1.5 months after inoculation. (B) Disease severity of roots 3 months after inoculation using disease index as follows; 0-healthy, 1-rotted part of main root was less than 50%, 2-rotted part of main root was more than 50%, 3-main root was totally destroyed and no living fine root around the main root was observed. Bar represents mean index of 10 plants with standard errors.

4.4 Discussion

Genomic rearrangements are common in human, animal, plant and fungal viruses in the family *Reoviridae*, and their genome organization and functions have been extensively surveyed (Desselberger, 1996; Taniguchi and Urasawa, 1995; Nuss, 1984; Sun and Suzuki, 2008; Eusebio-Cope *et al*., 2010). However, the extent of genomic rearrangement in other dsRNA viruses has rarely been investigated. This study describes the first example of genomic rearrangements of a newly identified dsRNA virus, RnMBV1, in *C. parasitica*, resulting in RnMBV1-RL2, which showed the expansion of dsRNA2 (Fig. 1 Chapter 3, Fig. 2 and 3 this chapter). Unfortunately, the genome sequence of RnMBV1-RL2 was difficult to determine. Results from RT-PCR and AGE suggested that dsRNA of Δ*dcl*-2/RnMBV1-RL2 is still undergoing rearrangement and the dsRNA profile observed before is not yet in its stable form. Surprisingly, the same biological properties between RnMBv1 and RnMBV1-RL2 were observed in *C. parasitica* (compare biological properties between Chapter 3 and 4) except for vertical transmission rate, which is higher in RnMBV1-RL2 than in RnMBV1, 1.98% compared to 0.48%.

Other rearranged genome was observed in *R. necatrix,* resulting in RnMBV1-RS1, one of the characteristic features of RnMBV1-RS1 is the complete loss of dsRNA2. The combinant dsRNAS1a and S1b contain only sequences derived from dsRNA1; therefore, dsRNAS1a and S1b probably resulted due to intragenic rearrangement of dsRNA1. DsRNA1 and dsRNA2 of RnMBV1 were assumed to be packaged into virions separately, as the molecular ratio of each doesn't show equimolar ratio and dsRNA1 is variably less abundant than dsRNA2 in fungal mycelia depending on culture conditions (Chiba *et al*., 2009). The results of protoplast transfection with diluted virions in this study (Fig. 12) support this notion. Fungal colonies harboring dsRNA1 alone changed their dsRNA profile to that of RnMBV1-RS1 (containing dsRNA1 and dsRNAS1) during sub-culture (Fig.12), indicating the instability of viral strains containing dsRNA1 alone. Once established, RnMBV1-RS1 was maintained stably after ten subcultures without any obvious change in dsRNA1 and dsRNAS1a and -S1b

profiles. Based on these data, a model for the generation of RnMBV1-RS1 was proposed (Fig. 21), suggesting that two genomic segments (dsRNA1 and 2 in the wild-type RnMBV1; dsRNA1 and S1 in RnMBV1-RS1) are required for stable maintenance of RnMBV1. As-yet-unraveled transactivation in the replication and/or encapsidation between the two segments might give a selective advantage to wild-type RnMBV1 and RnMBV1-RS1.

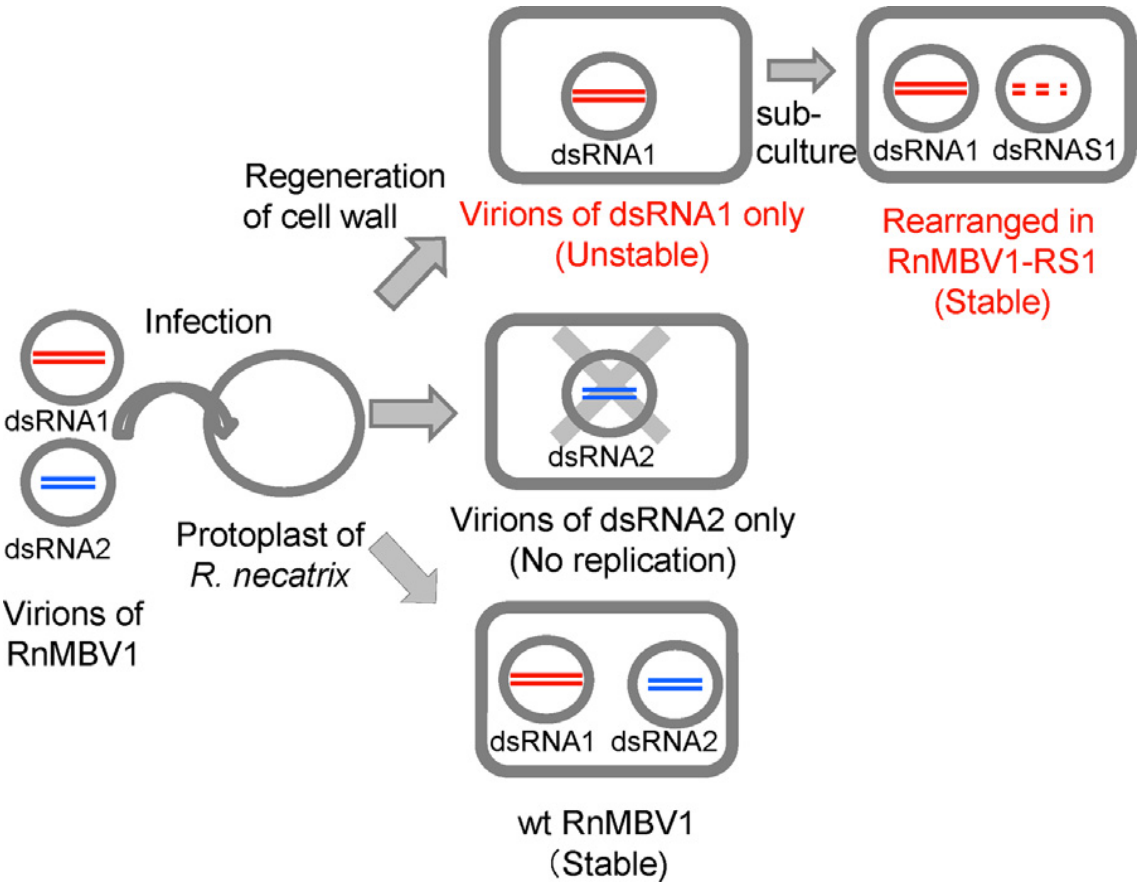

Fig. 21. Schematic diagram of the generation process of RnMBV1-RS1 in *R. necatrix* after transfection with virions from wild-type RnMBV1.

Furthermore, the observation that particles of RnMBV1-RS1 comprising dsRNA1 and dsRNAS1a or dsRNAS1b still infected to *R. necatrix*, provided an interesting insight into the roles of these ORFs in replication. Replication competence is retained despite the complete loss of dsRNA2 in RnMBV1-RS1. However, less RnMBV1-RS1

accumulated than the wild-type RnMBV1 in fungal strains W97 and W370T1 (Fig. 14). Therefore, while ORF3 and ORF4 are not necessary for replication and packaging, they, and particularly ORF3, may influence replication efficiency. An other noteworthy point is that several field isolates of the family *Megabirnaviridae*, including RnMBV1-W779 (Chiba *et al.,* 2009), RnMBV1-W958, and RnMBV2-W8 (Sasaki and Kanematsu, unpublished) also carry dsRNA1 and dsRNA2. This implies an unidentified functional role for dsRNA2 in natural conditions. The RnMBV1 genome has a long 5' UTR (approximately 1.6 kbp) and a relatively short 3' UTR (approximately 60 bp). The dsRNAS1a and -S1b segments of RnMBV1-RS1 reside in the 5' UTR and were shortened to 565 bp in both dsRNAS1a and -S1b. The long 5' UTR of the RnMBV1 genome segments is predicted to play a role allowing non-canonical translation of ORFs1 and 3 (Chiba *et al*., 2009). The terminal sequences of dsRNAS1a and S1b were conserved in the 3'UTR. The infectivity of RnMBV1-RS1 particles and its stable maintenance in *R. necatrix* indicate that RnMBV1-RS1 dsRNAS1a and -S1b retain essential cis-acting elements for RNA replication and virion packaging that are usually located at the terminal portions of viral genomic RNAs. Further experiments are necessary to determine if dsRNAS1 transcripts can serve as translation templates. RNA recombination is common in RNA viruses. The arranged segments of RnMBV1-RS1, dsRNAS1a and -S1b, were derived from dsRNA1 when complete deletion of one ORF and duplication of the other occurred concurrently (Fig. 13). Head to tail duplication of ORFs in rearrangements are frequently observed in Reoviridae (Gault *et al*., 2001; Kojima *et al*., 1996) including mycoviruses (Sun and Suzuki, 2008; Tanaka *et al*., 2011). The specific mechanism of RnMBV1-RS1 rearrangement is unknown. Replicase driven errors during RNA synthesis are most likely to occur during their combination event. No remarkable short stretches of direct or inverted repeats were observed between donor and recipient RNA sequences around rearrangement sites, which are postulated to facilitate recombination (Nagy and Simon, 1997). Instead, there is a prominent AU rich sequence at the recombination site in the 5' UTR (Fig. 13). AU-rich templates in the donor sequence efficiently promote RNA recombination of tombusviruses by replicase driven template switching (Cheng and Nagy, 2003; Shapka and Nagy, 2004). This study clearly indicated that phenotypic alterations in *R. necatrix* by infection with RnMBV1 are moderated by infection with RnMBV1-RS1 (Figs. 15

and 16). In addition, RnMBV1-RS1 accumulates less than RnMBV1 in *R. necatrix* (Fig. 14). Based on these data, two possibilities may account for symptom induction of RnMBV1: (1) proteins coded by dsRNA2 are involved in efficient RnMBV1 replication and/or hypovirulence in *R. necatrix* infection, or (2) the ability to induce symptoms and confer hypovirulencec or relates with levels of dsRNA1, and less accumulation of dsRNA1 in RnMBV1-RS1 causes attenuation. These possibilities are not mutually exclusive. In addition, dsRNAS1a and -S1b segments may act as defective interfering (DI) RNAs, playing a role in the reduction of RnMBV1-RS1 compared with the wild type in *R. necatrix*. Some mycoviral proteins have previously been identified as symptom determinants. Examples include the Cryphonectria hypovirus 1 (CHV1) multifunctional protein p29 that represses pigment production and enhances homologous and heterologous viruses (Craven *et al*., 1993; Sun *et al*., 2006) and K1 killer toxin encoded by M1 dsRNA of *Saccharomyces cerevisiae* virus L-A that kills strains lacking M1 (Wickner, 1992). Recently, the dsRNA4-coded protein of *Magnaporthe oryzae* chrysovirus1 has been shown to induce aberrant cytoloplasm in a non-host fungus, *S. cerevisiae* (Urayama *et al*., 2012). In the preliminary study, significant phenotypic alteration was not detected in transformants containing ORF3 and ORF4 proteins in *R. necatrix* (Shimizu *et al*., 2013). Further studies will be needed to elucidate the function of dsRNA2 in RnMBV1 and the mechanisms of hypovirulence of RnMBV1. The polyketide synthesis (PKS) gene family has been shown to be required for bio synthesis of melanin in several fungi (e.g. Takano *et al*., 1995). This study found that RnMBV1 caused a considerable reduction of melanin production in *R. necatrix*, while infection with RnMBV1-RS1 is shown here to result in partial restoration, albeitnot to the level of virus free strains (Fig. 15C). However, the extent of melanization is not directly relevant to *R. necatrix* virulence, as albeit no strains of W97 with a PKS gene knockdown retained virulence (Shimizuetal., 2013). Alteration of pigment production has also been observed in other virus/fungal host interactions, such as suppression of orange pigmentation by the prototype hypovirus, CHV1-EP713, in *Cryphonectia parasitica* (Hillman *et al*., 1990) and enhancement of pink pigmentation by infection with *Fusarium graminearum* virus 1-DK21 (Chu *et al.,* 2002). Taken together, it is interesting to hypothesize that altered pigmentation is a manifestation of host fungus stress response and/or defense/counter-defense response between host fungi

and viruses. Interesting connections between DI RNA generation and viral RNA silencing have been noted in several fungal hosts. CHV1 has been shown to be a target of RNA silencing; the generation and maintenance of CHV1 DI RNA requires host RNA silencing key components (Segers *et al*., 2007; Sun *et al*., 2009). Enhanced RNA replication, symptom induction, and elimination of CHV1 DI RNA are observed in RNA silencing-defective fungal strains (Zhang *et al*., 2013). Recently, another dsRNA virus, *Rosellinia necatrix* partitivirus 2, has been shown to be targeted by host RNA silencing and its DI RNA has been shown to reduce the accumulation of helper virus and alleviate symptoms regardless of whether RNA silencing is competent in the host fungus, *C. parasitica* (Chiba *et al*., 2013a). However, RNA silencing components appear to be dispensable for maintenance of RnPV2 DI RNA, unlike for CHV1 DI RNAs. It was confirmed that RnMBV1 could be the target of RNA silencing in a silencing-defective *C. parasitica* strain. By using exogenous GFP gene and endogenous host genes, *R. necatrix* contains RNA silencing machinery was confirmed (Yaegashi *et al*., 2013b; Shimizu *et al*., 2013). Therefore, it will be intriguing to investigate whether RnMBV1 dsRNAS1 can occur in RNA silencing-defective fungal strains and to determine how dsRNA1 accumulation and phenotypic alteration are related. *R. necatrix* hosts a wide range of mycoviruses across at least five families, including *Rosellinia necatrix* partitivirus 1 and 2 (RnPV1, 2), *Rosellinia necatrix* quadrivirus 1 and 2 (RnQV1, 2), mycoreovirus3 (MyRV3), *Rosellinia necatrix* victorivirus1 (RnVV1), and RnMBV1. Among these viruses, only RnMBV1 and MyRV3 confer hypovirulence in *R. necatrix* (Chiba *et al*., 2009; Kanematsu *et al*., 2004); the others are asymptomatic. The variety of wild-type and mutant viruses, as described in this and previous studies, offer an attractive model system for analyzing mycovirus/fungal interactions in *R. necatrix*.

Chapter 5. General Discussion

Since the discovery of mycoviruses in the 1960s the field of mycovirology has gradually expanded. However, in comparison to the understanding related to viruses in plants and animals, the knowledge of fungal viruses is still considered to be in its formative years. The work done so far in the mycovirus field has focused largely on obtaining sequences and the characterization of these viruses. Predominantly, this work has focused on dsRNA mycoviruses. Typically, mycoviral infections have varied presentations ranging from deleterious, to symptomless and even positive effects on the host fungus. Of particular interest are those viruses that confer a hypovirulent phenotype (Pearson *et al*., 2009). Although many symptoms of mycoviral infections are described and recognized, very little is still known about the exact mechanisms underlying the relationship between the virus and its host. Also, little work has been done on the incidence, diversity and spread of mycoviruses.

White root rot, caused by the ascomycete *Rosellinia necatrix*, is a devastating disease worldwide particularly in fruit trees in Japan. The pathogen is mainly disseminated in the form of mycelia and can survive in the soil for many years. This soil-borne fungus is difficult to control by conventional methods. Therefore, mycoviruses that can attenuate the virulence of their plant-pathogenic fungus attract interests as biocontrol agents. A variety of mycovirus-related dsRNAs have been found in the over 1000 *R. necatrix* isolates collected. Molecular characterization of these viruses revealed that *R. necatrix* hosts a number of mycoviruses belonging to at least 5 families: *Partitiviridae, Quadriviridae*, *Reoviridae, Totiviridae* and *Megabirnaviridae.* This study represents a thorough molecular and biological characterization of a novel mycovirus, termed *Rosellinia necatrix megabirnavirus* 1 (RnMBV1) using the natural host and an experimental host fungus. The work presented in this thesis focuses on one of these mycoviruses, *Rosellinia necatrix* W779, and the effects of this mycovirus on its host *R. necatrix*. *R. necatrix* W779 showed 2 dsRNA segments after agarose gel electrophoresis with sizes ranging about 9 and 7.2 kb for dsRNA1 and dsRNA2, respectively. Sequence analysis of each segment was performed. As part of this study, several PCR-based

methods for the sequence determination of dsRNA templates were optimized. The 2 dsRNA segments of *R. necatrix* W779 were completely sequenced and a two ORFs per segment were identified. DsRNA1 and 2 were 8931 and 7180 nucleotides long, respectively. DsRNA1 and 2 each possess 2 ORFs coding for all 4 proteins. And the long 5'UTR of approximately 1.6 kbps of both segments show high level of sequence similarity. The BLAST search detected low level of sequence similarities only between dsRNA-1 ORF2 and RdRp of members of *Totiviridae* and *Chrysoviridae.* Phylogenetic tree-generated based on RdRp sequence alignment reveals that RdRp clusters of *R. necatrix* W779 strain is placed separately from related dsRNA mycoviruses. Deduced amino acid of P1, 3 and 4 did not yield any hits in BLAST search. Virus particles of about 50 nm in diameter were successfully purified by means of sucrose and $CsSo_4$ equilibrium-centrifugation and observed under the electron microscope. SDS-PAGE of particles showed a single major band corresponding to 135 kDa and a minor protein at 250 kDa. No major band was detected in virus free W1015. The 135 kDa protein from SDS-PAGE possibly represents the major capsid protein. PMF analysis were performed and found the results from PMF perfectly matched with deduced amino acid coded by dsRNA1 ORF1. The results support that dsRNA1 ORF1 possibly codes for the capsid protein. Phylogenic study of its RdRp and capsid proteins supports that *R. necatrix* W779 would possibly be the candidate as a novel virus, *Rosellinia necatrix megabirnavirus 1* (RnMBV1) in the new family *Megabirnaviridae.*

Particles of dsRNA viruses are believed to contain all of the enzymatic activities necessary for transcription and the synthesis of viral mRNA, leading to the onset of infection. This study clearly established a virus etiology for the reduced virulence and vegetative mycelial growth of *R. necatrix*. Curing of RnMBV1 in W779 results in the generation of an isogenic fungal strain, W1015, that shows an enhanced growth rate and virulence level. The virus is able to infect strains W370T1 and W97 via virion transfection and induce a similar set of phenotypic alterations, i.e., reduced mycelial growth and attenuated virulence (hypovirulence). From these RnMBV1-infected strains, virus particles encapsidating dsRNA1 and 2 were isolated. The transfected fungal strains, W97 and 370T1, belonging to MCG80 and MCG139, are vegetatively incompatible with W779 (MCG351) and unable to receive RnMBV1 when cocultured

with W779. It was confirmed that the transfected strains carried the phenotypic markers of their parents. To determine the virological potential of RnMBV1, virulence assay were performed on apple rootstocks. The apple rootstocks were inoculated with virus free and virus infected *R. necatrix* strain W97 and W370T1. Fungal colony without the virus induced lethal phenotypes more than the plants that have been inoculated with virus infected fungal colony. The more severe symptoms were also observed in root inoculated with fungal colony without the virus. The mortality of apple rootstocks was much greater when they were inoculated with virus free strain. These combined results indicate that the RnMBV1 is a novel bipartite dsRNA virus, with potential for biological control (virocontrol).

From the virulence data, RnMBV1 were studied further, unfortunately there are some limitations to study RnMBV1 in its original host, *R. necatrix,* such as *R. necatrix* conidia rarely germinate and develop into mycelia in the laboratory condition. Spheroplasts are difficult to store as their competence is short term only and therefore requires preparing fresh spheroplasts every time experiments were performed. The *R. necatrix* genome is not yet available online. Introducing RnMBV1 to experimental host, *C. parasitica*, provides more opportunity to study on RnMBV1. *C. parasitica,* with its genome sequence already available publicly, has been use as a phytopathogenic fungus model for investigation of virus/host or virus/virus interactions. Availability of various mutants that include an RNA silencing-defective strain, Δ*dcl-2* makes this fungus suitable as an experimental host. The two fungal strains, standard RNA silencing-competent EP155 and RNA silencing-defective Δ*dcl-2* showed different responses to RnMBV1 infection. RnMBV1 replicated at a much higher level (20-fold) in Δ*dcl-2* than in EP155. This indicates that RNA silencing targets the megabirnavirus in *C. parasitica* but it remains unknown whether RnMBV1 encodes an RNA silencing suppressor. As expected from the different replication levels, RnMBV1 induced distinct phenotypic alteration in the strains; only a mild alteration of colony morphology in the standard RNA silencing-competent EP155, and a reduced growth rate with an irregular colony margin in Δ*dcl-2*. Both infected fungal strains retained similar levels of sporulation, relative to virus-free Δ*dcl-2* or EP155. This symptom expression remained

phenotypically stable after horizontal and vertical transmission. It was surprising that RnMBV1 conferred hypovirulence to the *C. parasitica* wild-type strain, as in the case of Δ*dcl-2*, in spite of the limited effects on colony morphology. The phenotypic effects of RnMBV1 on *C. parasitica* have not previously been studied in depth. The effects of other mycoviruses (typically dsRNA viral elements) on the fitness of their hosts have usually been assessed by in-vitro growth on a medium such as potato dextrose agar (PDA) plus pathogenicity assays on detached plant leaves and fruit (Elad, 2004). The studies performed in this thesis tested several in-vitro fitness criteria (linear growth, sporulation and virulence assay), in order to come to a better understanding of the effects of the virus RnMBV1 on *C. parasitica*. To understand how RnMBV1 affects field populations of host, awareness of how it is transmitted is important. A common and significant difference between the genomes of mycoviruses and plant viruses is the absence of genes for movement proteins. It is therefore assumed that mycoviruses only move intercellularly during cell division (e.g. sporogenesis) or via hyphal fusion (Ghabrial, 1994; Ghabrial & Suzuki, 2009). Vertical transmission via asexual spores and sexual recombination and horizontal transmission via hyphal anastomosis are intercellular routes of virus movement. Studies on vertical transmission of dsRNA mycoviruses via asexual spores have recorded varied rates of transmission, ranging from 0-100% (Ghabrial & Suzuki, 2009; Pearson *et al*., 2009). In black Aspergilli*, A. flavus* and *A. nidulans*, 100% of tested conidiospores was infected with dsRNA mycovirus (Coenen *et al*., 1997; Van Diepeningen *et al*., 1997; Van Diepeningen *et al*., 2006). However, in *Fusarium graminearum* the rate of transmission to conidia was 50%. This pattern of varying rate of transmission is seen in *Heterobasidion annosum* with the transmission rate of dsRNA varying from 3% and 55% in two examined isolates (Ihrmark *et al*., 2002). Although it is generally assumed that mycoviruses move passively through the cytoplasm by streaming (Sasaki *et al*., 2006) it is not known specifically how RnMBV1 is transported within its host, *R. necatrix*, or in experimental host, *C. parasitica*. Based on previous studies of dsRNA element, it has been suggested that dsRNA mycoviruses are eliminated by the sexual cycle (Brown, 1999). Similarly, mycoviruses have not been observed in natural isolates of some *Aspergillus* species, which are able to undergo a sexual cycle (Varga & Samson, 2008). Exclusion of dsRNA segments from spores was also observed in *Gaeumannomyces framinis* , *Ophiostoma*

ulmi, *Epichloë festucae* and *Helicobasidium mompa* (Varga & Samson, 2008). Mycovirus transmission through sexual reproduction has been shown in other fungi including in the basidiospores of *Agaricus brusnnescens*, *Ustilago maydis* and *Heterobasion annosum* (Pearson *et al*., 2009; Varga & Samson, 2008). In other words RnMBV1 must be able to infect other healthy fungus. Horizontal transmission of mycoviruses is only known to occur via hyphal anastomosis (Ghabrial, 1998; Pearson *et al*., 2009). Horizontal transmission of mycoviruses between different fungal strains via hyphal anastomosis is a well-established phenomenon and has been used to transmit mycoviruses experimentally (Suzaki *et al*., 2005; Xie *et al*., 2006). Successful anastomosis relies on the two fungi being vegetatively compatible and since mycoviruses exist within the cytoplasm, they should be included in the exchange of cytoplasm and organelles during anastomosis. In our experiments we successfully anastomosed an RnMBV1 positive with two fungus free negative. RnMBV1 infection was detected in recipient strains, after 2 weeks growth. The findings here add to the literature and show that RnMBV1 can be transmitted via hyphal anastomosis. In summary the transmission experiments show that RnMBV1 is transmitted freely in horizontally by hyphal anastomosis but rarely vertically via spores.

From the previous data on SDS-PAGE using this virus particle as a sample, 135 kDa protein corresponding to capsid protein encoded by ORF1 was observed. A minor protein of 250 kDa, which suspected to be a fusion protein of ORF1 and 2 because the genetic organization shows that ORF2 is in -1 frame relative to ORF1. However, it remained unclear how the upstream ORF1, preceded by extremely long UTRs, and the downstream ORF2 are expressed. This study succeeded to provide a clue to the nature of the expression of the downstream ORF2 on dsRNA1. Antibodies against ORF1-encoded proteins detected the CP as well as a minor protein of 250 kDa in purified virus preparations, confirming the previous conclusion that the RnMBV1 CP is encoded by ORF1 (Chiba *et al.*, 2009). The observation that the minor 250-kDa protein reacted specifically with an antibody against ORF2-coded protein (Fig. 17B) indicate that the RdRp domain encoded by ORF2 is expressed as a CP-fusion product. As described by Chiba (2009), the presence of the consensus slippery sequence and subsequent stem-loop/pseudo-knot structure implies that RnMBV1 RdRp is expressed via -1

frameshifting. The identity of the mature proteins of ORF3 is still unclear. The 150-kDa, 30-kDa, and 23-kDa products were detectable specifically in infected RnMBV1-infected *C. parasitica* cells. On the basis of its coding capacity, it seems likely that the 150-kDa protein is the full-length product encoded by ORF3. The smaller products observed in this study may be derived from the N- and/or C- terminal portions after programmed catalytic cleavage or site-specific degradation. This notion is based on the fact that the antiserum used in this study was directed against the N and C terminal portions of the ORF3 product. Further investigation is required for unraveling the ORF3-protein function.

Not only wild type RnMBV1 was able to be detected in *C. parasitica* but also RnMBV1 rearranged genome. From the same transfection, genomic rearrangements of a newly identified dsRNA virus, RnMBV1, in *C. parasitica*, resulting in RnMBV1-RL2, which showed the expansion of dsRNA2 and authentic dsRNA2. Results from RT-PCR and AGE investigated that dsRNA of Δ*dcl*-2/RnMBV1-RL2 is still undergoing rearrangement and that the dsRNA profile observed before is not yet in its stable form. Surprisingly, the same biological properties between RnMBV1 and RnMBV1-RL2 were observed in *C. parasitica* except for vertical transmission rate, in which rate is higher in RnMBV1-RL2 than in RnMBV1, 1.98% compared to 0.48%.

The other rearranged genome was observed in *R. necatrix,* resulting in RnMBV1-RS1, one of the characteristic features of RnMBV1-RS1 is the complete loss of dsRNA2. These combinant dsRNAS1a and S1b contain only sequences derived from dsRNA1; therefore, dsRNAS1a and S1b are probably due to intragenic rearrangement of dsRNA1. DsRNA1 and dsRNA2 of RnMBV1 were assumed to be packaged into virions separately, as the molecular ratio of each is not equimolar and dsRNA1 is variably less abundant than dsRNA2 in fungal mycelia depending on culture conditions. RnMBV1-RS1 was maintained stably after ten subcultures without any change. Based on these data, a model for the generation of RnMBV1-RS1 was proposed, suggesting that two genomic segments are required for stable maintenance of RnMBV1. Replication competence is retained despite the complete loss of dsRNA2 in RnMBV1-RS1. However, less RnMBV1- RS1 accumulated than the wild type RnMBV1 in fungal

strains W97 and W370T1. Therefore, while ORF3 and ORF4 are not necessary for replication and packaging, they, and particularly ORF3, may influence replication efficiency. The dsRNAS1a and S1b segments of RnMBV1-RS1 reside in the 5' UTR and were shortened to 565 bp in both dsRNAS1a and S1b. The terminal sequences of dsRNAS1a and S1b were conserved in the 3'UTR. The infectivity of RnMBV1-RS1 particles and its stable maintenance in *R. necatrix* indicate that RnMBV1-RS1 dsRNAS1a and S1b retain essential cis-acting elements for RNA replication and virion packaging that are usually located at the terminal portions of viral genomic RNAs. RNA recombination is common in RNA viruses but the specific mechanism of RnMBV1-RS1 rearrangement is unknown.

This study clearly indicated that phenotypic alterations in *R. necatrix* by infection with RnMBV1 are moderated by infection with RnMBV1-RS1. In addition, RnMBV1-RS1 accumulates less than RnMBV1 in *R. necatrix*. Based on these data, two possibilities may account for symptom induction of RnMBV1, proteins coded by dsRNA2 are involved in efficient RnMBV1 replication and/or hypovirulence in *R. necatrix* infection, or the ability to induce symptoms and confer hypovirulence or relates with levels of dsRNA1, and less accumulation of dsRNA1 in RnMBV1-RS1 causes attenuation. These possibilities are not mutually exclusive.

The research conducted in this thesis was to study the transmission and interactions occurring between the mycovirus RnMBV1 and its fungal host, *R. necatrix*, and its experimental host, *C. parasitica*. Currently, control of most plant pathogenic fungi relies predominantly on the use of fungicides. In addition to the health hazards and the risks to the environment, the use of fungicides is often cost prohibitive and fungi frequently develop fungicide resistance (Elad, 2004). The need for novel biocontrol measures to combat fungal diseases cannot be overemphasized. Mycoviruses may be able to contribute to sustainable agriculture as biological control agents but to do this they must have a measurable effect on their host fungi and be able to efficiently move through the fungal population. Consequently these two aspects need to be evaluated to determine the potential of mycoviruses as biological control agents. Furthermore, study of virus/host interactions is a significant area of modern virology, in which mycoviruses

can be used as tools to explore the physiology of their fungal hosts (Ghabrial &Suzuki, 2009).

Chapter 6. Summary

White root rot, caused by the ascomycete *Rosellinia necatrix*, is a devastating disease worldwide particularly in fruit trees in Japan. The pathogen is mainly disseminated in the form of mycelia and can survive in the soil for many years. This soil-borne fungus is difficult to control by conventional methods. Therefore, mycoviruses that can attenuate the virulence of their plant-pathogenic fungus attract interests as biocontrol agents. A variety of mycovirus-related dsRNAs have been found in the over 1000 *R. necatrix* isolates collected. Molecular characterization of these viruses revealed that *R. necatrix* hosts a number of mycoviruses belonging to at least 5 families: *Partitiviridae, Quadriviridae*, *Reoviridae, Totiviridae* and *Megabirnaviridae.* This study represents a thorough molecular and biological characterization of a novel mycovirus, termed *Rosellinia necatrix megabirnavirus* 1 (RnMBV1) using the natural host and an experimental host fungus.

RnMBV1was shown to encompass two double-stranded (ds) RNAs, dsRNA1 (8931 bp) and dsRNA2 (7180 bp), which was isolated from a field strain of *R. necatrix*, W779. Besides the strictly conserved 5' (24 nts) and 3' (8 nts) terminal sequences, both segments show high levels of sequence similarities at the long 5' untranslated region of approximately 1.6 kbp. DsRNA1 and dsRNA2 each possess two open reading frames (ORFs) termed 1 to 4. Although the protein encoded by the 3' proximal ORF2 on L1 shares sequence identities of 20-25% with RNA-dependent RNA-polymerases from members of the families *Totiviridae* and *Chrysoviridae*, the remaining three virally-encoded proteins lack sequence similarities with any reported mycovirus proteins. Phylogenetic analysis showed that the W779 virus belongs to a separate clade distinct from those of other known mycoviruses. Purified virions of ~50 nm in diameter consisted of dsRNA1 and dsRNA2, and a single major capsid protein of 135 kDa, which was shown by peptide mass fingerprinting to be encoded by dsRNA1 ORF1. A recently developed transfection protocol with purified virions shows that the virus was responsible for reduction of virulence and mycelial growth in several host strains. That is, transfection of RnMBV1-cured strain W1015, W370T1 and the standard strain W97 results in severe virulence attenuation. The latter two strains are genetically different

from W779 and belong to a different mycelial compatibility group (MCG) than W779 which impairs lateral viral transmission. These combined results indicate that RnMBV1 is a novel bipartite dsRNA virus, with potential for biological control (virocontrol) that belongs to a new virus family.

Purified RnMBV1 particles were transfected in to the experimental host, *Cryphonectria parasitica*, a filamentous fungus that has been used as a model for mycovirus research for further studies. This study provides an additional example of *C. parasitica* serving as a versatile, heterologous fungus for exploring virus–host interactions and virus gene expression strategies. Transfection of RnMBV1 particles with into an RNA silencing-defective strain (Δ*dcl-2*) of *C. parasitica* and subsequent anastomosis with the wild type strain (EP155) resulted in stable persistent infection in both host strains. However, accumulation levels in the two strains were different, being ~20-fold higher in Δ*dcl*-2 than in EP155. Intriguingly, whilst RnMBV1 reduced both virulence and growth rate in Δ*dcl-2*, it attenuated virulence without affecting significantly other traits in EP155. Western blot analysis using antiserum against recombinant proteins encoded by either ORF1 or ORF2 demonstrated the presence of a 250 kDa protein in purified virion preparations, suggesting that RdRp is expressed as a CP fusion product via a -1 frameshift. Antiserum against the ORF3-encoded protein allowedthe detection of 150, 30 and 23 kDa polypeptides specifically in RnMBV1-infected mycelia. Some properties of an RnMBV1 mutant with genome rearrangements, which occurred after transfection of Δ*dcl-2*and EP155, were also presented. From the same transfection, genomic rearrangements of a newly identified dsRNA virus, RnMBV1, in *C. parasitica*, was resulting in RnMBV1-RL2, which showed the expansion of dsRNA2 and authentic dsRNA2. Resulted from RT-PCR and AGE investigated that dsRNA of Δ*dcl*-2/RnMBV1-RL2 is still undergoing rearrangement and the dsRNA profile observed before is not yet in its stable form. Surprisingly, the same biological properties between RnMBv1 and RnMBV1-RL2 were observed in *C. parasitica* except for vertical transmission rate, which higher in RnMBV1-RL2 than in RnMBV1, 1.98% compared to 0.48%. Not only in *C. parasitica* but genome rearrangement of RnMBV1 also observed in *R. necatrix*. RnMBV1 with genome rearrangements (RnMBV1-RS1) that retained dsRNA1, encoding capsid protein (ORF1) and RNA- dependent RNA polymerase

(ORF2), and had a newly emerged segment named dsRNAS1, but with loss of dsRNA2 were detected. Analyses of two variants of dsRNAS1 revealed that they both originated from dsRNA1 by deletion of ORF1 and partial tandem duplication of ORF2, retaining a much shorter 50 untranslated region (UTR). *R. necatrix* transfected with RnMBV-RS1virions showed maintenance of virulence on host plants compared with infection with RnMBV1. This suggests that dsRNAS1 is able to be transcribed and packaged, as well as suggesting that dsRNA2, while dispensable for virus replication, is required to reduce the virulence of *R. necatrix.* It was subsequently examined whether RnMBV1 could infect different phtopathogenic fungi and attenuate their virulence. Purified RnMBV1 particles were transfected in to the experimental host, *Cryphonectria parasitica*, a filamentous fungus that has been used as a model for mycovirus research. Transfection with purified RnMBV1 particles into an RNA silencing-defective strain (Δ*dcl-2*) of *C. parasitica* and subsequent anastomosis with the WT strain (EP155) resulted in stable persistent infection in both host strains. However, accumulation levels in the two strains were different, being ~20-fold higher in Δ*dcl-2* than in EP155. Importantly, whilst RnMBV1 reduced both virulence and growth rate in Δ*dcl-2*, it attenuated virulence without affecting significantly other traits in EP155. This experimental system was further utilized for the virus gene expression strategy. Western blot analysis using antiserum against recombinant proteins encoded by either ORF1 or ORF2 demonstrated the presence of a 250 kDa protein in purified virion preparations, suggesting that RdRp is expressed as a CP fusion product via a -1 frameshift. Antiserum against the ORF3-encoded protein allowed the detection of 150, 30 and 23 kDa polypeptides specifically in RnMBV1-infected mycelia. Some properties of an RnMBV1 mutant with genome rearrangements, which occurred after transfection of Ddcl-2 and EP155, were also presented. This study provides an additional example of *C. parasitica* serving as a versatile, heterologous fungus for exploring virus-host interactions and virus gene expression strategies.

While a number of transfectants of *R. necatrix* and *C. parasitica* were analyzed for electropherotype, some transfectant strains were found to carry unusual genome profiles different from wild-type RnMBV1. Examples include RnMBV1-RL2 that occurred

originally in Δ*dcl-2* that harbored normal dsRNA and an extended form of dsRNA2. Surprisingly, RnMBV1-RL2 and wild-type RnMBV1 manifested similar biological properties between RnMBV1 and RnMBV1-RL2 in *C. parasitica* except for vertical transmission rate, which higher in RnMBV1-RL2 than in RnMBV1, 1.98% compared to 0.48%. Another type of rearranged RnMBV1 genomes were observed in transfected *R. necatrix*. RnMBV1 with genome rearrangements (RnMBV1-RS1) that retained dsRNA1, encoding capsid protein (ORF1) and RNA-dependent RNA polymerase (ORF2), and had a newly emerged segment named dsRNAS1, but with loss of dsRNA2 were detected. Analyses of two variants of dsRNAS1 revealed that they both originated from dsRNA1 by deletion of ORF1 and partial tandem duplication of ORF2, retaining a much shorter 50 untranslated region (UTR). This study clearly indicated that degrees of phenotypic alterations of the host fungus, *R. necatrix,* by infection with RnMBV1-RS1, were compromised relative to those by infection with parental strain RnMBV1. In addition, RnMBV1-RS1 was accumulated less than RnMBV1 in *R. necatrix*. Based on these data, two possibilities are considered to account for symptom induction of RnMBV1, 1) The ability to induce symptoms and confer hypovirulence correlates with levels of dsRNA1, and less accumulation of dsRNA1 in *R. necatrix* strains infected with RnMBV1-RS1 attenuates it, 2) proteins coded by dsRNA2 are involved in efficient RnMBV1 replication and/or hypovirulence conference in *R. necatrix*. *R. necatrix* transfected with RnMBV-RS1virions showed maintenance of virulence on host plants compared with infection with RnMBV1. This suggests that dsRNAS1 is able to be transcribed and packaged, as well as suggesting that dsRNA2, while dispensable for virus replication, is required to reduce the virulence of *R. necatrix.*

These combined results indicate that RnMBV1 is a novel bipartite dsRNA virus, with potential for biological control (virocontrol) of the natural host white root rot fungus as well as the heterologous chestnut blight fungus. The mutant RnMBV1 strains will provide additional tools for further functional analyses of RnMBV1.

Chapter 7. Acknowledgement

This thesis would not have been possible without the help of many people. It is my pleasure that I have the opportunity to express my gratitude to them.

First and foremost, I respect and thank Professor Nobuhiro Suzuki, my major advisor, for his guidance, support and knowledge during the conduct of this thesis. The enthusiasm and interest for the completion of my thesis were derived from his constant encouragement and motivation.

Appreciation and sincere thanks are due to Drs. Ivan Galis and Maki Katsuhara for being my co-supervisors and for editing the manuscript.

Special thanks to Drs. Akio Tani, Satoko Kanematsu, Atsuko Sasaki and Naoyuki Miyazaki.

I would also like to thank the lab members in PMI group for their help and guidance in the laboratory: to Dr. Hideki Kondo for all advices; to Kazuyuki Maruyama and Hisano Sakae for their kind and help at all times. To the previous and present lab members: Drs. Ana Eusebio-Cope, Soutaro Chiba, Sun Li-Ying, Ida Bagus Andika, Atiff Jamal and Ms. Zhang Rui for being my friend. It was a great pleasure to meet and work with all of you.

Grateful thanks to Ana and Noel, I could not imagine my life here without their helps. They always make me feel like home. Knowing them is the best part of my life here.

I would like to acknowledge the Japanese Ministry of Education, Culture, Science and Sports for my scholarship. The Naito Foundation, and the Program for Promotion of Basic and Applied Researches for Innovations in Bio-Oriented Industries for the financial support.

Special thanks to Thai community in Okayama, Jay&J-walkerz, my previous

supervisors and bosses; Asst. Prof. Tiparat Hongpattarakeree, Assoc. Prof Supasil Maneerat, K. Sirichai Atiwattananon and Han Family.

To my old friends back home, Kerng&Wing, Klang, Mai-Somrudee, Mai-Thidarat, Kerd&Ray, Wongsakol family and others for their love and support. They always make me happy.

Last but not the least, to my own family; they are the reasons for what I am doing right now. To Papa, who did not just give me live but provided me a good and comfortable life to enjoy. He is a loving dad and glorious father. To Mama, if there were no her, there would absolutely be no me. Her blessings and love have nurtured me into what I am today. There are no words to thank you enough. To my younger brother, it is nice growing up and sharing everything with someone like him-someone to lean on, someone to count on and someone to talk to. For the good times and bad times, we always have each other's back. We've been through so much and I believe our day will come.

I dedicate this work to you guys……

"Those with academic knowledge must maintain good moral values to make the country survive and prosper. Those values are conscience - or knowing right and wrong - honesty in thought and deed, gratitude to the country and all protagonists, selflessness, non-aggression or non-harassment of others, sincerity and goodwill, and most importantly, diligence, doing the work oneself steadfastly, aiming for results. These qualities are factors that make education complete and beneficial."

22/06/1979 H.M. King Bhumibol Adulyadej

Hini mitabi mi o kaerimishi inishieno Hito no kokoro ni naraite shigana.

Thrice daily a wise man of old reflected on himself; now I, In the spirit of the sage wish to do the same.

Empress Shouken

Chapter 8. References

Aivanesan, A. and Holliday, D. 1985. Descriptios of pathogenic fungi and bacteria *Rosellinia necatrix*. Commonwealth Mycological Institue, No. 352.

Altschul, S. F., Madden, T. L., Schaffer, A. A., Zhang, J., Zhang, Z., Miller, W. and Lipman, D. J. 1997. Gapped BLAST and PSI-BLAST: a new generation of protein database search programs. Nucleic Acids Res 25, 3389-3402.

Anagnostakis, S. L. 1982. Biological control of chestnut blight. Science. 215, 466-471.

Anselmi, N. and Giorcelli, A. 1990. Factors influencing the incidence of *Rosellinia necatrix* Prill in poplars. European Journal of Forest Pathology. 20, 175-183.

Aoki, N., Moriyama H., Kodama M., Arie T., Teraoka T. and Fukuhara T. 2009. A novel mycovirus associated with four double-stranded RNAs affects host fungal growth in *Alternaria alternata*.Virus Res. 140, 179-187.

Arakawa, M., Nakamura, H., Uetake, Y., Nitta, H., Naganawa, T., Kakishima, M., Okabe, I. and Matsumoto, N. (2001). Double-stranded RNA in the white root rot fungus, *Rosellinia necatrix*, as a hypovirulence factor. Jpn J Phytopathol 67, 192.

Arakawa, M., Nakamura H., Uetake Y., and Matsumoto N. 2002. Presence and distribution of double-stranded RNA elements in the white root rot fungus *Rosellinia necatrix*. Mycoscience. 43, 21-26.

Asamizu, T., Summers, D., Motika, M. B., Anzola, J. V., and Nuss, D. L. 1985. Molecular cloning and characterization of the genome of wound tumor virus: A tumor-inducing plant reovirus. Virology. 144, 398-409.

Behdad, E. 1976. The influence of several new systemic fungicides on *Rosellinia necatrix* (Hartig) Berlese. Iranian Journal Plant Pathology. 12, 40-41.

Belsham, G. J. 2009. Divergent picornavirus IRES elements. Virus Res. 139, 183-192.

Belshaw, R., Watson, J., Katzourakis, A., Howe, A., Woolven-Allen, J., Burt, A. and Tristem, M. 2007. Rate of recombinational deletion among human endogenous retroviruses. J. Virol. 81, 9437-9442.

Boyce, M., Celma, C. C. and Roy, P., 2008. Development of reverse genetics systems for bluetongue virus: recovery of infectious virus from synthetic RNA transcripts. J. Virol. 82, 8339-48.

Brown, J. K. M. 1999. The evolution of sex and recombination in fungi. Population and Community Biology series, 25, 73-96.

Bruenn, J. A. 2003. A structural and primary sequence comparison of the viral RNA-dependent RNA polymerases. Nucleic Acids Res. 31, 1821-1829.

Buck, K. W. 1998. Molecular variability of viruses of fungi. In Molecular Variability of Fungal Pathogens (P. Bridge, Y. Couteaudier & J. Clarkson, eds): 53-72. CAB International, Wallingford.

Burgya´n, J. and Havelda, Z. 2011. Viral suppressors of RNA silencing. Trends Plant Sci.16, 265-272.

Byun, Y., Moon S. and Han K. 2007. A general computational model for predicting ribosomal frameshifts in genome sequences. Comput. Biol. Med. 37, 1796-1801.

Cai, G., Krychiw, J. F., Myers, K., Fry, W. E. and Hillman, B. I. 2013. A new virus from the plant pathogenic oomycete Phytophthora infestans with an 8 kb dsRNA genome: the sixth member of a proposed new virus genus. Virology. 435, 341–349.

Cai, G., Myers K., Hillman B. I. and Fry W. E. 2009. A novel virus of the late blight pathogen, *Phytophthora infestans*, with two RNA segments and a supergroup 1 RNA-dependent RNA polymerase. Virology doi:10.1016/j.virol.2009.06.040.

Cazorla-López, F., Bloemberg, G. V. and Lugtenberg, B. J. J. 2001. Biocontrol of white root rot on avocado plants using rhizobacterial strains. Biological control of fungal and bacterial plant pathogens. IOBC/WPRS Bulletin. 4, 79-82.

Charoenpanich, J., Tani A., Moriwaki N., Kimbara K., and Kawai F. 2006. Dual regulation of a polyethylene glycol degradative operon by AraC-type and GalR-type regulators in Sphingopyxis macrogoltabida strain 103. Microbiology. 152, 3025-3034.

Chen, B., Chen, C. H., Bowman, B. H. and Nuss, D. L. 1996. Phenotypic changes associated with wild type and mutant hypovirus RNA transfection of plant pathogenic fungi phylogenetically related to *Cryphonectria parasitica*. Phytopathology. 86, 301-310.

Chen, B., Choi G. H. and Nuss D. L. 1994. Attenuation of fungal virulence by synthetic infectious hypovirus transcripts. Science. 264, 1762-1764.

Cheng, C. P. and Nagy, P. D. 2003. Mechanism of RNA recombination in carmo- and tombusviruses: evidence for template switching by the RNA-dependent RNA polymerase in vitro. J. Virol. 77, 12033-47.

Chiba, S., Salaipeth, L., Lin, Y. H., Sasaki, A., Kanematsu, S. and Suzuki, N. 2009. A novel bipartite double-stranded RNA mycovirus from the white root rot fungus *Rosellinia necatrix*: molecular and biological characterization, taxonomic considerations, and potential for biological control. J Virol. 83, 12801-12812.

Chiba, S., Kondo, H., Tani, A., Saisho, D., Sakamoto, W., Kanematsu, S. and Suzuki, N. 2011. Widespread endogenization of genome sequences of non-retroviral RNA viruses into plant genomes. PLoS Pathog. 7, e1002146.

Chiba, S., Lin, Y. H., Kondo, H., Kanematsu, S. and Suzuki, N. 2013a. A novel victorivirus from a phytopathogenic fungus, *Rosellinia necatrix*, is infectious as particles and targeted by RNA silencing. J Virol. 87, 6727-6738.

Chiba, S., Lin, Y. H., Kondo, H., Kanematsu, S. and Suzuki, N. 2013b. Effects of defective interfering RNA on symptom induction by, and replication of, a novel partitivirus from a phytopathogenic fungus, Rosellinia necatrix. J Virol. 87, 2330-2341.

Choi, G. H. and Nuss D. L. 1992. Hypovirulence of chestnut blight fungus conferred by an infectious viral cDNA. Science. 257, 800-803.

Chu, Y. M., Jeon, J. J., Yea, S. J., Kim, Y. H., Yun, S. H., Lee, Y. W. and Kim, K. H. 2002. Double-stranded RNA mycovirus from Fusarium graminearum. Appl. Environ. Microbiol. 68, 2529-34.

Chung, B. Y.-W., Miller, W. A., Atkins, J. F. and Firth, A. E. 2008. An overlapping essential gene in the Potyviridae. Proceedings of the National Academy of Sciences of the USA. 105, 5897-5902.

Coenen, A., Kevei, F. and Hoekstra, R. F. 1997. Factors affecting the spread of double-stranded RNA viruses in *Aspergillus nidulans.* Genetical research*,* 69(1), 1-10.

Craven, M.G., Pawlyk, D.M., Choi, G. H. and Nuss, D. L. 1993. Papain-like protease p29 as a symptom determinant encoded by a hypovirulence-associated virus of the chestnut blight fungus. J. Virol. 67, 6516-6521.

Dawe, A. L. and Nuss D. L. 2001. Hypoviruses and chestnut blight: exploiting viruses to understand and modulate fungal pathogenesis. Ann. Rev. Genet. 35, 1-29.

Dawe, A. L. and Nuss, D. L. 2013. Hypovirus molecular biology: from Koch's postulates to host self-recognition genes that restrict virus transmission. Adv. Virus Res. 86, 109-147.

Delmas, B., Kibenge, F. S. B., Leong, J. C., Mundt, E., Vakharia, V. N. and Wu, J. L. 2005. Family *Birnaviridae*. p. 561-569. In Fauquet, C. M. et al., (ed.). Virus Taxonomy: Eighth Report of the International Committee for the Taxonomy of Viruses. Academic Press, San Diego.

Deng, F., Xu, R. and Boland, G.J. 2003. Hypovirulence-associated double-stranded RNA from *Sclerotinia homoeocarpa* is conspecific with Ophiostoma novo-ulmi mitovirus 3a-Ld. Phytopathology. 93 (11), 1407-1414.

Deng, F. and Nuss D. L. 2008. Hypovirus papain-like protease p48 is required for initiation but not for maintenance of virus RNA propagation in the chestnut blight fungus *Cryphonectria parasitica*. J. Virol. 82, 6369-6378.

Deng, F., Allen T. D. and Nuss D. L. 2007. Ste12 Transcription factor homologue 611 CpST12 is down-regulated by hypovirus infection and required for virulence and female fertility of the chestnut blight fungus *Cryphonectria parasitica*. Eukaryot. Cell. 6, 235-244.

Desselberger, U. 1996. Genome rearrangements of rotaviruses. Adv. Virus. Res. 46, 69-95.

Dinman, J. D. and Wickner, R. B. 1992. Ribosomal frameshifting efficiency and gag/gag-pol ratio are critical for yeast M1 doublestranded RNA virus propagation. J Virol. 66, 3669–3676.

Dinman, J. D., Icho, T. and Wickner, R. B. 1991. A -1 ribosomal frameshift in a double-stranded RNA virus of yeast forms a gag-pol fusion protein. Proc Natl Acad Sci USA. 88, 174-178.

Dolja, V.V., McBride, H.J. and Carrington, J.C. 1992. Tagging of plant potyvirus replication and movement by insertion of beta-glucuronidase into the viral polyprotein. Proc Natl Acad Sci U S A. 89(21), 10208-10212.

Domingo, E., Escarmıs, C., Sevilla, N., Moya, A., Elena, S. F., Quer, J., Novella, I. S. and Holland, J. J. 1996. Basic concepts in RNA virus evolution. FASEB Journal 10, 859-864.

Duan, C. H., Tsai, W. H. and Tu, C. C. 1990. Dissemination of white root rot disease of loquat and its control. Journal of Agricultural Research of China. 39, 47-54.

Elad, Y. 2004. Botrytis: biology, pathology and control: Springer.

Esteban, R. and Fujimura T. 2003. Launching the yeast 23S RNA Narnavirus shows 5' and 3' cis-acting signals for replication. Proc. Natl. Acad. Sci. USA. 100, 2568-2573.

Eusebio-Cope, A., Suzuki, N., Sadeghi-Garmaroodi, H. and Taga, M. 2009. Cytological and electrophoretic karyotyping of the chestnut blight fungus *Cryphonectria parasitica*. Fungal Genet Biol. 46, 342-351.

Eusebio-Cope, A., Sun, L., Hillman, B. I. and Suzuki, N. 2010. Mycoreovirus 1 S4-coded protein is dispensable for viral replication but necessary for efficient vertical transmission and normal symptom induction. Virology. 397, 399-408.

Faruk, M. I., Eusebio-Cope A. and Suzuki N. 2008. A host factor involved in hypovirus symptom expression in the chestnut blight fungus, *Cryphonectria parasitica*. J.

Virol. 82, 740-754.

Faruk, M., Izumino M. and Suzuki N. 2008. Characterization of mutants of the chestnut blight fungus (*Cryphonectria parasitica*) with unusual hypovirus symptoms. J. Gen. Plant. Pathol. 74, 425-433.

Fauquet, C. M., Mayo, M. A., Maniloff, J., Desselberger, U. and L. Ball, A. [eds.]. 2005. Virus taxonomy: VIIIth report of the International Committee on Taxonomy of Viruses. Elsevier Academic.

Freeman, S., Sztejnberg, A. and Chet, I. 1986. Evaluation of *Trichoderma* as a biocontrol agent for *Rosellinia necatrix*. Plant and Soil, 94, 163-170.

Finn, R.D., Tate J., Mistry J., Coggill P.C., Sammut J.S., Hotz H.R., Ceric G., Forslund K., Eddy S.R., Sonnhammer E.L. and Bateman A. 2008. The Pfam protein families database. Nucleic Acids Res. Database Issue. 36, D281-D288.

García-Jiménez, J., Busto, J., Vicent, A., and Armengol, J. 2004. Control of *Dematophora necatrix* on *Cyperus esculentus* tubers by hot-water treatment. Crop Protection. 23, 619-623.

Gault, E., Schnepf, N., Poncet, D., Servant, A., Teran, S., and Garbarg-Chenon, A. 2001. A human rotavirus with rearranged genes 7 and 11 encodes a modified NSP3 protein and suggests an additional mechanism for gene rearrangement. J. Virol. 75, 7305-14.

González-Sánchez, M. A., Cazorla, F. M., Ramos, C., de Vicente, A. and Pérez-Jiménez, R. M. 2004. Studies of soil and rhizosphera bacteria to improve biocontrol of avocado white root rot caused by *Rosellinia necatrix*. Management of plant diseases an arthropod pests by BCAs and their integration in agricultural systems. IOBC/WPRS Bulletin. 27, 169-172.

Ghabrial, S. A. 1994. New developments in fungal virology. Advances in Virus Research, 43, 303-388.

Ghabrial, S. A. 1998. Origin, adaptation and evolutionary pathways of fungal viruses. Virus Genes 16, 119-131.

Ghabrial, S. A. 2001. Fungal viruses. p. 478-483. In Maloy, O. & Murray, T. (ed.) Encyclopedia of Plant Pathology. vol. 1. John Wiley & Sons, New York.

Ghabrial, S. (2008). Totiviruses. In Encyclopedia of Virology, 3rd edn, pp. 163-174. Edited by B. W. J. Mahy & M. H. V. Van Regenmortel. Oxford: Elsevier.

Ghabrial, S. A., and Suzuki N. 2009. Viruses of plant pathogenic fungi. Annu. Rev. Phytopathol. 47, 353-384.

Glass, N.L. and Dementhon, K. 2006. Non-self recognition and programmed cell death in filamentous fungi. Current opinion in microbiology. 9(6): 553-8.

Guo, L., Sun L.-Y, Chiba S., Araki H., and N. Suzuki. 2009. Coupled termination/reinitiation for translation of the downstream open reading frame B of the prototypic hypovirus CHV1-EP713. Nucleic Acids Res. 37, 3645-3659.

Gupta, V. K. 1977. Possible use of Carbendazim in the control of *Dematophora* root rot of apple. Indian Phytopathology. 30, 527-531.

Heiniger, U. and Rigling D. 1994. Biological control of chestnut blight in Europe. Annu. Rev. Phytopathol. 32, 581-599.

Hillman, B. I., Halpern, B. T. and Brown, M. P. 1994. A viral dsRNA element of the chestnut blight fungus with a distinct genetic organization. Virology. 201, 241-250.

Hillman, B. I. and Suzuki N. 2004. Viruses in the chestnut blight fungus. Adv. Virus Res. 63, 423-472.

Hillman, B. I., Shapira, R. and Nuss, D. L. 1990. Hypovirulence associated suppression of host function in *Cryphonectria parasitica* can be partially relieved by high-light intensity. Phytopathology. 80, 950-956.

Hillman, B. I., Supyani S., Kondo H. and Suzuki N. 2004. A reovirus of the fungus *Cryphonectria parasitica* that is infectious as particles and related to the Coltivirus genus of animal pathogens. J. Virol. 78, 892-898.

Ihrmark, K., Johannesson, H., Stenström, E., and Stenlid, J. 2002. Transmission of double-stranded RNA in *Heterobasidion annosum*. Fungal Genetics and Biology, 36(2), 147-154.

Ikeda, K., Nakamura H., Arakawa M. and Matsumoto N. 2004. Diversity and vertical transmission of double-stranded RNA elements in root rot pathogens of trees, *Helicobasidium mompa* and *Rosellinia necatrix*. Mycol. Res. 108, 626-634.

Ikeda, K., Nakamura H. and Matsumoto N. 2005. Comparison between *Rosellinia necatrix* isolates from soil and diseased roots in terms of hypovirulence. FEMS Microbiol. Ecol. 54, 307-315.

Ten Hoopen, G. M. and Krauss, U. 2006. Biology and control of *Rosellinia bunodes* , *Rosellinia necatrix* and *Rosellinia pepo*: A review. Crop Protection, 25 (2), 89-107.

Ito, S. and Nakamura N. 1984. An outbreak of white root-rot and its environmental conditions in the experimental arboretum (in Japanese) J. Jpn For. Soc. 66, 262-267.

Jiang D. and Ghabrial S. A. 2004. Molecular characterization of *Penicillium chrysogenum* virus: reconsideration of the taxonomy of the genus Chrysovirus. J. Gen. Virol. 85, 2111-2121.

Kanadani, G., Date, H. and Nasu, H. 1998. Effect of Fluazinam soildrench on white root rot of grapevine. Annals of the Phytopathological Society of Japan, 64, 139-141.

Kanematsu, S., Arakawa M., Oikawa Y., Onoue M., Osaki H., Nakamura H., Ikeda K., Kuga-Uetake Y., Nitta H., Sasaki A., Suzaki K., Yoshida K. and Matsumoto N. 2004. A reovirus causes hypovirulence of *Rosellinia necatrix*. Phytopathology. 94, 561-568.

Kanematsu, S., Sasaki, A., Onoue, M., Oikawa, Y. and Ito, T. 2010. Extending the fungal host range of a partitivirus and a mycoreovirus from *Rosellinia necatrix* by inoculation of protoplasts with virus particles. Phytopathology. 100, 922-930.

Kobayashi, T., Antar, A. A., Boehme, K. W., Danthi, P., Eby, E. A., Guglielmi, K. M., Holm, G. H., Johnson, E. M., Maginnis, M. S., Naik, S., Skelton, W. B., Wetzel, J. D., Wilson, G. J., Chappell, J. D. and Dermody, T. S. 2007. A plasmid-based reverse genetics system for animal double-stranded RNA viruses. Cell Host Microbe. 1, 147-57.

Kojima, K., Taniguchi, K., Urasawa, T. and Urasawa, S. 1996. Sequence analysis of normal and rearranged NSP5 genes from human rotavirus strains isolated in nature: implications for the occurrence of the rearrangement at the step of plus strand synthesis. Virology. 224, 446-52.

Komoto, S., Sasaki, J. and Taniguchi, K. 2006. Reverse genetics system for introduction of site-specific mutations into the double-stranded RNA genome of infectious rotavirus. Proc. Natl. Acad. Sci. USA 103, 4646-51.

Kondo, H., Kanematsu, S. and Suzuki, N. 2013. Viruses of the white root rot fungus, *Rosellinia necatrix*. Adv Virus Res. 86, 177-214.

Kozak, M. 1989. The scanning model for translation: an update. J. Cell Biol. 108, 229-241

Kozlakidis, Z., Hacker, C. V., Bradley, D., Jamal, A., Phoon, X., Webber, J ., Brasier, C. M., Buck, K. W. and Coutts, R. H. 2009. Molecular characterisation of two novel double-stranded RNA elements from *Phlebiopsis gigantea*. Virus Genes. 39, 132-136.

Kubo, Y., Suzuki, K., Furusawa, I., and Yamamoto, M. 1985. Melanin biosynthesis as a prerequisite for penetration by appressoria of *Colletotrichum lagenarium*: site

inhibition by melanin-inhibiting fungicides and their action on appressoria. Pest. Biochem Physiol. 47-55.

Lai, M.M. 1992. RNA recombination in animal and plant viruses. Microbiol Rev. 56(1), 61-79.

Lee, K. M., Yu, J., Son, M., Lee, Y. W. and Kim, K. H. 2011. Transmission of *Fusarium boothii* mycovirus via protoplast fusion causes hypovirulence in other phytopathogenic fungi. PLoS ONE. 6, e21629.

Li, L., Wang, A. L. and Wang, C. C. 2001. Structural analysis of the 21 ribosomal frameshift elements in giardiavirus mRNA. J Virol. 75, 10612-10622.

Lin, Y.S. and Duan, C.H. 1988. White root rot of loquat and its pathogen. J Agric Res China. 37, 305-312.

Lin, Y. H., Chiba, S., Tani, A., Kondo, H., Sasaki, A., Kanematsu, S. and Suzuki, N. 2012. A novel quadripartite dsRNA virus isolated from a phytopathogenic filamentous fungus, *Rosellinia necatrix*. Virology. 426, 42-50.

Lin, Y. H., Hisano, S., Yaegashi, H., Kanematsu, S. and Suzuki, N. 2013. A second quadrivirus strain from the phytopathogenic filamentous fungus Rosellinia necatrix. Arch Virol. 158, 1093-1098.

Liu, H., Fu Y., Jiang D., Li G., Xie J., Peng Y., Yi X. and Ghabrial S. A. 2009. A novel mycovirus that is related to the human pathogen hepatitis E virus and rubi-like viruses. J. Virol. 83, 1981-1991.

Lynch, M. 2006. Streamlining and simplification of microbial genome architecture. Annu Rev Microbiol.60, 327-349.

Matsumoto, N. 1998. Biological control of root diseases with dsRNA based on population structure of pathogenes. JARQ. 32, 31-35.

Mendoza, R. A., Ten Hoopen, G. M., Kass, D. C. J., Sánchez, V. A. and Krauss, U. 2003. Evaluation of mycoparasites as biocontrol agents of *Rosellinia* root rot in cocoa. Biological Control. 27, 210-227.

Milgroom, M. G. and Cortesi P. 2004. Biological control of chestnut blight with hypovirulence: a critical analysis. Annu. Rev. Phytopathol. 42, 311-338.

Mundt, E. and Vakharia, V. N., 1996, Synthetic transcripts of double-stranded Birnavirus genome are infectious. Proc. Natl. Acad. Sci. USA. 93, 11131-6.

Nakamura, H., Ikeda, K., Arakawa M. and Matsumoto, N. 2002. Conidioma production of the white rooto rot fungus in axenic culture under near-ultravioret light radiation. Mycoscience. 43, 251-254.

Nuss, D. L., 1984. Molecular biology of wound tumor virus. Adv. Virus Res. 29, 57-93.

Nuss, D.L. and Summers, D., 1984. Variant dsRNAs associated with transmission-defective isolates of wound tumor virus represent terminally conserved remnants of genome segments. Virology. 133, 276-88.

Nuss, D. L. 2005. Hypovirulence: Mycoviruses at the fungal-plant interface. Nat. Rev. Microbiol. 3, 632-642.

Pearson, W. R. and Lipman, D. J. 1988. Improved tools for biological sequence comparison. Proc. Natl. Acad. Sci. USA. 85, 2444-2448.

Pearson, M. N., Beever, R. E., Boine, B., and Arthur, K. 2009. Mycoviruses of filamentous fungi and their relevance to plant pathology. Mol Plant Pathol. 10(1), 115-128.

Pérez-Jiménez, R. M. 2006. A review of Biological control and pathogenicity of Rosellinia necatrix- the cause of white root rot disease of fruit trees and plants. J. Phytopathology. 154, 257-266.

Pérez-Jiménez, R. M., Jiménez-Díaz, R. M., and López-Herrera, C. J. 2002. Somatic incompatibility of *Rosellinia necatrix* on avocado plants in southern Spain. Mycological Research. 106, 239-244.

Petrini, L.E. 1993. Rosellinia species of the temperate zones. Sydowia. 44, 169-281.

Pliego, C., Kanematsu S., Ruano-Rosa D., de Vicente, A. López-Herrera, C., Cazorla, F. M. and Ramos, C. 2009. GFP sheds light on the infection process of avocado roots by *Rosellinia necatrix*. Fungal Genet. Biol. 46, 137-145.

Pliego, C., López-Herrera, C., Ramos, C. and Cazorla, F.M. 2012. Developing tools to unravel the biological secrets of *Rosellinia necatrix*, an emergent threat to woody crops. Mol. PlantPathol.13, 226-239.

Runia, W. T. 2000. Steaming methods for soils and substrates. Acta Horticulturae, 532, 115–123.

Sambrook, J. and Russell, D. W. 2001. Molecular cloning: a laboratory manual, 3rd ed. Cold Spring Harbor Laboratory, Cold Spring Harbor, N.Y.

Salaipeth, L., Chiba, S., Eusebio-Cope, A., Kanematsu, S. and Suzuki, N. 2013. Biological properties and expression strategy of Rosellinia necatrix megabirnavirus1analyzed in an experimental host, *Cryphonectria parasitica*. J. Gen. Virol. (inpress).

Sasaki, A., Onoue, M., Kanematsu, S., Suzaki, K., Miyanishi, M., Suzuki, N., Nuss, D.

L. and Yoshida, K. 2002. Extending chestnut blight hypovirus host range within Diaporthales by biolistic delivery of viral cDNA. Mol Plant Microbe Interact.15, 780-789.

Sasaki, A., Miyanishi, M., Ozaki, K., Onoue, M. and K. Yoshida. 2005. Molecular characterization of a partitivirus from the plant pathogenic ascomycete *Rosellinia necatrix*. Arch. Virol. 150, 1069-1083.

Sasaki A., Kanematsu, S., Onoue, M., Oikawa, Y., Nakamura, H. and Yoshida, K. 2007. Artificial infection of Rosellinia necatrix with purified viral particles of a member of the genus mycoreovirus reveals its uneven distribution in single colonies. Phytopathology. 97, 278-286.

Sasaki A., Kanematsu, S. Onoue, M. Oyama, Y. and Yoshida, K. 2006. Infection of *Rosellinia necatrix* with purified viral particles of a member of *Partitiviridae* (RnPV1-W8). Arch. Virol. 151, 697-707.

Saupe, S. J. 2000. Molecular genetics of heterokaryon incompatibility in filamentous ascomycetes. Microbiol Mol Biol Rev. 64, 489-502.

Schena, L. and Ippolito, A. 2003. Rapid and sensitive detection of *Rosellinia necatrix* in roots and soils by real time Scorpion-PCR. Journal of Plant Pathology. 85, 15-25.

Segers, G. C., Zhang, X., Deng, F., Sun, Q. and Nuss, D. L. 2007. Evidence that RNA silencing functions as an antiviral defense mechanism in fungi. Proc. Natl. Acad. USA. 104, 12902-12906.

Shapka, N. and Nagy, P. D. 2004. The AU-rich RNA recombination hot spot sequence of Brome mosaic virus is functional in tombusviruses: implications for the mechanism of RNA recombination. J. Virol. 78, 2288-300.

Simon, A. E. and Bujarski, J. J. 1994. RNA-RNA recombination and evolution in virus-infected plants. Annual Review of Phytopathology. 32, 337-362.

Smart, C. D., Yuan, W., Foglia, R., Nuss, D. L., Fulbright, D. W. and Hillman, B. I. 1999. Cryphonectria hypovirus 3, a virus species in the family hypoviridae with a single open reading frame. Virology. 265, 66-73.

Spear, A., Sisterson, M. S., Yokomi, R. and Stenger, D. C. 2010. Plant-feeding insects harbor double-stranded RNA viruses encoding a novel proline-alanine rich protein and a polymerase distantly related to that of fungal viruses. Virology. 404, 304-311.

Strauss, J.H. and Strauss, E.G. 1988. Evolution of RNA viruses. Annu Rev Microbiol. 42, 657-683.

Sun, L., Nuss, D. L. and Suzuki, N. 2006. Synergism between a mycoreovirus and a hypovirus mediated by the papain-like protease p29 of the prototypic hypovirus CHV1-EP713. J Gen Virol. 87, 3703-3714.

Sun, Q., Choi, G. H., and Nuss, D. L. 2009a. Hypovirus-responsive transcription factor gene pro1 of the chestnut blight fungus Cryphonectria parasitica is required for female fertility, asexual spore development, and stable maintenance of hypovirus infection. Eukaryot. Cell. 8, 262-270.

Sun, Q., Choi, G. H. and Nuss, D. L. 2009b. A single Argonaute gene is required for induction of RNA silencing antiviral defense and promotes viral RNA recombination. Proc. Natl. Acad. Sci. USA. 106, 17927-17932.

Sun, L.-Y. and Suzuki., N. 2008. Intragenic rearrangements of a mycoreovirus induced by the multifunctional protein p29 encoded by the prototypic hypovirus CHV1-EP713. RNA 14, 2557-2571.

Suzaki, K., Ikeda, K., Kanematsu, S., Matsumoto, N., and Yoshida, K. 2005. Horizontal transmission and host-virulence attenuation of totivirus in violet root rot fungus *Helicobasidium mompa*. Journal of General Plant Pathology, 71, 161-168.

Suzuki, N. and Nuss, D. L. 2002. The contribution of p40 to hypovirus-mediated modulation of fungal host phenotype and viral RNA accumulation. J. Virol. 76, 7747-7759.

Suzuki, N., Maruyama, K., Moriyama, M. and Nuss, D. L. 2003. Hypovirus papain-like protease p29 is an enhancer of viral dsRNA accumulation and vertical transmission. J. Virol. 77, 11697-11707.

Suzuki, N., Sugawara, M., Nuss, D. L. and Matsuura, Y. 1996. Polycistronic (tri- or bicistronic) phytoreoviral segments translatable in both plant and insect cells. J Virol. 70, 8155-8159.

Suzuki, N., Supyani, S., Maruyama, K. and Hillman, B. I. 2004. Complete genome sequence of Mycoreovirus 1/Cp9B21, a member of a new genus within the family Reoviridae, from the chestnut blight fungus Cryphonectria parasitica. J. Gen. Virol. 85, 3437-3448.

Sztejnberg, A., Freeman, S., Chet, I., and Katan, J. 1987. Control of *Rosellinia necatrix* in soil and apple orchard by solarization and *Trichoderma harziarum*. Plant Disease. 71, 365-369.

Sztejnberg, A. Madar, Z. and Chet, I., 1980. Induction and quantification of microsclerotia in *Rosellinia necatrix*. Phytopathology. 70, 525-527.

Takano, Y., Kubo, Y., Shimizu, K., Mise, K., Okuno, T. and Furusawa, I., 1995. Structural analysis of PKS1, a polyketide synthase gene involved in melanin biosynthesis in *Colletotrichum lagenarium*. Mol. Gen. Genet. 249, 162-7.

Tanaka, T., Sun, L., Tsutani, K. and Suzuki, N., 2011. Rearrangements of mycoreovirus 1 S1, S2 and S3 induced by the multifunctional protein p29 encoded by the prototypic hypovirus Cryphonectria hypovirus 1 strain EP713. J. Gen. Virol. 92**,** 1949-59.

Taniguchi, K. and Urasawa, S., 1995. Diversity in rotavirus genomes. Semin. Virol. 6, 123-131.

Taniguchi, K., Kojima, K. and Urasawa, S., 1996. Nondefective rotavirus mutants with an NSP1 gene which has a deletion of 500 nucleotides, including a cysteine-rich zinc finger motif-encoding region (nucleotides 156 to 248), or which has a nonsense codon at nucleotides 153-155. J. Virol. 70, 4125-30.

Teixeira de Sousa, A. J., Guillaumin, J. J., Sharples, G. P. and Whalley, A. J. S. 1995. *Rosellinia necatrix* and white root rot of fruit trees and other plants in Portugal and nearby regions. Mycologist, 9, 31-33.

Thompson, J. D., Gibson, T. J., Plewniak, F., Jeanmougin, F. and Higgins, D. G. 1997. The CLUSTAL_X windows interface: flexible strategies for multiple sequence alignment aids by quality analysis tools. Nucleic Acids Res. 25, 4876-4882.

Tseng, M. N., Chung, P. C., and Tzean, S. S. 2011. Enhancing the stress tolerance and virulence of an entomopathogen by metabolic engineering of dihydroxynaphthalene melanin biosynthesis genes. Appl. Environ. Microbiol. 77**,** 4508-19.

Urayama, S., Ohta, T., Onozuka, N., Sakoda, H., Fukuhara, T., Arie, T., Teraoka, T. and Moriyama, H., 2012. Characterization of Magnaporthe oryzae chrysovirus 1 structural proteins and their expression in *Saccharomyces cerevisiae*. J. Virol. 86, 8287-95.

Van Diepeningen, A. D., Debets, A. J. M. and Hoekstra, R. F. 1997. Heterokaryon incompatibility blocks virus transfer among natural isolates of black Aspergilli. Current Genetics, 32(3), 209-217.

Van Diepeningen, A. D., Debets, A. J. M. and Hoekstra, R. F. 1998. Intra-and interspecies virus transfer in Aspergilli via protoplast fusion. Fungal Genetics and Biology, 25(3), 171-180.

Varga, J., Rigo, K., Toth, B., Teren, J. and Kozakiewicz, Z. 2003. Evolutionary relationships among Aspergillus species producing economically important mycotoxins. Food Tech Biotech 41(1), 29-36.

Varga, J. and Samson, R. A. 2008. Aspergillus In The Genomic Era: Wageningen Academic Publishers.

Vogel, H. 1956. A convenient growth medium for Neurospore (medium N). Microb Genet Bull 13, 42-43.

Wei, C. Z., Osaki, H., Iwanami, T., Matsumoto, N. and Y. Ohtsu. 2004. Complete nucleotide sequences of genome segments 1 and 3 of Rosellinia anti-rot virus in the family Reoviridae. Arch. Virol. 149, 773-777.

Whalley, A. J. S. (1996) The xylariaceous way of life. Mycological Research 100, 897-922.

Wickner, R. B., Ghabrial, S. A., Nibert, M. L., Patterson, J. L. and Wang, C. C. 2011. Family Totiviridae. In Virus Taxonomy: Ninth Report of the International Committee for the Taxonomy of Viruses, pp. 639-650. Edited by A. M. Q. King, M. J. Adams, E. B. Carstens & E. J. Lefkowits. New York: Elsevier/Academic Press.

Wu, Q., Wang, X. and Ding, S. W. 2010. Viral suppressors of RNAbased viral immunity: host targets. Cell Host Microbe 8, 12-15.

Xie, J., Wei, D., Jiang, D., Fu, Y., Li, G., Ghabrial, S.A. and Peng, Y. 2006. Characterization of debilitation-associated mycovirus infecting the plant-pathogenic fungus Sclerotinia sclerotiorum J. Gen. Virol., 87 (1), pp. 241–249

Yaegashi, H., Sawahata, T., Ito, T. and Kanematsu, S. 2011. A novel colony-print immunoassay reveals differential patterns of distribution and horizontal transmission of four unrelated mycoviruses in Rosellinia necatrix. Virology 409, 280–289.

Yaegashi, H., Yoshikawa, N., Ito, T. and Kanematsu, S. 2013. A mycoreovirus suppresses RNA silencing in the white root rot fungus, Rosellinia necatrix. Virology 444, 409-416.

Yasuda, M., and Katoh, K. 1989. Characteristics of bacteria isolated from soil and roots of fruit trees. Soil Science and Plant Nutrition. 35, 501-508.

Yu, J., Kwon, S. J., Lee, K. M., Son, M. and Kim, K. H. 2009. Complete nucleotide sequence of double-stranded RNA viruses from Fusarium graminearum strain DK3. Arch Virol 154, 1855-1858.

Yu, X., Li, B., Fu, Y., Jiang, D., Ghabrial, S. A., Li, G., Peng, Y., Xie, J., Cheng, J. and other authors 2010. A geminivirus-related DNA mycovirus that confers hypovirulence to a plant pathogenic fungus. Proc Natl Acad Sci U S A 107, 8387-8392.

Zuker, M. 2003. Mfold web server for nucleic acid folding and hybridization prediction. Nucleic Acids Res. 747 31: 3406-3415.